Norwegian University
of Life Sciences

Master's Thesis 2022   30 ECTS
Faculty of Science and Techonology

An Assessment of the Design Model for Glulam Members subjected to Compression Perpendicular to the Grain with Reinforcement

Eldbjørg Aaraas Hånde and Kari Ryen Thunberg
Structural Engineering and Architecture

Preface

This master thesis concludes our master's degree in Structural Engineering and Architecture at the Norwegian University of Life Sciences (NMBU). Many academic questions have been discussed with each other, our supervisor, and collaborators during this work. This thesis has both been demanding and educational, which has given us new acknowledgment and understanding of the topic.

We would like to give our deepest gratitude to our supervisors Assoc Prof. Ebenezer Ussher and Prof. Roberto Tomasi. We appreciate the valuable guidance and feedback throughout the whole period, as well as for giving us the opportunity to write this thesis. Furthermore, we would like to thank Xiaojun Gu for the support during the experimental work.

The experimental work is conducted at the Wood Laboratory at NMBU. We would like to thank RealTek and MINA for letting us use their facilities and the equipment. The laboratory work has given us a deeper understanding of the material and test executions. Furthermore, we appreciate Frode Anker Røsstad for his guidance and help with the test preparations. A great thanks are given to the steel laboratory at NMBU for its effectiveness and solution orientations. Additionally, we appreciate Moelven, SFS, and Rothoblaas for letting us use their products in our experimental work.

Finally, we would like to thank our supervisors and CEN committee for evaluating our work and comments to prEN 1995-1-1, version of November 2021.

Eldbjørg Aaraas Hånde and Kari Ryen Thunberg
Ås, June 2022

Abstract

This master thesis presents an empirical assessment of glulam subjected to compression perpendicular to the grain (CPG) with reinforcement. prEN 1995-1-1 will replace the current Eurocode 5, NS-EN 1995-1-1 - *Design of timber structures*. prEN 1995 introduces a design model concerning reinforced members subjected to CPG. However, there is a gap in knowledge concerning the proposed design model and experimental data.

Demanding design situations with CPG occur in timber structures with high concentrated loads. The consideration of CPG introduces complexity into the design process due to the reduced bearing strength of the member in the perpendicular direction. However, the bearing strength can increase considerably by reinforcing the member with fully threaded self-tapping screws. For members subjected to CPG with reinforcement, three failure modes may occur; failure due to pushing-in of screws, buckling of screws, or timber failure. These failure modes give the basis of determining the decisive capacity in the design model, prEN 1995-1-1.

In this study, the reliability of the design model is investigated through experimental tests. The load cases considered are discrete support with a concentrated or uniformly distributed load. Moreover, the capacity of one screw without the timber contribution is tested by torx tests. The reinforcement applied has varying lengths, diameters, screw heads, and screw arrangements.

The comparison of the design model and test results present an inaccuracy in the design model. For some configurations, the predicted failure mode is not corresponding to the achieved failure mode in the tests. In addition, the overall predicted capacity is overly conservative. Despite the inaccuracies, the evaluation of the first part of the design model presents a good correlation between the predictions and test results.

This study considers the possibility of harmonizing the design model, and two proposals are presented. Proposal 1 is a modification of the design model in prEN 1995, where the $k_{c,90}$ is evaluated. Proposal 2 is derived based on stress concentration along the effective dispersion length.

The study of this thesis strengthens the scientific data of reinforced members subjected to CPG. Proposal 2 enlightens another aspect of the stress consideration at the tip of the screws. The approach corresponds with test capacities and failure modes.

Sammendrag

Denne masteroppgaven omhandler en empirisk evaluering av trykk vinkelrett på fiberretning (CPG) i et armert limtreelement. prEN 1995-1-1 vil erstatte dagens Eurokode 5, NS-EN 1995-1-1 - *Prosjektering av trekonstruksjoner*. prEN 1995-1-1 introduserer en beregningsmodell for CPG med armering. I denne beregningsmodellen er det et kunnskapshull knyttet til nøyaktigheten i modellen, dette har sin bakgrunn i begrenset tilgang på eksperimentelle tester.

Utfordringer relatert til CPG oppstår i trekonstruksjoner med høye konsentrerte laster. CPG er et krevende område i dimensjoneringsprosessen. Dette er knyttet opp til treverkets reduserte bæreevne vinkelrett på fiberretning. Kapasiteten kan økes betraktelig ved å forsterke trevirke med helgjengede skruer. Tre feilmekanismer kan oppstå ved CPG for armerte elementer: Svikt på grunn av innpressing av skruer, knekking av skruer eller svikt i trevirket. Feilmekansimene gir grunnlag for bestemmelse av dimensjonerende kapasitet i bergeningsmodellen gitt i prEN 1995-1-1.

I denne studien er beregningsmodellens pålitelighet evaluert gjennom eksperimentelle tester. Last-situasjonene som vurderes er en fritt opplagt bjelke med én punktlast eller jevnt fordelt last. I tillegg testes kapasiteten til én skrue uten å belaste trevirket gjennom torx-tester. Skruene som benyttes som armering har varierende lengde, diameter, skruehode og plassering.

Sammenligningen av beregningsmodellen og testresultatene viser en uoverensstemmelse. For flere av konfigurasjonene samsvarer ikke den beregnede feilmekanismen med det som ble påvist i de utførte testene. Med bakgrunn i testene er den beregnede kapasiteten i overkant konservativ. Til tross for unøyaktighetene, viser evalueringen av den første delen av beregningsmodellen en høy korrelasjon mellom testresultatene og modellen.

I denne studien er det i tillegg evaluert muligheten for å harmonisere beregningsmodellene for CPG i henholdsvis armert- og uarmert limtre og to forbedringsforslag presenteres. Forslag 1 er en modifisering av beregningsmodellen i prEN 1995, hvor $k_{c,90}$ er evaluert. Forslag 2 er utledet basert på en spenningskonsentrasjon langs den effektive spredningslengden.

Denne oppgaven styrker de vitenskapelige dataene til armerte limtreelementer utsatt for CPG. Forslag 2 belyser et annet perspektiv med hensyn til spenningskonsentrasjonen ved tuppen av skruen. Dette forslaget til modifisering samsvarer godt med feilmekanismene og kapasitetene oppnådd i testene.

Contents

Figures

Tables

1. Introduction

1.1 Background

Timber buildings are traditionally found in the Nordic countries, primarily in one- or two-story buildings [1]. The need for more sustainable buildings due to population growth has resulted in an increased application of timber for the construction of buildings [2, 3]. Acknowledge the potential in timber regarding low emission, advanced multi-story structures are of interest. Consequently, this requires the design to utilize the full potential of the timber properties.

Compression perpendicular to the grain, (CPG) is a demanding area regarding the design of timber structures. The mechanical properties in timber differ in the three main directions of the grain. Considering GL 28h; the compressive strength parallel to grain is $f_{c,0,k} = 28\ N/mm^2$. For the same material the strength perpendicular is $f_{c,90,k} = 2.5\ N/mm^2$ [4]. Consequently, this is a $\frac{1}{11}$ reduction of the capacity when a member is subjected to CPG. Accordingly, an increase in the CPG capacity could be obtained by applying reinforcement in timber members [5].

In 2012, the European Committee for Standardization (CEN) made a program to develop the second generation of Eurocodes. The development purpose is to extend the existing rules to include new materials and construction methods. Moreover, improve the designer's efficacy and reduce the number of national parameters [6]. Eurocode 5 - *design of timber structures*, NS-EN 1995-1-1, presents the design model for CPG. Regarding the second generation of Eurocodes, a working draft of EN 1995-1-1 has been released. The presented design model of CPG is an evolution of the current Eurocode, and a section implementing reinforced members subjected to CPG is added. The reinforcement is fully threaded self-tapping screws.

The working draft, prEN 1995 of November 2021, presents a new improved design model for non-reinforced members. This model introduces a material behaviour and deformation factor, k_p. In addition, the load arrangement factor, $k_{c,90}$, is adopted to take into account the load dispersion in relation to the contact area. However, the design model for reinforced members is introduced in the current consolidated draft of the Eurocode. From a compatibility point of view, it is suggested to harmonize the approach in the design model of reinforced and non-reinforced members. Based on this, a study of glulam members considering compression perpendicular to the grain with reinforcement is of interest.

1.2   Problem Statement and Research Questions

In the light of Eurocode 5, an investigation regarding the design model of CPG of glulam members with reinforcement is desired. The prediction of capacities and failure modes should be confirmed by experimental tests. Accordingly, the following problem statement is developed:

There is a gap in knowledge concerning the test data that strengthens and validate the design model given in the proposed Eurocode 5.

The work of this thesis will give strength to the following research questions:

  i What is the level of accuracy, reliability, and robustness of the design model for CPG of reinforced members in prEN 1995?

 ii Is it possible to harmonize the proposed approaches for reinforced and non-reinforced members subjected to CPG?

1.3   Research Objectives and Scientific Contributions

The objective of this work is to investigate the reliability of the new Eurocode 5 concerning CPG with reinforcement. In this thesis, the evaluation of the design model is based on experimental results. A preliminary study of former research regarding CPG with reinforcement is performed to validate the work. A sensitivity study of the design model strengthens the evaluations and describes the model in detail with varying parameters. Furthermore, an assessment of harmonizing the design model with the non-reinforced design model is presented. The scientific contribution of this work is to strengthen the knowledge concerning the design model of reinforced timber members under CPG demands. Additionally, this thesis enlighten a different view of the design model.

1.4   Limitations

In this thesis, the following assumptions and decisions are made:

 • The design model and determination of the screw capacity are assumed to be correct, and the design model of the screw capacity is not criticized.

 • The experimental campaign carried out, forms the basis of the harmonization proposed for the design model of reinforced timber members subjected CPG.

1.5 Structure of the thesis

- Chapter 1 - Introduces the outline of the thesis.

- Chapter 2 - Addresses the theory of timber as a material and CPG of non-reinforced members.

- Chapter 3 - Presents the state of the art of members subjected to CPG with reinforcement, and a preliminary investigation based on earlier experimental work.

- Chapter 4 - Covers sensitivity analysis that addresses the capacity of non-reinforced and reinforced members with varying geometrical parameters.

- Chapter 5 - Contains the experimental campaign, where the method and test execution is presented.

- Chapter 6 - Consists of the experimental results.

- Chapter 7 - Evaluates the experimental results and the design model, as well as presents two proposal.

- Chapter 8 - Gives the final remarks.

2. Compression perpendicular to the grain

2.1 General introduction to timber

Timber performs as a highly anisotropic material reflecting that the direction of the grain influences the mechanical properties [7]. In the parallel direction to the grain, timber tends to be very strong and stiff due to its cellular structure. However, in the direction perpendicular to the grain, the strength and stiffness are considerably lower [7]. In particular, timber is an orthotropic material. The mechanical properties differ in three mutually perpendicular directions, see Figure 2.1. The longitudinal direction (L) is aligned parallel to the grain. The radial direction (R) and tangential direction (T) refers to properties perpendicular to the grain [8].
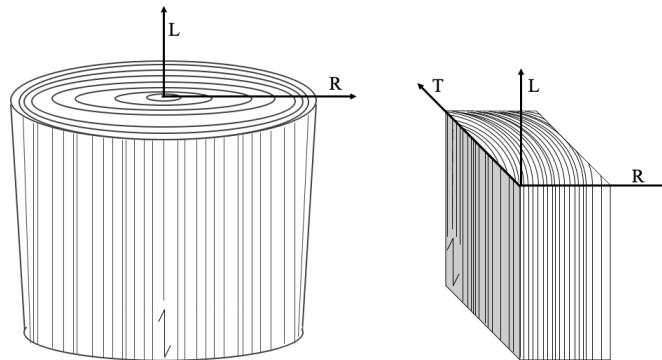
Figure 2.1: Principal direction of timber [7]

The fibers in a timber member are tubular in section and elongated. The cell walls of the fibers are glued together with the organic substance lignin. Lignin strengthens the bond between the cell walls that provides the basis for the strength of the timber [9]. CPG failure leads to a collapse of the cellular tubes and acts as a failure along the tubular layers [10]. The failure of the cell structure is shown in Figure 2.2. The thickness of the cell walls gives timber strength and stiffness. However, other parameters such as annual rings and growth impact the mechanical properties. Earlywood tends to have a thinner cell wall than latewood and will result in a higher modulus of elasticity with a thicker cell wall [11].
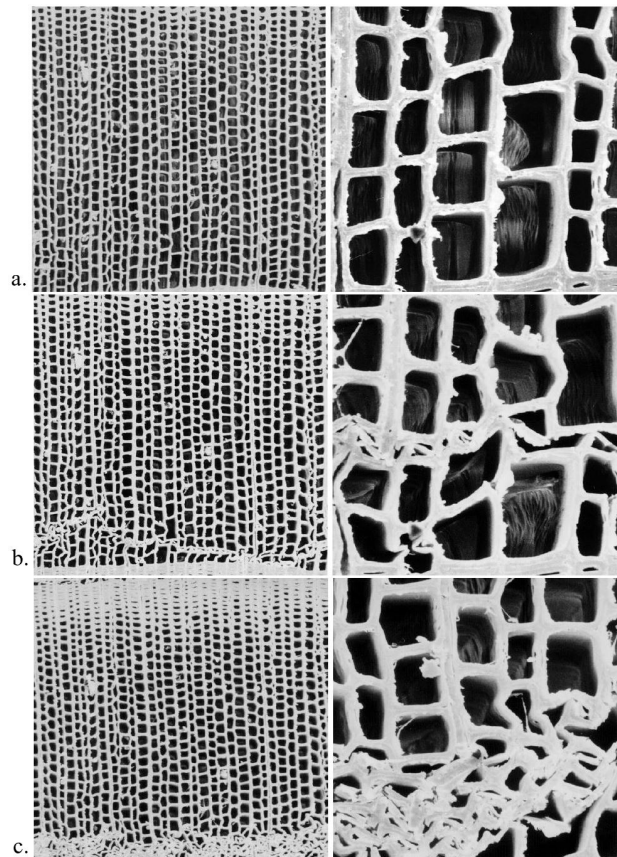
Figure 2.2: a) Undeformed; b) Failure of a single layer; c) Failure of multiple layers [10]

Beams, trusses, and multi-story buildings are examples of design situation where CPG can occur. Failure due to CPG will typically not lead to collapse. The failure of CPG is potential a problem within the range of the serviceability limit state (SLS). However in Eurocode 5, CPG is regarded as a ultimate limit state (ULS) problem to avoid load failure of structural systems [12]. The mode of failure appears over an effective contact area. Figure 2.3 shows how deformation resulting from CPG appears. As the compressive load increases, the fibers will buckle. This compression will transmit to neighboring fibers as a chain reaction. Due to the deformation, greater loads are achievable by increasing the loaded length with the dispersion length [12].
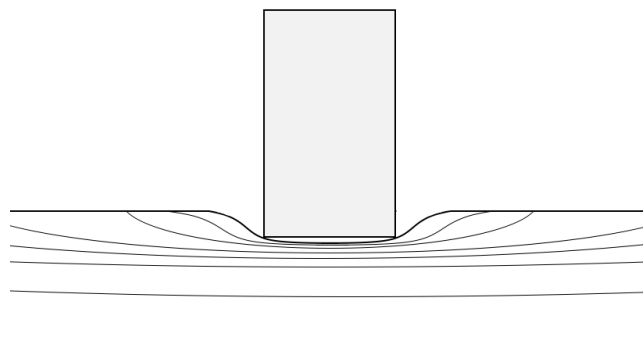
Figure 2.3: Compression perpendicular to grain

2.2   Elasticity and plasticity of timber

Elastic behavior is the force a member can withstand, resulting in non-permanent deformation. Once releasing the force, the material will turn back to its original shape. The relationship between stress and strain is linear. Consequently, Hooke's law is valid. The limit for elastic behavior, the proportional limit, is determined by the modulus of elasticity [13].

In contrast to elastic behavior, plastic behavior results in permanent deformation. The material undergoes plastic deformation when the member is beyond the proportional limit (elastic behavior). By increasing deformation, many materials will eventually reach the fracture point. The stress-strain diagram in Figure 2.4 shows the elastic and plastic behavior for a general material [13].
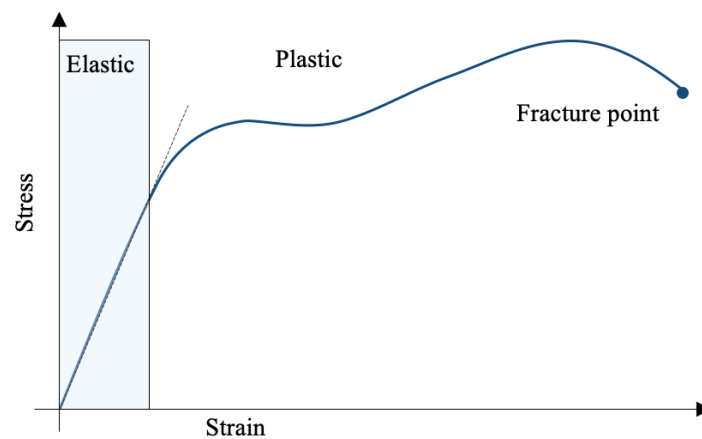
Figure 2.4: Stress-strain general material behavior

Timber has an elastic-plastic behavior. The limit for elastic behavior is determined by the modulus of elasticity. Since timber is an orthotropic material, the modulus of elasticity corresponds to the direction of the fiber, E_L, E_R, and E_T. There is no clearly defined ultimate stress for CPG, where the material is assumed to be infinitely stiff under the condition of CPG [11]. Consequently, EN 408 reports the ultimate strength for CPG by the proportional limit [14].
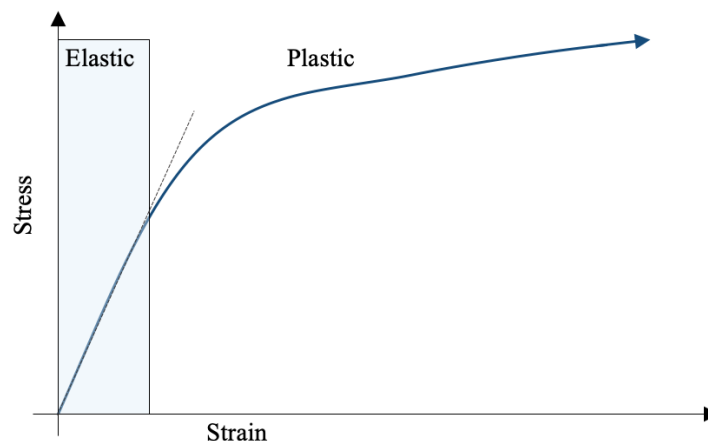
Figure 2.5: Stress-strain timber behavior

2.3   Definition of strength (NS-EN 408)

In Europe, the test method to determine the strength and stiffness of structural timber is given by EN 408. EN 408 includes compression perpendicular to grain as well-defined basic material properties instead of properties related to typical use or applications [15]. The mechanical properties are determined by loading the specimen with a uniformly distributed load over the full surface.

The setup of the test method is shown in Figure 2.6. The contact plates on the top and bottom transfer the load as a uniformly distributed load. The sensors to measure the deflection are located centric within the gauge length, h_t, which is equal to 60 % of the height of the test specimen. The maximum load $F_{c,90,est}$ should be reached within 300 seconds, ± 120 seconds [14].
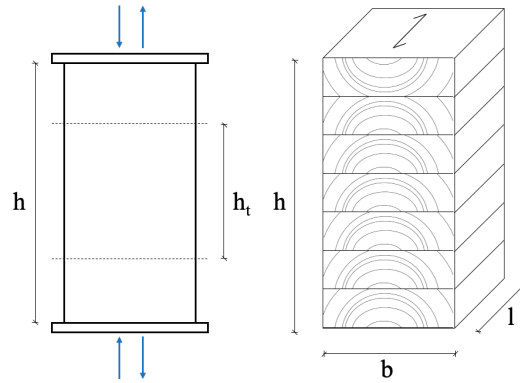
Figure 2.6: Glulam test specimen according to EN 408

The compressive strength, $f_{c,90}$, of the test specimens can be determined from Equation 2.1.

$$f_{c,90} = \frac{F_{c,90,max}}{b \cdot l} \tag{2.1}$$

Where, the value of $F_{c,90,max}$ can be determined by an iterative process where EN 408 describes the procedure as follows:

Estimate a value for the load $F_{c,90,max}$. Use the test results to plot the curve of the deformation due to the applied load; see Figure 2.7. Line 1 refers to the elastic strength of the test specimen. A linear line corresponding to the proportional limit, between 10 % and 40 % of the estimated compressive strength determines line 1. Line 2 is parallel to line 1, with 1 % offset to the gauge length. The intersection between line 2 and the load-deformation curve determine the compressive strength, $F_{c,90,max}$. If the value is within 5 % of the $F_{c,90,est}$ is the value of $F_{c,90,max}$ valid, otherwise, repeat the process until the value is within the 5 % tolerance. Consequently, this method accounts for the differences in elastic stiffness in species [15].
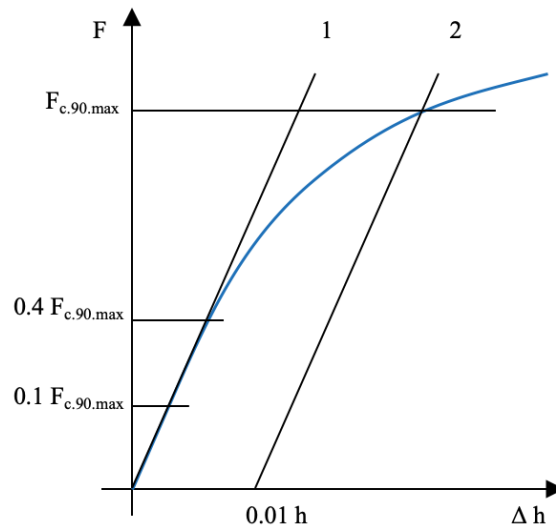
Figure 2.7: Load-deformation curve for compression

2.4 Load dispersion

The capacity of compression perpendicular to the grain depends on the loading area and the length of the unloaded part. Consistent with the yield theory, the stress induced by a load is considered to be distributed over the height of the material [16]. In 1938, Suenson conducted tests to investigate the influence of the unloaded length for non-reinforced members subjected to CPG [17]. The study presents five load cases where the specimen is loaded differently.

- Case A represents the block test, where the whole specimen is loaded. Resulting in uniform compression in the fibers. At the onset of yielding, the deformation will increases greatly with a relatively low enlarging in loading.

- Case B represents the rail test, which is a case where only parts of the specimen are loaded. The load will disperse into the material. The loaded fibers will transfer some of the load to adjacent fibers.

- Cases C, D, and E have a greater unloaded length which will increase the strength and stiffness. This results in higher capacities.
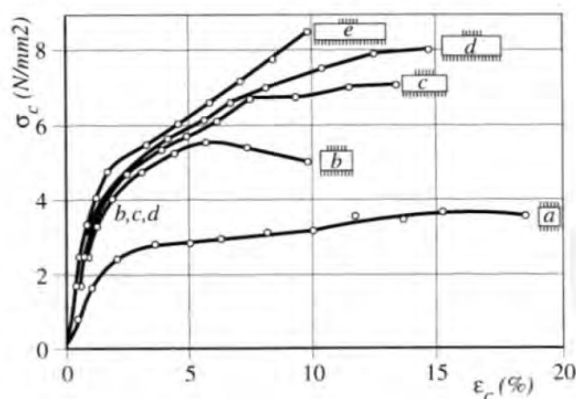
Figure 2.8: Stress-strain curve according to different load cases [17].

Figure 2.8 shows the relationship between strain and stress for different load cases. The test results from Suenson show that the load will disperse, and the unloaded part of the timber will increase the strength and stiffness. The study by Suenson was later confirmed by Reichegger [18].

2.5   Design model of non-reinforced members (NS-EN 1995-1-1)

The design model in the current Eurocode 5 is presented as follows [19]:

$$\sigma_{c,90,d} \leq k_{c,90} \cdot f_{c,90,d} \tag{2.2}$$

Where, $\sigma_{c,90,d}$ is the level of stress given by the effective contact area. $k_{c,90}$ is the factor that accounts for load configuration, the risk of splitting, and the deformation. Generally, this factor is considered equal to 1.0, but for specific support conditions the CPG capacity can be increased. The different support conditions are further specified in the Eurocode 5.

The effective contact area, A_{ef}, account for the contribution of adjacent fibers. An increase of 30 mm of the contact length on both sides of the contact area is recommended. The effective length considers the load distribution of the CPG stress, where the stress distributes to parts of the timber that are not loaded directly.
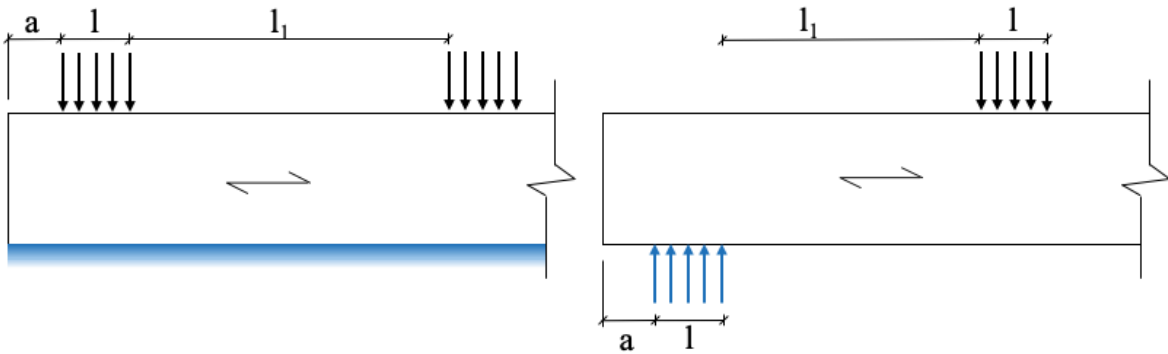
Figure 2.9: CPG according to NS-EN1995-1-1, continuous support and discrete support

See NS-EN 1995-1-1, Eurocode 5 for the full description of the the design model [19].

2.6   Design model of non-reinforced members (prEN 1995-1-1)

In the proposed changes in the consolidated draft, the design model for CPG according to prEN 1995 states that the verification should be as follows [20]:

$$\sigma_{c,90,d} \leq k_p \cdot k_{c,90} \cdot f_{c,90,d} \tag{2.3}$$

Where, $\sigma_{c,90,d}$ is the level of stress given by the contact area. The k_p factor takes into account the material behavior and the deformation perpendicular to the grain. In prEN 1995, k_p is determined by considering the damage or level of deformation allowed for a member. The values for k_p is shown in Table 2.1.

Table 2.1: Values for k_p from prEN 1995, valid for solid timber, glulam, and CLT

Cases	Case A	Case B	Case C
Deformation	2.5 %	10 %	20 %
k_p-factor	1.4	2.1	2.7

$k_{c,90}$ is the load arrangement factor and describes the spreading of the load, calculated according to Equation 2.6. l_c is the contact length of the applied force. l_{ef} is the spreading of the load in an angle of 45 ° in a effective height depending on the support condition. Equation 2.4 and 2.5 presents the effective height, h_{ef}.

Continuous supports:
$$h_{ef} = min\{h; 280mm\} \qquad (2.4)$$

Discrete supports:
$$h_{ef} = min\{0.4 \cdot h; 140mm\} \qquad (2.5)$$

$$k_{c.90} = \sqrt{\frac{l_{ef}}{l_c}} \leq 4.0 \qquad (2.6)$$
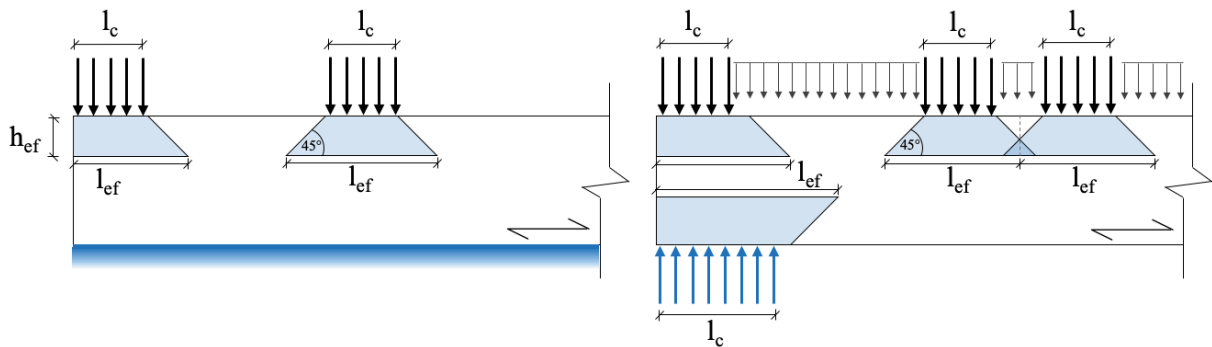
Figure 2.10: CPG according to prEN1995-1-1, load dispersion for continuous and discrete support

See Appendix A, section A.1 for the extract of this section in prEN 1995.

3. Literature review of reinforced members

3.1   General description

The consolidated version, prEN 1995-1-1 (November, 2021) has implemented a section of reinforcement in timber members subjected to CPG. The bearing strength can be increased considerably by reinforcing the member with fully threaded self-tapping screws. The screws can vary in diameter, head, and length. Threads along the whole length will reduce the risk of pushing-in due to the bond between the screws and timber.

3.2   Design model of reinforced members (prEN 1995-1-1)

The design model for characteristic resistance of reinforced members subjected to CPG is presented as follows [20]:

$$F_{c,90,Rk} = \min \begin{cases} k_{c,90} \cdot b_c \cdot l_{ef,1} \cdot f_{c,90,k} + n \cdot \min\{F_{w,k}, F_{c,k}\} \\ b \cdot l_{ef,2} \cdot f_{c,90,k} \end{cases} \tag{3.1}$$

The design model is an evolution of the current model presented in section 2.5 for non-reinforced members. Three failure modes may occur for members subjected to CPG with reinforcement. The design model considers either failure due to withdrawal of the screw, failure due to buckling of the screw, or failure of the timber. The first part of the Equation 3.1 considers the capacity of the reinforced area. The second part considers the capacity of the timber. Withdrawal resistance, $F_{w,k}$, compression resistance, $F_{c,k}$ and, the number of screws, n, give basis to the characteristic resistance of the screws. In section 3.3, the failure modes are further described.

The effective contact length, $l_{ef,1}$, is increased by up to 30 mm. The effective contact length considers that the stress will distribute to adjacent fibers. Furthermore, the load will disperse in the depth of the screws length, given an angle of 45 °. The effective length at the screw tip is defined by $l_{ef,2}$, as shown in Figure 3.1.
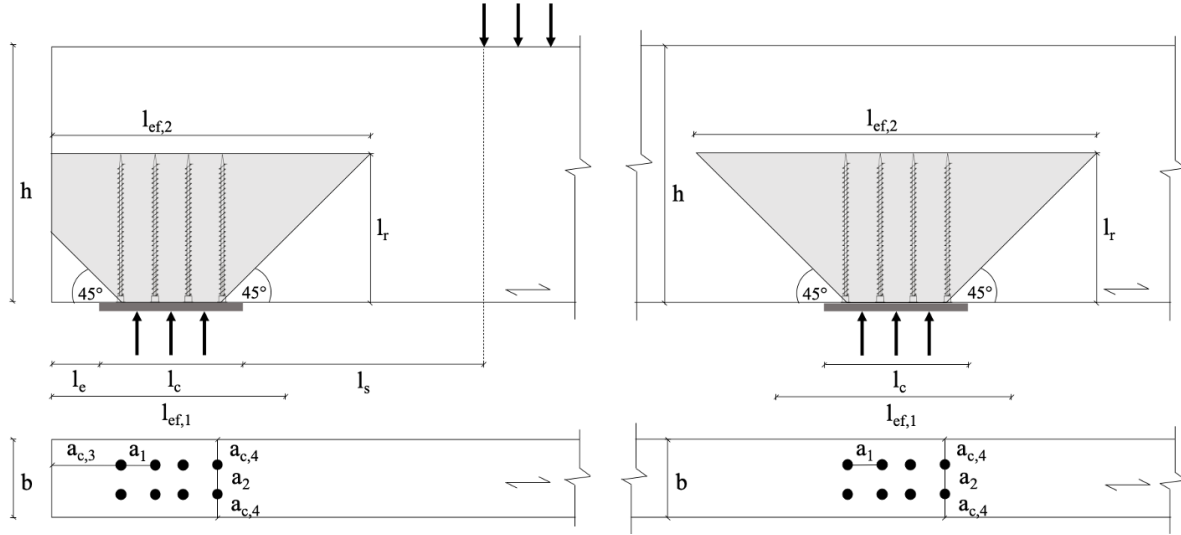
Figure 3.1: Geometry, reinforced members subjected to CPG

See Appendix A, section A.2 for the extract of this section in prEN 1995.

3.2.1   Comments to prEN 1995-1-1

prEN 1995 is a consolidated version and is currently under development to become the new Eurocode 5. Consequently, prEN 1995 is under preparation, which involves a continuous process of inspecting the precision of the model to improve the designer's efficacy. Accordingly, some remarks have been made concerning the presented design model in prEN 1995 of November 2021. The calculations in this study are executed according to the remarks, which are further described.

The effective length and the effective dispersion length for both intermediate and edge supports are given in Equation 3.2 and 3.3.

$$l_{ef,1} = l_c + min\{30mm; l_c\} + min\{30mm; l_c; l_e\} \tag{3.2}$$

$$l_{ef,2} = l_r + (n_0 - 1) \cdot a_1 + min\{l_r; a_{3,c}\} \tag{3.3}$$

In contrast to prEN 1995, the contact length, $l_{ef,1}$, is increased up to 30 mm on both sides within the limit of the support length and distance to the edge. This is grounded in theory presented in Eurocode 5 and Bejtka [5, 19]. Furthermore in this study, the distance to a concentrated load is omitted since a force on the opposite face will not impact the imprint of the load. The appearance of concentrated loads within a distance of 30 mm on the same front is unusual.

The definition of $l_{ef,2}$ is unchanged. However, the Equation 3.3 considers both intermediate and edge supports to improve the efficacy.

For the consideration of the withdrawal resistance, $F_{w,k}$, and compression resistance, $F_{c,k}$, the following sections are applied for the calculated resistances. The sections applies to prEN 1995 dated November 2021.

- $F_{w,k}$ - Section 11.2.3 in prEN 1995 - Withdrawal resistance
- $F_{c,k}$ - Section 11.2.5 in prEN 1995 - Compression resistance

3.3 Failure modes

A study performed by Bejtka and Blass at the University of Karlsruhe considered the behavior of reinforced members subjected to CPG [21]. Through observations of experimental tests, Bejtka and Blass noted three failure modes. The design model in prEN 1995 considers the same failure modes.

3.3.1 Pushing-in of the screw

The first failure mode corresponds the pushing-in capacity of the screws. The exceedance of the bearing resistance leads to penetration of the screws into the timber member. Numerous studies at the University of Karlsruhe have shown that the capacity of pushing-in is equal to the withdrawal capacity. This failure mode occurs mainly with the use of short screws [5]. The withdrawal capacity, $F_{w,k}$, is determined by the following Equation 3.4.

$$F_{w,k} = \pi \cdot d \cdot l_w \cdot f_{w,k} \tag{3.4}$$

Where, l_w is the anchorage depth and d is the outer thread diameter of the screw. The characteristic withdrawal strength, $f_{w,k}$, is calculated as follows:

$$f_{w,k} = 8.2 \cdot k_w \cdot k_{mat} \cdot d^{-0.33} \cdot (\frac{\rho_k}{350})^{k_\rho} \tag{3.5}$$

The formula accounts for number of penetrated layers, where the capacity can increases by a factor k_{mat}. For glulam is the factor k_w equal to 1.0. In the case with screws perpendicular to the grain is the k_ρ equal to 1.10.

See Appendix A, section A.3 for the extract of the withdrawal resistance according to prEN 1995.

3.3.2 Buckling of the screw

The second failure mode occurs due to the compressive resistance of the screw. Pure compressive pressure along the screw's axis can result in instability. As a result of instability, the screws will fail due to buckling. The failure mode occurs mainly for long and slender screws. The characteristic buckling capacity, $F_{c,k}$ is calculated according to Equation 3.6.

$$F_{c,k} = 1.18 \cdot \kappa_c \cdot N_{pl,k} \tag{3.6}$$

Where, the κ_c is the buckling factor. The buckling factor accounts for the relative slenderness of the screw. The $N_{pl,k}$ is the characteristic yield capacity of the screw, and is calculated as follows:

$$N_{pl,k} = \pi \cdot \frac{d_1^2}{4} \cdot f_{y,k} \tag{3.7}$$

The Equation 3.7 considers the inner thread diameter, d_1, and the characteristic yield strength, $f_{y,k}$. See Appendix A, section A.4 for the extract of the compression resistance according to prEN 1995.

3.3.3   Failure of timber

The third failure mode occurs due to the failure of the timber at the screw tips. The characteristic of this failure mode is lateral expansion perpendicular to the grain and results in cracks at the point of the screw tip. The characteristic capacity of timber at the screw tip is according to Equation 3.8:

$$F_{c,90,k} = b \cdot l_{ef,2} \cdot f_{c,90,k} \tag{3.8}$$

This failure mode is observed by Bejtka with small loading areas, and short screws [5]. At the end of the screw, the force is transferred to the timber. The maximum pressure in the timber emerges at the screw tip and depends on the effective dispersion length and width. The effective length depends on the screws length, the screw arrangement, and the design situation, see Figure 3.1.

3.4 Preliminary investigation

3.4.1 General introduction

In an article by Leijten, he investigated different proposed design models for CPG without reinforcement and presented nine load cases, shown in Figure 3.2 [16]. These load cases distinguish the different loading types related to design situations, with the exception of load case A. Load case A is a standard test specimen according to EN 408. In the following sections, load cases are referred to as presented by Leijten.
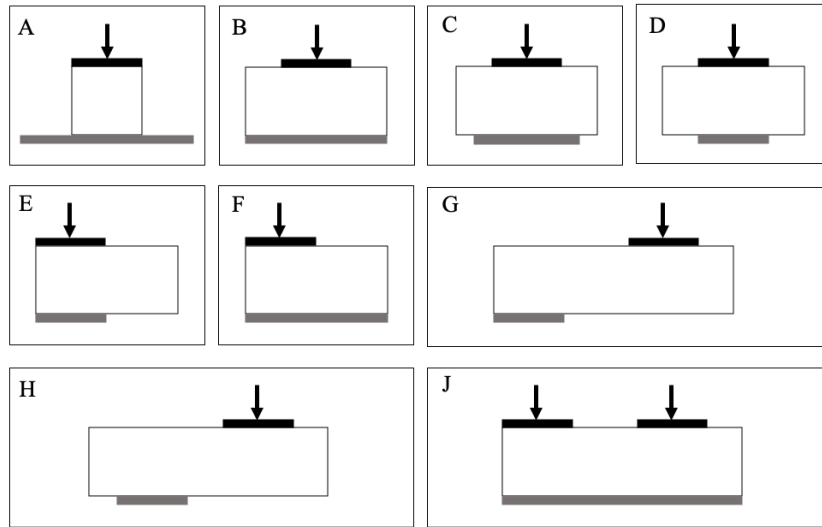
Figure 3.2: Load cases [16]

Further, to describe the design model abbreviation is applied. Therefore, A_1 is the capacity corresponding to the failure of the screw. A_{11} and A_{12} describe the contribution from the timber and the screws, respectively. Accordingly, A_2 is the capacity related to the failure of the timber at the tip of the screw. The abbreviation is stated in Equation 3.9.

$$F_{c,90,Rk} = \min \begin{cases} k_{c,90} \cdot b_c \cdot l_{ef,1} \cdot f_{c,90,k} + n \cdot \min\{F_{w,k}, F_{c,k}\} \\ b \cdot l_{ef,2} \cdot f_{c,90,k} \end{cases} = \min \begin{cases} A_{11} + n \cdot A_{12} & = A_1 \\ A_2 \end{cases} \quad (3.9)$$

3.4.2 Dietsch

In 2019, Philipp Dietsch performed a study investigating the use of self-tapping screws as reinforcement in timber [22]. The study aimed to apply screws with an overlap. Additionally, the study presents a numerical analysis of CPG with single-sided reinforcement.

The numerical investigations confirmed the effective length, $l_{ef,2}$. The model indicates that the stress along the effective length varies considerably, where a stress concentration occurs at the tip of the screws. The level of stress is shown in Figure 3.3. However, the stress concentration will be compensated by stress redistribution due to the elastic-plastic behavior of the mechanical properties of timber [22].
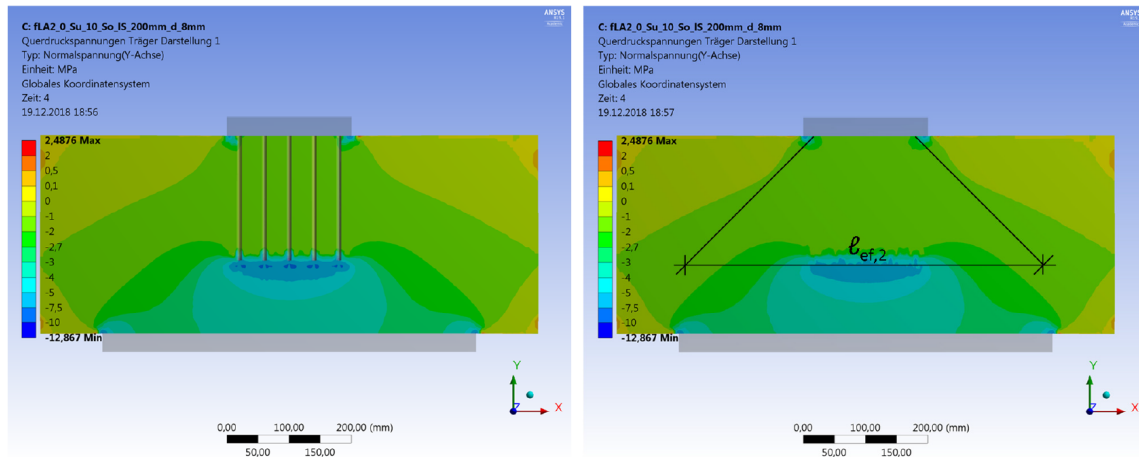
Figure 3.3: Dietsch, Stress distribution of reinforced members [22]

Figure 3.4 displays the distribution of stress in a horizontal plane along $l_{ef,2}$ with screw group of four, six, and ten screws. The Figure 3.4 shows how the stress increase around the screw tips. The study concludes with a recommendation for the use of screws with overlap to transmit the stress concentration efficient.
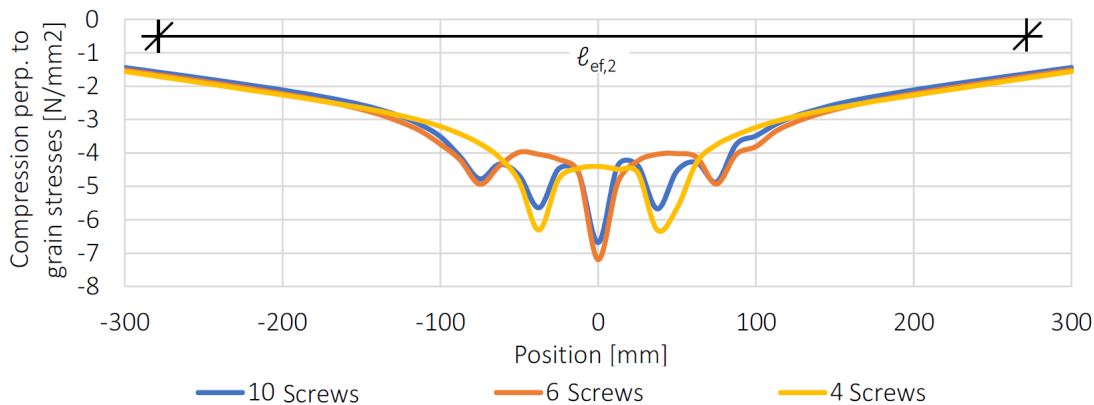
Figure 3.4: Dietsch, Distribution of the stress along $l_{ef,2}$ at the screw tips [22]

3.4.3   Karlsruhe

In 2005, Bejtka wrote Volume 2 of the series of Karlsruhe reports in Timber Engineering, considering CPG with reinforcement of timber components with fully threaded screws [5]. During this work, Bejtka studied the failure mechanisms, the influence of the screws, and produced laboratory tests to verify the increase of capacity with reinforcement.

Studying the test result of Möhler/Freiseis and Colling, including his own result, Bejtka observed three failure modes. The characteristic of these failure modes are the following:

1. Failure caused by the screws being pushed into the member, withdrawal

2. Failure caused by buckling of the screws

3. Failure caused by the CPG strength of the timber at the tip of the screw.

These failure modes are described in detail in section 3.3.

Bejtka carried out tests with and without reinforcement in the Karlsruhe report. Table 3.1 shows the geometry of test specimens, screws, and the result with a corresponding increase in capacity compared with the non-reinforced test specimen.

Table 3.1: Results form the Karlsruhe report [5]

Name	Specimens		Screws			Contact area		Test result	
	Width	Height[a]	d	l_r	n	b_c	l_c	$F_{c,90,k}$	[%]
A_ohne_1	100	-	-	-	-	100	80	43.2	-
A_7_2	100	-	7.5	180	2	100	80	77.5	79 %
A_8_2	100	-	8	340	2	100	80	92.0	113 %
A_10_2	100	-	10	200	2	100	80	104.0	141 %
A_7_4	100	-	7.4	180	4	100	120	126.0	192 %
A_10_4	100	-	10	200	4	100	120	133.0	208 %
A_ohne_2	120	540	-	-	-	120	90	57.1	-
A_6_6	120	540	6.5	160	6	120	90	132.0	131 %
D_ohne_1	100	-	-	-	-	100	80	46.0	-
D_7_2	100	-	7.5	180	2	100	80	96.1	109 %
D_8_2	100	-	8	340	2	100	80	98.0	113 %
D_10_2	100	-	10	200	2	100	80	104.0	126 %
D_7_4	100	-	7.5	180	4	100	120	127.0	176 %
D_8_4	100	-	8	340	4	100	120	169.0	267 %
D_10_4	100	-	10	200	4	100	120	173.0	276 %
D_ohne_2	120	240	-	-	-	120	90	56.4	-
D_7_6	120	220	7.5	180	6	120	90	195.0	245 %
D_8a_6	120	300	8	260	6	120	90	228.0	304 %
D_8b_6	120	480	8	400	6	120	90	242.0	329 %

[a] Not reported specimen height corresponds to either 540 mm or 1000 mm

A significant increase can be accomplished with a minimum of effort. The test result shows that the capacity of CPG can be increased up to 329 % by applying reinforcement. The capacity is achieved with six screws with dimension of 8 x 400 mm. It is possible to increase the capacity further by using several screws. The screws enables an increase in effective stiffness in the perpendicular direction to the grain. This may also reduce the deformation of the supports.

In the report of Karlsruhe, Bejtka performed an analytical test with the program Ansys concentrating on the behavior of the screw. A design model for reinforced members was developed from the analytical and experimental test results. The design model is presented as the Model of Karlsruhe in Equation 3.10 [5].

$$F_{c,90,Rk} = \min \begin{cases} k_{c,90} \cdot b_c \cdot l_{ef} \cdot f_{c,90,k} + n \cdot R_{S,k} \\ b \cdot l_{ef,2} \cdot f_{c,90,k} \end{cases}$$ (3.10)

Where:

$$R_{S,k} = \min \begin{cases} R_{ax,k} = d \cdot l_s \cdot f_{ax,k} \\ R_{c,k} = \kappa_c \cdot N_{pl,k} \end{cases}$$ (3.11)

The design model for reinforced members presented in prEN 1995 is based on this approach. However, there is a deviation regarding the definition of some parameters. In the model of Karlsruhe the following parameters differs:

- l_{ef}
  $$l_{ef} = l_c + 30 + \min \{30 \, mm \, ; \, l_e\}$$

- $R_{ax,k}$
  Different design approach compared to prEN 1995, based on numerical analysis with a different approach for the characteristic withdrawal strength parameter.

- $R_{c,k}$
  Different design approach, based on numerical analysis and are derived based on a tabulated value for the critical load. Depends on the screws length in contrast to prEN 1995.

Additionally, Bejtka evaluate the calculations in relation to the test result with the characteristic and mean strength perpendicular to grain, $f_{c,90,k} = 3.0 \, N/mm^2$ and $f_{c,90} = 5.0 \, N/mm^2$. The predicted capacity is minor compared to the test results when applying $f_{c,90,k} = 3.0 \, N/mm^2$. However, better correlation is observed with $f_{c,90} = 5.0 \, N/mm^2$. The strength properties perpendicular to grain is derived from the the test result [5].

See Appendix A, section A.5 for a extract of the Karlsruhe report for detailed approach.

3.4.4 Nilsson

In 2002, Karin Nilsson wrote a master thesis with the aim to investigate the influence of members subjected to CPG with reinforcement [23]. To give answers to the study, Nilsson performed experimental tests. Multiple test glulam specimens with the dimension of 500 x 90 x 315 mm (length x width x height) are loaded. The screw used as reinforcement is SFS WT-T 8.2, where the length of the screws varies. The load situation is the torx and load case B, where the tests are performed with either one, four, six, or eight screws. In the torx test the performance of one screw is evaluated.

First, Nilsson performed tests where the screws are directly loaded at the screw head with a torx socket. The screws had different lengths, 160 mm, 220 mm, and 300 mm. The aim is to investigate the influence of one screw. Since the screw is directly loaded, the impact of the timber capacity is neglected. According to the obtained test results, the screw with a length of 220 mm gave the highest capacity.

Further, tests with varying screw arrangements are performed. The aim is to find a relationship between the number of screws and bearing strength. The group of screws is loaded through a steel plate with dimensions 90 x 150 x 10 mm or a timber plate with dimensions 90 x 150 x 16 mm. The failure modes described are due to the timber, either expansion near the contact plate or near the screws tip [23] , see Figure 3.5. Nevertheless, the magnitude of the expansion is not reported in the thesis. In addition, the test specimen is not split in proportion to assess the failure mechanism of the screw.
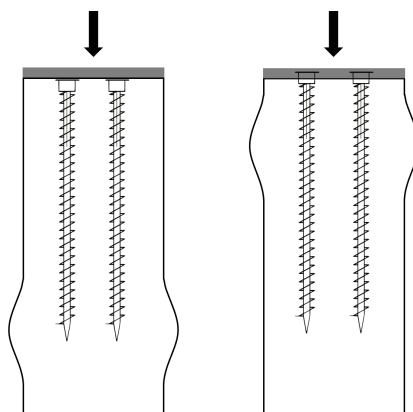
Figure 3.5: Nilsson, Expansion of timber with steel plate (left) and timber plate (right) [23].

Figure 3.6 shows the deformation curve of specimens with a steel plate and different numbers of screws. The deformation is measured with external sensors.
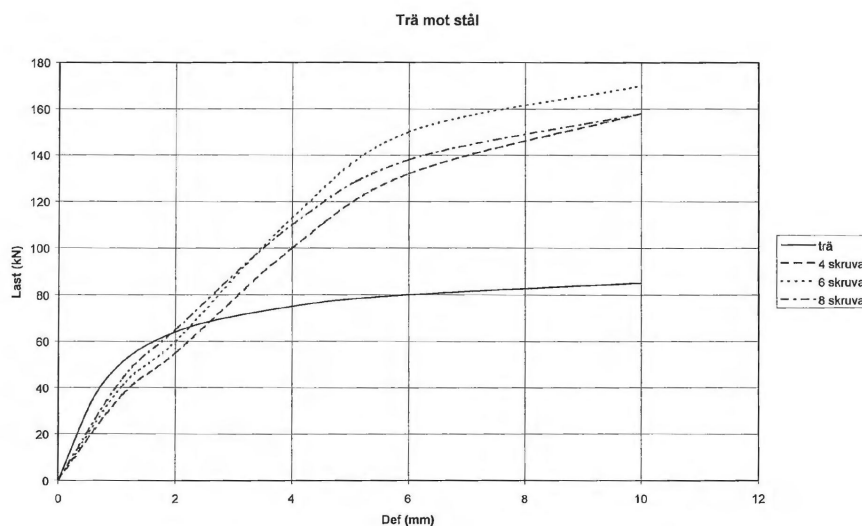
Figure 3.6: Nilsson, Load-displacement curve of non-reinforced, 4, 6 and 8 screws[23]

The capacity of each specimen is based on the procedure in EN 408. The maximum strength is measured at the intersection between the deformation curve and a parallel line to the curve with an offset according to 1 % of the gauge length. Given in Table 3.2, the properties and bearing strength is presented.

Table 3.2: Summary of capacities from tests performed by Nilsson [23]

Type	Specimen			Screws			Loading area		Test results	
	Length	Width	Height	d	l_r	n	b_c	l_c	Force [kN] Steel plate	Force [kN] Timber plate
Non-reinforcement	500	90	315	-	-	-	90	150	76	86
4 WT-T 8.2x220	500	90	315	8.2	190	4	90	150	141	96
6 WT-T 8.2x220	500	90	315	8.2	190	6	90	150	159	98
8 WT-T 8.2x220	500	90	315	8.2	190	8	90	150	140	108

The study concludes that using four screws as reinforcement and a steel plate as a contact plate is a sufficient method to increase the capacity for members subjected to CPG. However, the use of six screws gave higher capacity. Additionally, Nilsson observed that the capacity was almost similar by increasing the number of screws to eight. Nevertheless, when using a wooden plate as a contact plate, the use of eight screws is most efficient.

3.4.5   Reichegger

In 2004, Michael Reichegger performed a study considering the effect of self-tapping screws for members subjected to CPG [18]. The study concerns experimental tests and a comparison of test results against the design model of Karlsruhe. Furthermore, tests of non-reinforced members are executed with the aim of evaluating the effect of reinforcement regarding the capacity.

Glulam of spruce is applied in tests with strength class GL 24h according to EN 1194, where the compressive strength is $f_{c,90,k} = 2.7 \ N/mm^2$. The test specimens had dimensions of 400 x 120 x 200 mm and 600 x 120 x 400 mm (length x width x height). The test is executed according to load case B. The load is introduced through plates of steel or timber with dimensions of 80 x 120 and 120 x 120 mm, respectively. The timber contact plate is in strength class GL 24h. Two types of screws are applied: SFS WT-T and SPAX-S. The spacing of the screws is based on the recommended spacing in the ETA (European Technical Assessment).

Figure 3.7 shows the average stress-strain curve for non-reinforced and reinforced specimen, along with the different types of screws. The blue curve represents the non-reinforced specimens. Figure 3.7 a) represents the specimen with dimensions 400 x 120 x 200 mm, while Figure 3.7 b) is the 600 x 120 x 400 mm.

The determination of the compressive capacity of the non-reinforced and reinforced test specimens is based on EN 1193, which is the same procedure described in EN 408. Furthermore, the study compares the test result to the model of Karlsruhe. Table 3.3 shows properties and the comparisons of each test. From the tests, buckling of screws and withdrawal are recognized as failure mechanisms. In the case of the timber plate, the screws are sunk into the contact plate. With a steel plate, the capacity is increased by 33 % to 167 %. By applying a timber plate increases the capacity with 3 % and 124 % for WT-T 6.5 x 130 mm and SPAX-S 8 x 200 mm screws, respectively.
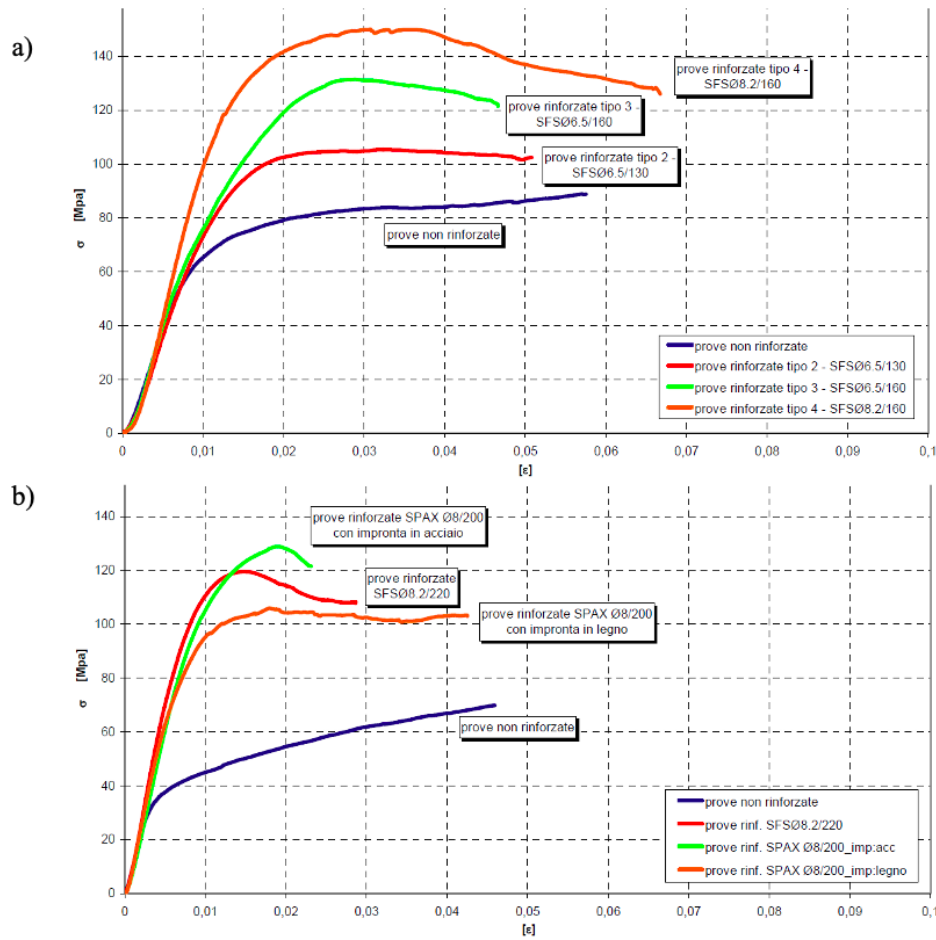
Figure 3.7: Reichegger, Stress-strain curves [18]

Table 3.3: Summary of capacities from tests performed by Reichegger, reinforced and non-reinforced members [18]

Type	Specimen			Screws			Loading area			Test results		Karlsruhe model
	Length	Width	Height	d	l_r	n	b_c	l_c	Plate	Force [kN]	Increase [%]	GL24h
Non-reinforcement	400	120	200	-	-	-	120	90	S/T	76.3	-	-
WT-T 6.5x130	400	120	200	6.5	80	4	120	90	S	101.5	33%	86.4
WT-T 6.5x160	400	120	200	6.5	130	4	120	90	S	123.7	62%	95.6
WT-T 8.2x160	400	120	200	8.2	130	4	120	90	S	136.3	79%	104.3
WT-T 6.5x130	400	120	200	6.5	80	4	120	90	T	78.7	3%	86.4
Non-reinforcement	600	120	400	-	-	-	120	120	S/T	65.7	-	-
WT-T 8.2x220	600	120	400	8.2	190	4	120	120	S	173.1	163%	141.4
SPAX-S 8x200	600	120	400	8.0	200	4	120	120	S	175.8	167%	136.2
SPAX-S 8x200	600	120	400	8.0	200	4	120	120	T	147.3	124%	136.2

The study of Reichegger validates the accuracy of the first part of the Karlsruhe model, accordingly, the capacity related to the screws. The predicted failure is in agreement with the failure in the executed test. Regarding the comparison of reinforced and non-reinforced members, it is stated that the use of screws increases the capacity considerably for members subjected to CPG.

3.5 Comparisons of design model and test results

This section presents a comparison between the design model in prEN 1995 and the test results obtained from earlier investigations.

Nilsson and Reichegger transfer the load by either a steel or timber plate, while Bejtka transfer the load with solely a steel plate. With a steel plate is the force evenly distributed over the surface of the timber's contact area and the screw heads. In the case of a timber plate is the screws penetrating the timber plate, and the increase of capacity due to reinforcement may not occur [5]. Due to the performance, the timber plate is omitted in the comparison.

3.5.1 Karlsruhe

The comparison between the design model and the average load-carrying capacity obtained by test results is shown in Table 3.4. There is a great deviation between the test results obtained by Bejtka and the predicted load-carrying capacity by the design model. The load configuration considered are load cases H and C, indirect, and direct load arrangement, respectively. The spacing between the load and the support is less than two times the height for load case H. Accordingly, $k_{c,90}$ is considered equal to 1.0 for both cases.

Table 3.4: Karlsruhe, comparison of the test results and design model

Name	Load case	Test results		Design model		Deviation
		Force [kN]	Failure mode	Force [kN]	Failure mode	
A_7_2	H	77.5	-	55.0	A_2	29 %
A_8_2	H	92.0	-	65.7	$A_1 \{F_{c,k}\}$	29 %
A_10_2	H	104.0	-	60.0	A_2	42 %
A_7_4	H	126.0	-	65.0	A_2	48 %
A_10_4	H	133.0	-	70.0	A_2	47 %
A_6_6	H	132.0	A_2	66.0	A_2	50 %
D_7_2	C	96.1	-	71.5	$A_1 \{F_{c,k}\}$	26 %
D_8_2	C	98.0	-	73.2	$A_1 \{F_{c,k}\}$	25 %
D_10_2	C	104.0	-	88.5	$A_1 \{F_{w,k}\}$	15 %
D_7_4	C	127.0	-	100.0	A_2	21 %
D_8_4	C	169.0	-	121.5	$A_1 \{F_{c,k}\}$	28 %
D_10_4	C	173.0	-	110.0	A_2	36 %
D_7_6	C	195.0	A_2 / $A_1 \{F_{w,k}\}$	117.0	A_2	40 %
D_8a_6	C	228.0	$A_1 \{F_{c,k}\}$	165.0	A_2	15 %
D_8b_6	C	242.0	$A_1 \{F_{c,k}\}$	168.0	$A_1 \{F_{c,k}\}$	14 %

The failure mode obtained in the tests is only reported for the performed preliminary tests. The failure mode reported by Bejtka for configuration D_8a_6 is buckling, while the design model predicts failure due to the timber. Otherwise, the failure modes reported correspond to the failure modes predicted by the design model.

The test results and the calculated capacities according to A_1 and A_2 are shown in the figures below. Figure 3.8 presents load case C, and Figure 3.9 presents load case H. The highest capacity is achieved with six screws or four screws with a diameter of 10 mm. The significant variation in capacity is due to the different use of length and diameter of the screw.
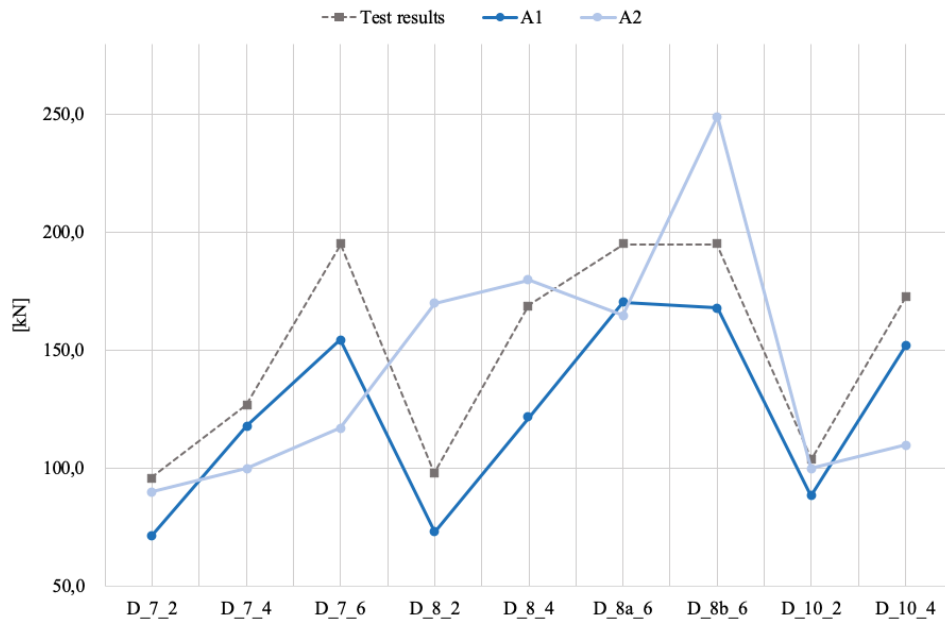
Figure 3.8: Bejtka, Test results, A_1 and A_2 presented in graph, load case C

Figure 3.8 shows that A_1 and the test results have the same tendency. However, for all configurations, the capacity according to A_1 is lower than the test results. In most cases A_2 is greater than A_1. In section 3.4, Bejtka states that the best correlation according to the Karlsruhe model is achieved by applying $f_{c,90,k} = 5.0 \ N/mm^2$. The design model in prEN 1995 is based on properties given in NS-EN 14080. The compressive strength, $f_{c,90,k}$ is equal 2.5 N/mm^2, and there is a consistent deviation, with an average value of 24 %.
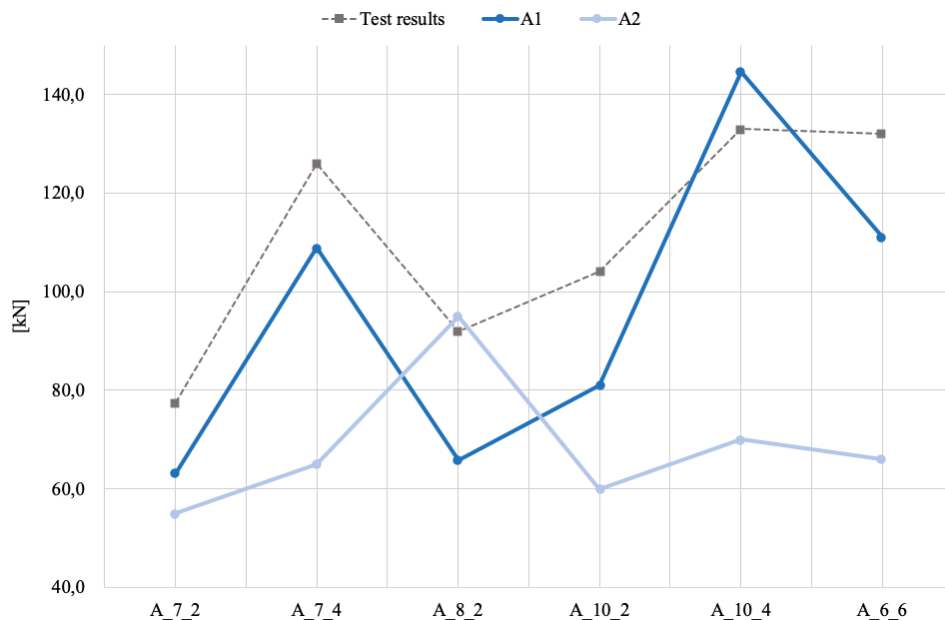
Figure 3.9: Bejtka, Test results, A_1 and A_2 presented in graph, load case H

Figure 3.9 presents load case H. In general, the achieved force and predictions are lower compared to load case C. Hence, the same tendency is observed for load case H regarding A_1. A_2 has an overall lower capacity than A_1. In contrast to load case C, the load dispersion is reduced considerably. This is caused by the support condition, since the member is loaded near the edge.

3.5.2   Nilsson

A comparison of the design model and the test results obtained by Nilsson is shown in Table 3.5. The predicted failure modes are according to A_2 for all configurations. Since the specimens are not splitted, the failure mode according to tests are omitted. The predicted capacity in the design model is consistent lower. According to the table, the mean deviation is 27 %. For the test configuration of eight screws, the capacity is lower than the configuration with six screws. However, the recommended minimum spacing is not satisfied. Accordingly, the risk of splitting increases and may results in a reduction in the capacity.

Table 3.5: Nilsson, comparison of the test results and design model

Name	Load case	Test results		Design model		Deviation
		Force [kN]	Failure mode	Force [kN]	Failure mode	
4 WT-T 8.2x220	B	141	-	102	A_2	27%
6 WT-T 8.2x220	B	159	-	108	A_2	32%
8 WT-T 8.2x220	B	140	-	108	A_2	23%

The test result and the design model is shown in Figure 3.10. The capacities according to A_1 are greater than A_2. The figure shows that A_1 varies linearly with the number of screws. For A_2, the capacity is equal for six and eight screws. The screw spacing and the number of screws parallel to the grain are equal. Consequently, the effective spreading length is mutual.
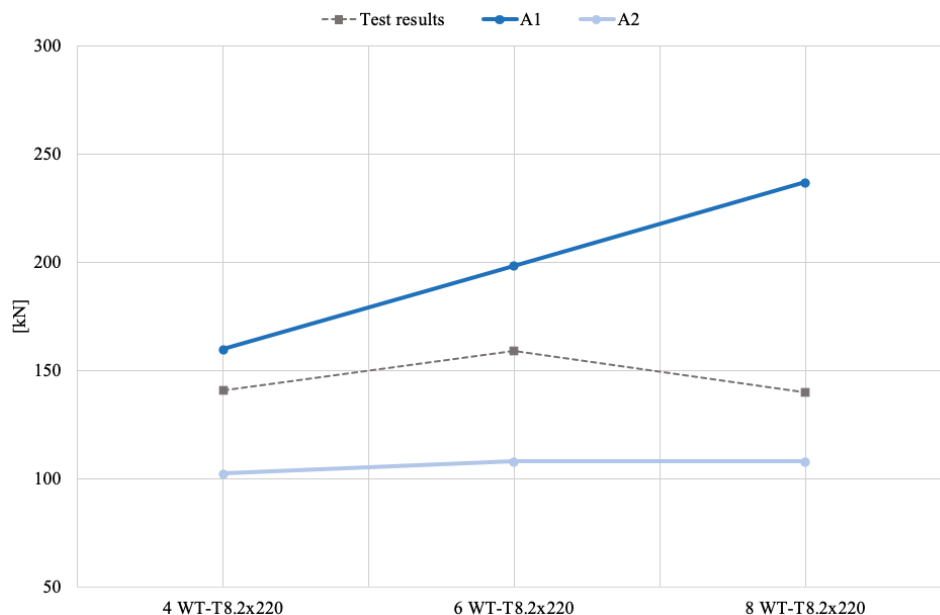
Figure 3.10: Nilsson, Test results, A1 and A2 presented in graph

Stated in subsection 3.4.4, the load situation presented is load case B. A_2 is the decisive capacity and is consistent lower for all configurations. Compared to the test results is the design model conservative. There is a greater gap between the A_1 and A_2. This gap occurs due to the consideration of the $k_{c,90}$ factor. In A_1 is $k_{c,90}$ equal to 1.75, whilst for A_2, $k_{c,90}$ is not considered.

3.5.3 Reichegger

In the study by Reichegger, the conducted tests achieve failure in the screws caused by either buckling or withdrawal. Table 3.6 shows the test results and the predictions according to the design model. According to the table is the decisive capacity due to A_2. The mean deviation between the predictions and the test results is 26 %.

Table 3.6: Reichegger, comparison of the test results and design model

Name	Load case	Test results		Design model		Deviation
		Force [kN]	Failure mode	Force [kN]	Failure mode	
SFS WT-T 6.5 x 130	B	101.5	$A_1 \{F_{w,k}\}$	57.0	A_2	44 %
SFS WT-T 6.5 x 160	B	123.7	$A_1 \{F_{w,k}\}$	88.0	A_2	29 %
SFS WT-T 8.2 x 160	B	136.3	$A_1 \{F_{w,k}\}$	90.3	A_2	34 %
SFS WT-T 8.2 x 220	B	173.1	$A_1 \{F_{c,k}\}$	126.3	A_2	27 %
SPAX-S 8 x 200	B	175.8	$A_1 \{F_{c,k}\}$	132.0	A_2	25 %

Figure 3.11 gives an overview of A_1 and A_2 in relation to the test results. The figure shows a good correlation between the test results and A_1. However, according to the design model, A_2 is the decisive capacity and is consistent lower.
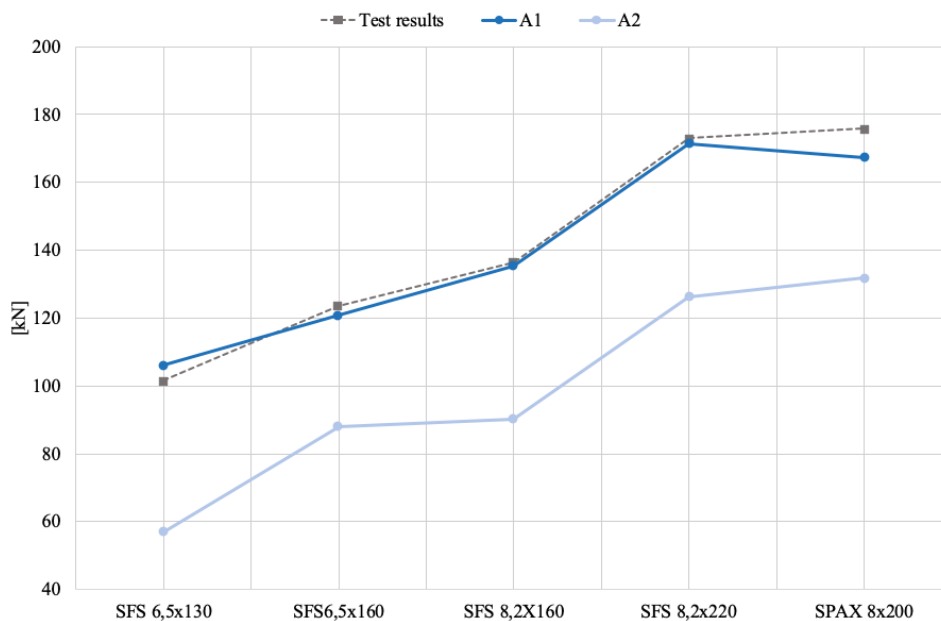
Figure 3.11: Reichegger, Test results, A1 and A2 presented in graph

The capacities for one screw are presented in Figure 3.12. The decisive capacity of the screws is accordingly the minimum of buckling and withdrawal. The predicted failure mode of WT-T 6.5 x 130 and WT-T 8.2 x 160 is withdrawal. This may be attributed to the fact that the screws are less slender due to the ratio of diameter and the effective screw length. The remaining screws fail due to buckling as a result of increasing length. As seen from the figure, the predicted failure mode corresponds to the failure of the test results, with the exception of SFS WT-T 6.5 x 160.
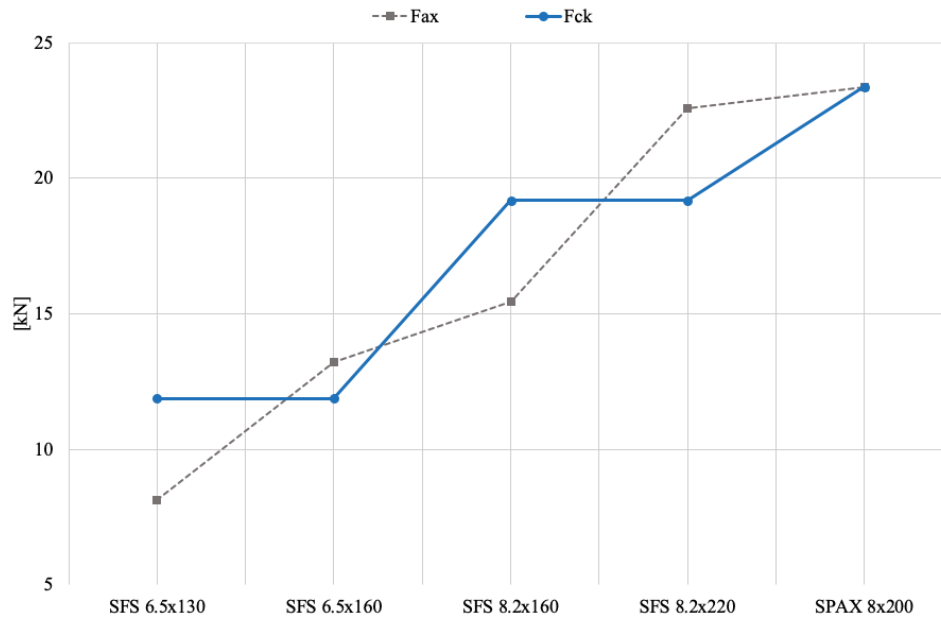
Figure 3.12: Reichegger, Withdrawal and buckling capacity for the screws

Finally, the study does not achieve failure corresponding to A_2 in the tests. Therefore, the design model's predictions result in inaccuracies corresponding to both the magnitude of capacity and the failure mode. However, A_1 is assumed to be very accurate and reliable based on the comparison.

3.5.4 Summary

The comparison between the test results by Nilsson and Reichegger shows a consistent lower predicted capacity. According to the design model failure occurs due to A_2. The mean capacity in Nilsson and Reichegger is approximately 27 % and 26 % too low, respectively. According to the comparison between the test by Bejtka and the design model, the capacity according to load case C is consistent lower. The design model shows that the failure mainly occurs in the screws. Similar for load case H, the capacity is lower, but the failure is mainly due to the timber.

The comparison of A_1 and the test results by Reichegger shows a good correlation. Nevertheless, the tendency of A_1 corresponds to the test results by Bejtka and Nilsson, but a deviation in capacity is observed.

In general, by reviewing previous literature with respect to the design model presented in prEN 1995, the prediction has a potential for improvement. Even though the predictions are adequate for some configurations, there is a substantial unfavorable deviation in some situations between the decisive capacity and the test result.

4. Sensitivity study

4.1 Introduction

This section concerns a sensitivity study of the design models for CPG. The aim is to determine the sensitivity of the parameters in the design model, i.e., how the capacity changes with different dimensions. In 2019, the CEN committee compared two models proposed for the Eurocode 5, considering non-reinforced members. The sensitivity study analyzed two approaches by Leijten or Blass, where the member's height and the implementation length varied. The study gives information on how the geometrical parameters of timber improve the capacity [24]. However, the design model for CPG presented in prEN 1995 is a modified approach by Leijten. The following sections describe a similar study with the approaches presented in prEN 1995 for non-reinforced and reinforced members. The study covers load cases B and C, see Figure 3.2. The varying properties are either geometrical parameters of the timber or the screws. The dimensions considered reflect the experimental work described in chapter 5.

4.2 Load-bearing capacity of non-reinforced members

The sensitivity analysis of the load-bearing capacity of non-reinforced members concerns varying contact length and height. The contact length is varied between 20 mm and 300 mm, while the height is varied between 20 mm and 1200 mm. The width and total length are constant and are equal to 140 mm and $(2000 + l_c)$ mm, respectively. The characteristic properties of GL 30c are applied in the analysis. The geometrical description of load cases B and C is shown in Figure 4.1.
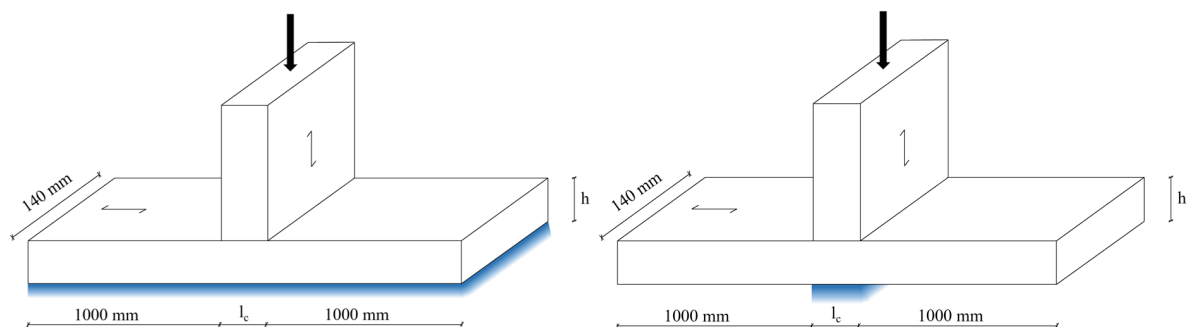
Figure 4.1: Non-reinforced members, description of the geometry load case B and load case C

The design model is described in section 2.6. Figure 4.2 displays the bearing capacity corresponding to 1.0 %, 2.5 %, and 10 % deformation. The design model considers a non-linear increase in capacity with increasing deformation. The increase is significantly higher between 2.5 % and 10 % deformation, compared to 1.0 % and 2.5 % deformation. For the 1.0 % deformation the material behavior factor, k_p, is equal to 1.0. For 2.5 % and 10 %, k_p is equal to 1.4 and 2.1, respectively [20].
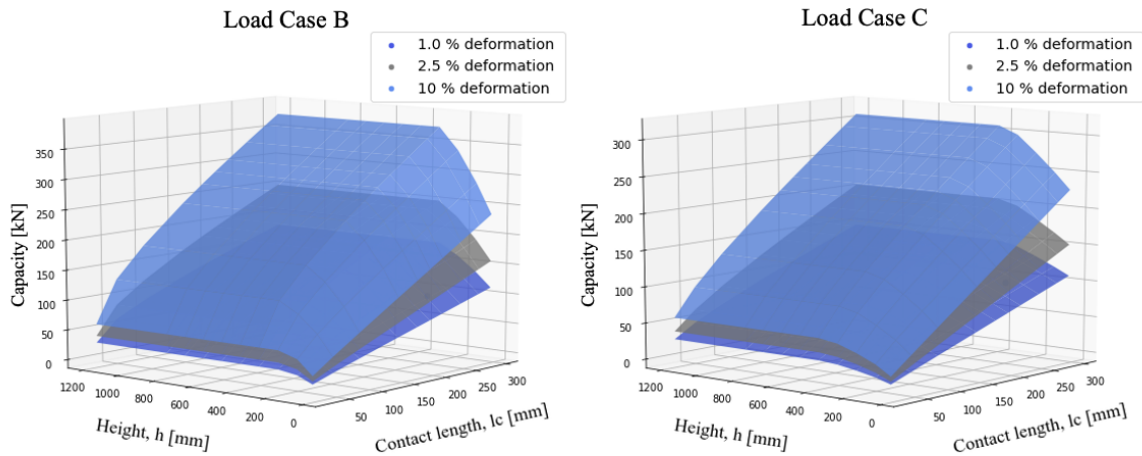
Figure 4.2: Non-reinforced members, bearing capacity for load case B and C

The difference between the two load cases is the load condition, which impacts the load arrangement factor, $k_{c,90}$. According to section 2.6 of non-reinforced members, load case B is considered as a continuous support. The load arrangement factor depends on the load dispersion due to the effective height and contact length. Discrete support limits the effective height to 140 mm, while continuous supports are limited to 280 mm. Consequently, the discrete supports have a lower $k_{c,90}$ factor. In the event of discrete support, the beam will additionally deforms due to the bending. This will have an impact on the load-bearing capacity. Hence, the load-bearing capacity is greater for load case B compared to load case C.

The limit of the effective height is confirmed in Figure 4.2. There is a significant increase in capacity in load case B until the height of 280 mm is reached. After this point, the resistance is constant considering increasing height. By increasing the contact length, the capacity increases linearly. The increase in capacity is steeper for load case B compared with load case C. For load case C, the member's height is reduced by employing $0.4 \cdot h$ until the limit is reached. Furthermore, load case C has the same tendency, but the enhancement of the capacity is reached at a minor member height.

Appendix B, and section B.1 gives fulfilled elaboration of the load-bearing capacity of non-reinforced members.

4.3   Load-bearing capacity of reinforced members

The sensitivity analysis of the design model applied to reinforced members concerns varying screw length and diameter. The reason for choosing these parameters as variables is their impact on the capacity. Both the diameter and length will affect the screw capacity, A_1, while A_2 is affected by the screw length. The screw length varies between 80 mm to 500 mm. The diameter follows the recommendations given by the standard, where it varies from 6 mm to 12 mm. Other parameters, such as contact length, member height, screw distance, and the number of screws, are considered constant. Characteristic values are used, and the material considered is GL 30c. The geometrical description of the setup for load cases B and C is shown in Figure 4.3.
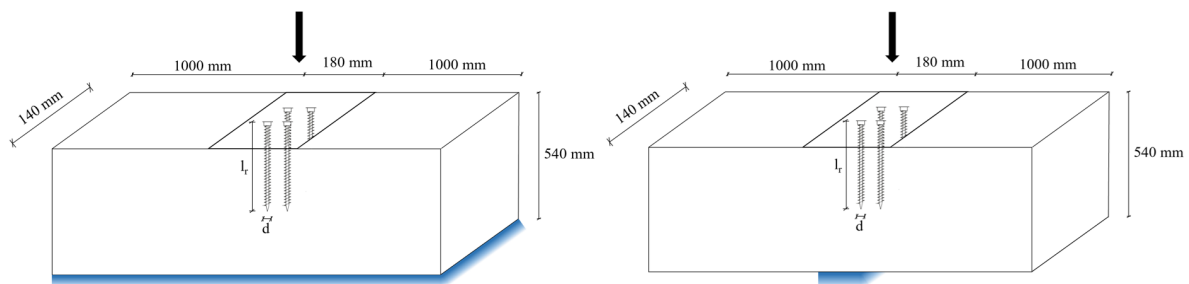
Figure 4.3: Reinforced members, description of the geometry load case B and load case C

The design model for reinforced members is presented in section 3.2. Figure 4.4 displays bearing capacity, which corresponds to the minimum of A_1 and A_2.
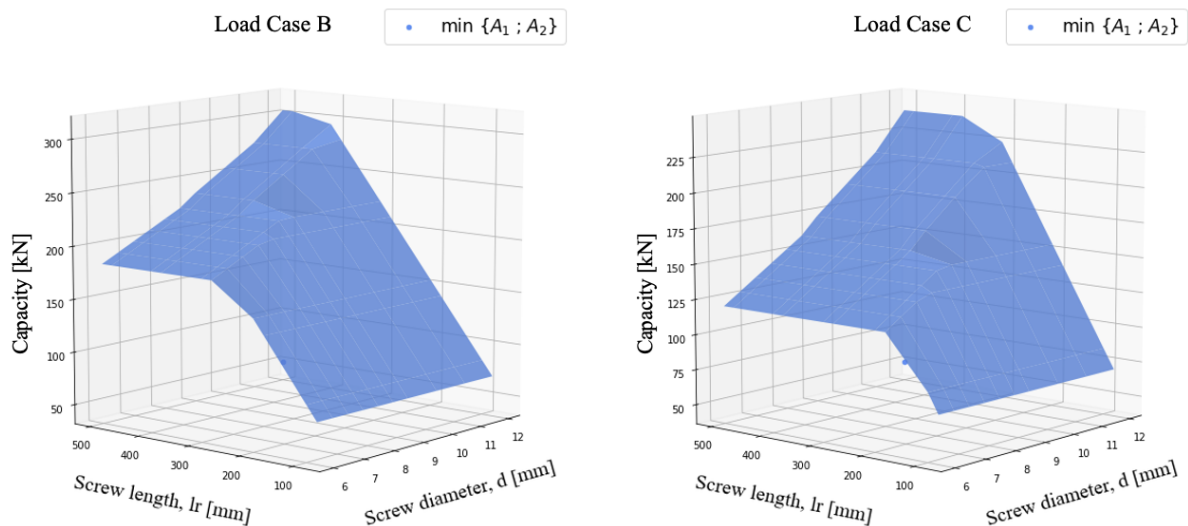
Figure 4.4: Reinforced members, bearing capacity for load case B and C

Load case B allows greater loads compared to load case C. The bearing capacity increases linearly to a certain screw length in both cases. Within this area, the screw diameter does not affect the capacity. When the screw length is extended to a specific length, the capacity does not increase, considering a constant diameter. After this point is reached, the capacity will increase with a greater diameter. Both load cases have the same tendency.

Figure 4.5 separates the equations in the design model. The blue plot is the load-bearing capacity according to A_1, and the grey plot is according to A_2.
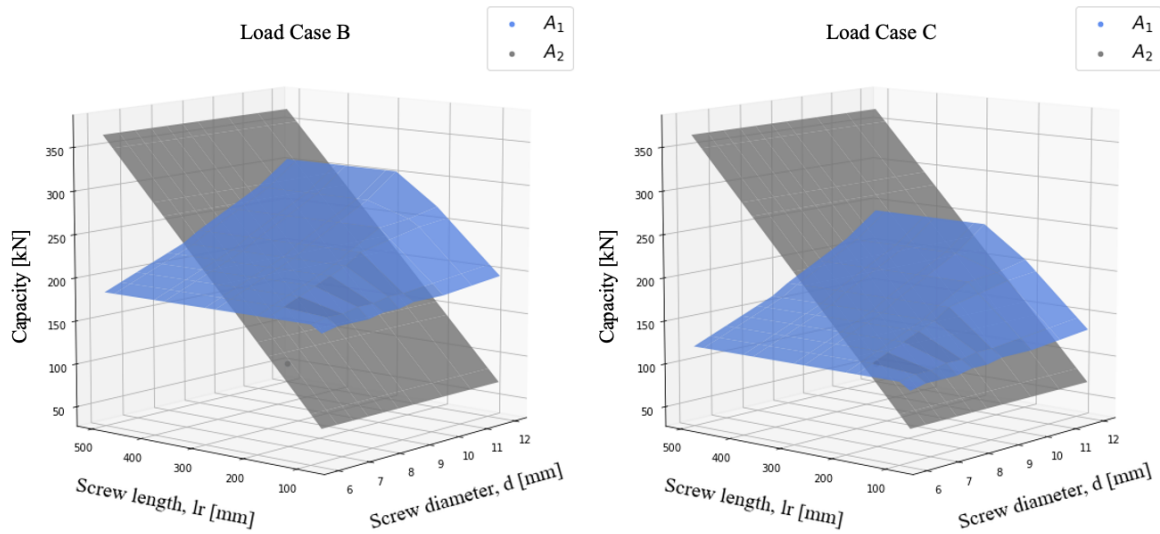
Figure 4.5: Reinforced members, A_1 and A_2 for load case B and C

A_2 is identical for both load cases. A_2 increases linearly with the length of the screw. However, the screw diameter does not impact the capacity. In situations where the screw length is small, the load-bearing capacity is determined by A_2. When the screw length increases will also the spreading length increase. When the spreading length increases to a certain level, the decisive capacity is A_1.

The curves corresponding to A_1 are similar, but the capacities are different for the two load cases. The determination of A_1 is more complex, where the capacity is based on the timber and the capacity of the screw. The capacity of the timber, A_{11} in Equation 3.9, is based on the load arrangement. The load arrangement factor, $k_{c,90}$, is equal to 1.75 for load case B, but for load case C it is equal to 1.0. This gives the basis for an increased capacity for load case B.

Figure 4.6 presents the capacity of one screw. The capacity of the screw is the minimum resistance of buckling and withdrawal, which is described in Figure 4.6 a). Figure 4.6 b) separates the withdrawal and buckling capacities.

Figure 4.6 a), F_k, shows the same tendency as A_1, but the resistance is reduced significantly. Described previously, the capacity stabilizes if the screw length reaches a specific level based on the screw diameter. Before this level is reached, the withdrawal capacity gives the minimum value. Subsequently, the buckling resistance gives the minimum capacity. The buckling depends on the slenderness ratio of the screw, which is determined by the characteristic yield capacity of screws and the buckling load. This is further described in section 3.3. The only parameter that varies in these formulas is the diameter. Since the buckling capacity is not dependent on the screw length, is the buckling capacity constant. In contrast, the withdrawal capacity depends on both the screw length and diameter. The withdrawal capacity is improved by increasing both parameters.

Appendix B, section B.3 and section B.4 gives fulfilled elaboration of the load-bearing capacity of reinforced members.
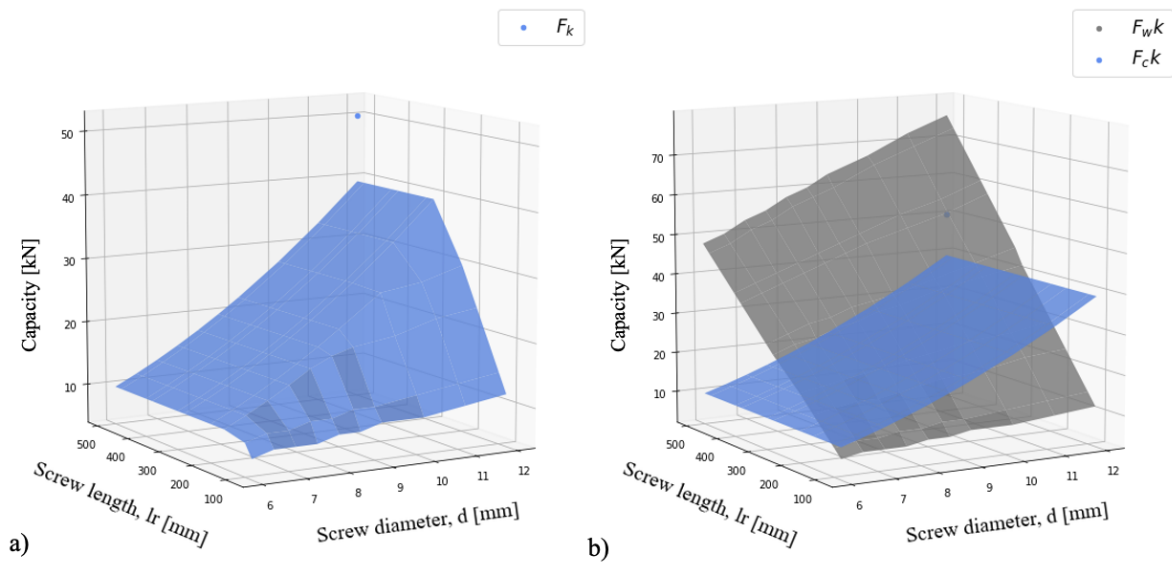
Figure 4.6: Capacity of the screws F_k, $F_{w,k}$ and $F_{c,k}$

4.4   Summary

In load case C, the capacity is significantly lower compared to load case B for both non-reinforced and reinforced specimens. Considering the minimum allowed load for a reinforced member, the capacity will increase considerably with the length of the screw for load case B.

Evaluating load cases B and C, the tendency is similar. However, the point of stabilization is considerably lower for load case C. This gives reason to say that the timber contribution is lower for load case C, regarding reinforced members. However, it is questionable if the jump in capacities between load cases B and C reflects the reality. The impact of the load situation and the timber contribution may therefore be further discussed.

5. Experimental campaign

5.1 Geometrical description

The test specimens are glue-laminated timber of strength class GL 30c, with dimensions of 800 x 140 x 225 or 1200 x 140 x 540 mm (length x width x height). The geometry of the specimens are design to get the full contribution from the load, i.e. the effective length and dispersion length. The applied reinforcement is screws produced by Rothoblaas and SFS. Required parameters, such as screw length, screw diameter, number of screws, and beam height, are investigated along with diverse load situations. The parameters enable an investigation of the design model's predicted failure mode and bearing capacity. Furthermore, varying load cases facilitate a detailed inquiry into timber behavior with reinforcement.

Figure 5.1 represents the load cases applied in this study. To compare the results, the load cases are executed with and without reinforcement. The experimental tests are based on EN 408 and ISO 6891. ISO 6891 presents the initial procedure of the test execution [25]. EN 408 describes the test procedure to determine the CPG strength, $f_{c,90,k}$, for a standard specimen without reinforcement [14]. The geometry of the specimens in load cases B and C deviates from the requirements in the standard. However, the same procedure of test execution is applied to these load cases for reinforced members. The load-displacement curve follows the requirements given by the standard, except the full member height is used to measure the displacement instead of the gauge length. This is in accordance with the study performed by Leijten, where similar load cases are investigated in the case of non-reinforced members [16].
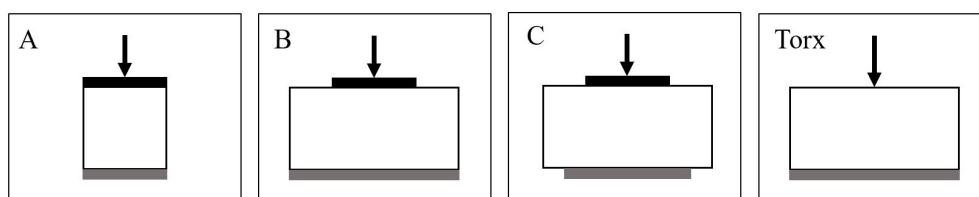
Figure 5.1: Experimental load cases

5.1.1 Design of test setup

Table 5.1 shows a schematic overview of the different screws. l_r is the effective screw length applied in the design model. The column named "*Head*" describes the geometry of the screw head. The predicted failure mode is according to the design model.

Table 5.1: Screw type

Screw type	Head	Diameter [mm]	Length [mm]	l_r [mm]	Predicted failure	Specimen height [mm]
WT-T	Cylindrical	8.2	160	130	$F_{w,k}$	225
VGZ	Cylindrical	7.0	160	160	$F_{c,k}$	225
HT-T	Countersunk	8.0	160	160	$F_{c,k}$	225
HT-T	Countersunk	8.0	180	180	$F_{c,k}$	225
HT-T	Countersunk	8.0	200	200	$F_{c,k}$	225
HT-T	Countersunk	8.0	300	300	$F_{c,k}$	540
HT-T	Countersunk	8.0	340	340	$F_{c,k}$	540
VGZ	Cylindrical	9.0	440	440	$F_{c,k}$	540

The screws are fully threaded self-tapping screws, except for the WT-T screw. The WT-T screw is double-threaded, where the effective length of the threaded part is applied. The screws are shown in Figure 5.2.

WT-T 8.2 x 160

VGZ 7.0 x 160

HT-T 8.0 x 160

HT-T 8.0 x 180

HT-T 8.0 x 200

HT-T 8.0 x 300

HT-T 8.0 x 340

VGZ 9.0 x 440
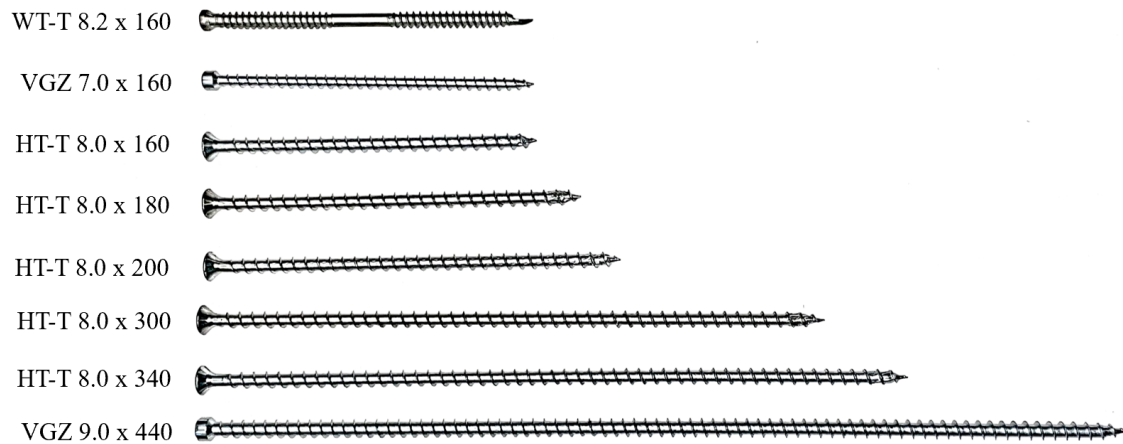
Figure 5.2: Screws

Three types of steel plates are applied to achieve the different load cases. Table 5.2 presents the properties of the steel plates along with their application.

Table 5.2: Steel plate

Length	Width	Thickness	Steel quality	Application
180	140	15	S355	Support
360	140	15	S355	Support / Load application plate
1200	200	15	S355	Load application plate

Each specimen is labeled with a unique name. The name of the test specimen is composed of its screw arrangement, screw diameter, screw length, load case, and test number, see left Figure 5.3. The non-reinforced specimens are described to the right. Section 5.1.2 describes the arrangement of the screws and their belonging names. Appendix A, section A.6 shows the screw properties from ETA.
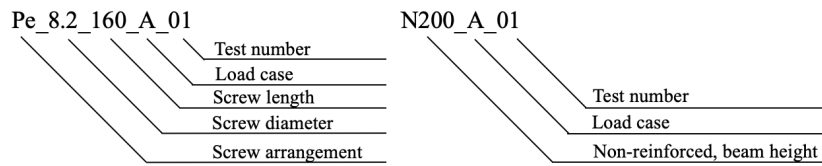
Figure 5.3: Name description for reinforced and non-reinforced test specimens

5.1.2 Screw arrangement

Due to the consideration of the effective spreading length and the increase in capacity, the screws are arranged in four situations, see Figure 5.4.
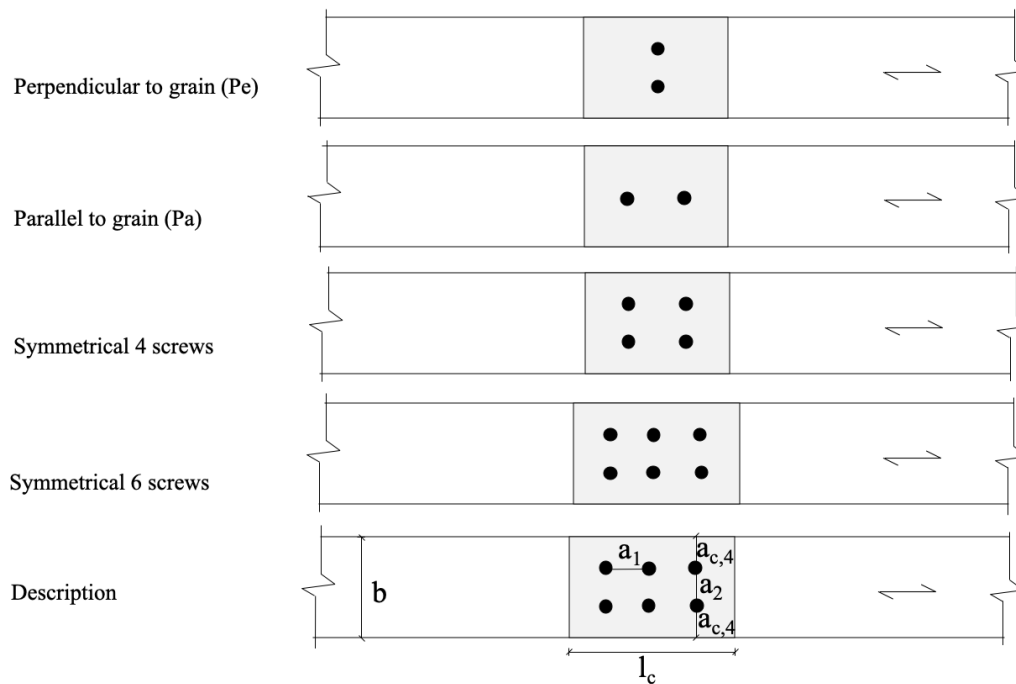
Figure 5.4: Screw arrangement

Table 5.3 shows the distance to edges and spacing between the screws. The distances and spacing are determined by the minimum distances in prEN 1995.

Table 5.3: Distances, edges and spacing

Screw arrangement	$a_{1\ min\{7d\}}$	$a_{2\ min\{5d\}}$	$a_{4,c\ min\{4d\}}$	l_c	n_0	n_{90}	n_{tot}
Pe (Perpendicular)	0	50	45	180	1	2	2
Pa (Parallel)	70	0	70	180	2	1	2
S (Symmetrical 4 screws)	70	50	45	180	2	2	4
S6 (Symmetrical 6 screws)	70	50	45	250	3	2	6

5.1.3   Load case A

Load case A represents the block test of the specimens according to EN 408. The dimensions of the specimens are based on the regulations in the standard. Table 5.4 shows the properties of the specimens and the prediction according to the design model.

The background for execution of load case A is to investigate the behavior of specimens with and without reinforcement corresponding to the requirements in EN 408. For reinforced specimens, the load will disperse from the screw head with a gradient of 45°. The dispersion of load is limited due to the length of the specimen. The predicted failure mode is the failure of A_2, failure of timber at the tip of the screws. In the case of non-reinforced, the failure appears right below the load application area. However, the predicted capacity for both configurations are equal.

Table 5.4: Properties for configurations, load case A

Type	Specimen			Screws			Loading area		Predicted capacity (prEN 1995)		
	Length	Width	Height	d	l_r	n	b_c	l_c	A_1 [kN]	A_2 [kN]	Failure mode
N200_A	180	140	200	-	-	-	140	180	-	63[a]	Timber
Pe_8.2_160_A	180	140	200	8.2	130	2	140	180	94	63	A_2

[a] Calculated according to non-reinforced design model (prEN 1995).

5.1.4   Load case B

Load case B considers discrete support with a uniformly distributed load. The load case considers the support with and without reinforcement. In contrast to load case A, the effective dispersion length for the reinforced specimens is completely utilized. The load disperses 45° from the screw head to the penetration depth of the screw. For the non-reinforced member, the load will disperse 45° from the loading area with a depth equal to the effective height. Table 5.5 shows the properties of the specimens and prediction according to the design models. The loading area represents the support. Appendix C, section C.3 shows an example of determining the design capacity for load case B.

Table 5.5: Properties for configurations, load case B

Type	Specimen			Screws			Loading area		Predicted capacity (prEN 1995)		
	Length	Width	Height	d	l_r	n	b_c	l_c	A_1 [kN]	A_2 [kN]	Failure mode
N225_B	800	140	225	-	-	-	140	180	-	118[a]	Timber
N540_B	1200	140	540	-	-	-	140	180	-	128[a]	Timber
Pe_7.0_160_B	800	140	225	7.0	160	2	140	180	171	112	A_2
Pa_7.0_160_B	800	140	225	7.0	160	2	140	180	171	137	A_2
Pe_8.2_160_B	800	140	225	8.2	130	2	140	180	178	91	A_2
Pe_8.0_180_B	800	140	225	8.0	180	2	140	180	178	126	A_2
Pe_8.0_200_B	800	140	225	8.0	200	2	140	180	178	140	A_2
S_7.0_160_B	800	140	225	7.0	160	4	140	180	196	137	A_2
S_8.2_160_B	800	140	225	8.2	130	4	140	180	209	116	A_2
S_8.0_160_B	800	140	225	8.0	160	4	140	180	210	137	A_2
S_8.0_180_B	800	140	225	8.0	180	4	140	180	209	151	A_2
S_8.0_200_B	800	140	225	8.0	200	4	140	180	209	165	A_2
S6_7.0_160_B	800	140	225	7.0	160	6	140	360	331	161	A_2
Pe_8.0_300_B	1200	140	540	8.0	300	2	140	180	178	210	$A_1\{F_{c,k}\}$
Pe_9.0_440_B	1200	140	540	9.0	440	2	140	180	188	308	$A_1\{F_{c,k}\}$
Pa_9.0_440_B	1200	140	540	9.0	440	2	140	180	188	333	$A_1\{F_{c,k}\}$
S_8.0_300_B	1200	140	540	8.0	300	4	140	180	209	235	$A_1\{F_{c,k}\}$
S_8.0_340_B	1200	140	540	8.0	340	4	140	180	209	263	$A_1\{F_{c,k}\}$
S_9.0_440_B	1200	140	540	9.0	440	4	140	180	229	333	$A_1\{F_{c,k}\}$
S6_9.0_440_B	1200	140	540	9.0	440	6	140	360	379	350	A_2

[a] Calculated according to non-reinforced design model (prEN 1995).

5.1.5 Load case C

Load case C represents discrete support with direct loading on the opposite face. The area with direct loading is not reinforced. It is desired to investigate the failure in the reinforced area. Hence, the loading area of direct loading is greater compared to the support, 360 x 140 mm (length x width). Both the reinforced and non-reinforced face, the load disperses by 45°. This will lead to an intersection of the dispersion length from both faces, and theoretically, the capacity is reduced. It is of interest to see how the specimens behave for this load case and investigate if the predictions correlate with the experimental results. Table 5.6 shows the properties of the specimens and prediction according to the design models. The loading area in the table represents the support. Appendix C, section C.4 shows an example of determining the design capacity for load case C.

Table 5.6: Properties for configurations, load case C

Type	Specimen			Screws			Loading area		Predicted capacity (prEN 1995)		
	Length	Width	Height	d	l_r	n	b_c	l_c	A_1 [kN]	A_1 [kN]	Failure mode
N225_C	800	140	225	-	-	-	140	180	-	89 [a]	Timber
N540_C	1200	140	540	-	-	-	140	180	-	101 [a]	Timber
Pe_7.0_160_C	800	140	225	7.0	160	2	140	180	108	112	$A_1\{F_{c,k}\}$
Pe_8.2_160_C	800	140	225	8.2	130	2	140	180	115	91	A_2
S_7.0_160_C	800	140	225	7.0	160	2	140	180	133	137	$A_1\{F_{c,k}\}$
S_8.2_160_C	800	140	225	8.2	130	2	140	180	146	116	A_2
S_8.0_160_C	800	140	225	8.0	160	2	140	180	147	137	A_2
Pe_9.0_440_C	1200	140	540	9.0	440	2	140	180	125	308	$A_1\{F_{c,k}\}$
S_9.0_440_C	1200	140	540	9.0	440	2	140	180	166	333	Timber [b]

[a] Calculated according to non-reinforced design model (prEN 1995).
[b] Failure due to CPG at the non-reinforced face.

5.1.6 Torx

This test aims to directly load the screw head and observe the failure of the screw alone. The load is mainly concentrated in the screw. However, some contributions from timber will occur. An area underneath the screw head due to the timber is accounted for in the predicted capacity A_1. Table 5.7 shows the properties and predictions according to the torx tests. The predicted failure mode is buckling for all screws, except the shorter screw, where the effective screw length is equal 130 mm.

Table 5.7: Properties for configurations, Torx

Type	Specimen			Screws			Loading area	Predicted capacity (prEN 1995)			
	Length	Width	Height	d	l_r	n	d_{head} [a]	A_1 [kN]	$F_{w,k}$ [kN]	$F_{c,k}$ [kN]	Failure mode
T_7.0_160	260	140	225	7.0	160	1	9.5	13.4	17.1	12.2	$A_1\{F_{c,k}\}$
T_8.0_160	260	140	225	8.0	160	1	14.8	18.3	18.7	15.4	$A_1\{F_{c,k}\}$
T_8.2_160	260	140	225	8.2	130	1	10	16.8	15.4	17	$A_1\{F_{w,k}\}$
T_8.0_180	260	140	225	8.2	180	1	14.8	18.3	21.0	15.4	$A_1\{F_{c,k}\}$
T_8.0_200	260	140	225	8.2	200	1	14.8	18.3	23.4	15.4	$A_1\{F_{c,k}\}$
T_8.0_300	260	140	225	8.2	300	1	14.8	18.3	35.0	15.4	$A_1\{F_{c,k}\}$
T_8.0_340	260	140	225	8.2	340	1	14.8	18.3	39.7	15.4	$A_1\{F_{c,k}\}$
T_9.0_440	400	140	540	9.0	440	1	11.5	22.1	55.6	20.4	$A_1\{F_{c,k}\}$

[a] d_{head} is the diameter of the screw head.

5.2   Preparations of test specimen

A detailed description of the preparation and processing of the test specimens is given in Table 5.8.

Table 5.8: Preparation and process

Delivery and storage	The specimens were delivered as long beams by Moleven Limtre. The specimens were stored at the laboratory of wood technology at NMBU. The temperature was constant at 20 degrees.
Cutting	The beams were cut into smaller pieces with a chainsaw to get the correct dimensions. There is some inaccuracy in the dimensions due to the thickness of the saw blade. This inaccuracy is accounted for when the dimensions of the specimens were designed.
Marking	All specimens were marked with a center, contact area, and screw distances to make the process more effective. Each specimen was labeled with a unique name.
Pre-drilling	All specimens were pre-drilled with a diameter 4.5 mm in a length of approximately 50 mm by using a bench pillar. The pre-drilling was performed to ensure a straight hole. Subsequently, were the specimens pre-drilled with the producer's recommended diameter and length. In some cases, there are some deviations.
Screwdriver drills	The pre-drilling and insertion of the screw were done by using electric drills by Bosch and Makita.
Screws	The screws were drilled with a right angle, and the head was in all cases flush with the timber surface. The specimen's screw configuration was prepared continuously during the process of testing. The reason for this was to evaluate the results while performing the test.
Documentation	Test sheets for all test configurations were made prior to the test execution. The test sheets defined all test properties concerning load application, predictions, and design of the specimen. During the tests, comments were made for each test. Two samples of the test sheets is shown in Appendix C, section C.2. Pictures prior to and after each test were taken, as well as after the splitting of the specimen.
Moisture content	The moisture content of each specimen was measured, see subsection 5.3.3
Splitting	The specimens were cut into smaller pieces by a band saw. The smaller pieces were marked with their own identity representing the test's name. The specimens were slotted either by a band saw or a circular saw. Further, each specimen was split with a chisel and hammer.

In Table 5.9 the drills are listed for the different screws. The dimensions of the drills are in accordance with the recommendations given in the ETA, but for the case of the VGZ 9.0 x 440 mm the diameter used differs.

Table 5.9: Pre-drilling

Screw	Drill	Drill diameter [mm]	Drill length [mm]
VGZ 7.0 x 160	PFX 4.5x235	4.5	160
WT-T 8.2 x 160	PFX 4.5x235	4.5	160
HT-T 8.0 x 160	PFX 4.5x235	4.5	160
HT-T 8.0 x 160	PFX 4.5x235	4.5	160
HT-T 8.0 x 180	PFX 4.5x235	4.5	160
HT-T 8.0 x 200	PFX 4.5x235	4.5	160
HT-T 8.0 x 300	PFX 5.0x315	5.0	290
HT-T 8.0 x 340	PFX 5.0x315	5.0	290
VGZ 9.0 x 440	HSS 6.0x600	6.0	360

5.3   Test procedure

The test machine is ZwickRoell Z1200. The specimens are subjected to a compressive force by the load cell of the machine. The machine has a built-in safety limitation of the load cell, where the machine is restricted to not pass a certain point. Due to this, the head of the load cell is built down with a cylindrical steel tube. Furthermore, brackets will prevent slipping sideways of the specimen. The brackets are applied because of safety reasons. The brackets do not take any load and are placed with a gap to the specimens.
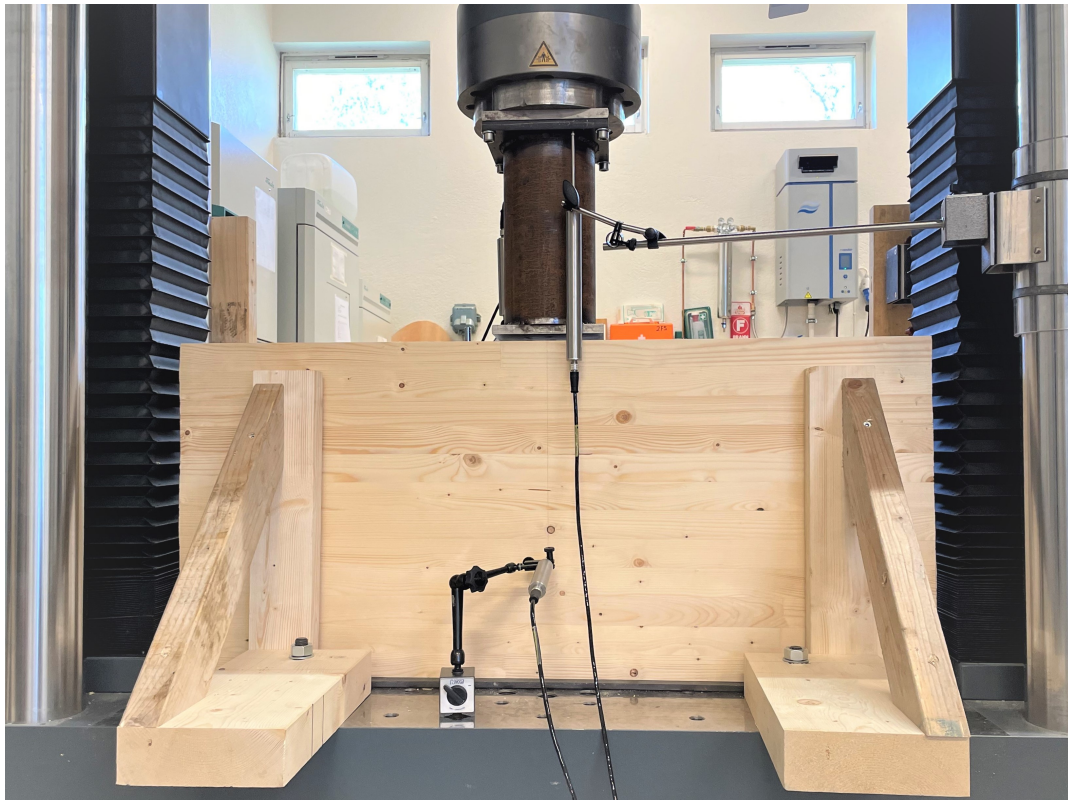
Figure 5.5: Setup of specimen with height 540 mm in ZwickRoell Z1200

5.3.1   Sensors

The deformation is measured through an integrated sensor in the load cell and external sensors. During the test execution, two horizontal and two vertical sensors are used, see Figure 5.6. The horizontal sensors are placed on each long side of the specimen in an area of the screw tip. The horizontal sensors will recognize any movement due to failure of the timber and sideways expansion.

The deformation used for the load-deformation curves is the change in depth of the specimen. According to EN 408, the sensors should be placed within the gauge length of the specimens. However, a similar study by Leijten for specimens without reinforcement applies the change in specimen depth. Using this provides more consistent results and is a preferred measuring method [16]. Otherwise, all evaluations are done in accordance with EN 408.

Figure 5.6: External sensors - vertical and horizontal

5.3.2   Load rate and phases

Certain characteristics of the test program have to be determined in advance of the tests. There is not any standard or procedure for testing reinforced members. According to EN 408, for the non-reinforced block test, the load shall be applied at a constant rate, where the rate is determined from preliminary tests. Since reinforced members achieve an ultimate load and reach failure at a clear point, it is not necessary with the preliminary tests. The estimated load F_{est}, either A_1 or A_2, applies directly to the load rate. In the case of non-reinforced members, not block test, the estimated force is determined by the non-reinforced design model with k_p equal to 1.0.

When determining the bearing capacity, the application of load is of importance. The test is divided into four phases in load cases B and C. The three initial phases are based on load rates, while the last is based on displacement per minute. In load cases A and torx, the test is only based on load rates, hence three phases.

Phases 1 and 2 are in accordance with ISO 6891, and are applied to avoid sizeable initial deformation and stabilize the loading area. Since the specimen is in the elastic range to a certain level of loading, the preliminary load application is adequate. The specimen is loaded until 40 % of F_{est}, held for 30 seconds before the load decreases to 10 % of F_{est}, and then held for 30 seconds [25].

The evaluation of the test starts in phase 3. According to EN 408, the maximum force shall be reached within 300 ± 120 seconds. To estimate the load rate, F_{est} is divided by 300 seconds. In situations with four phases, the phase 4 will occur when F_{est} is reached. Phase 4 is a load-displacements control with a 1.0 mm/min deformation rate [22]. The load-displacement control applies to those specimens where it is of interest to consider a certain level of deformation. The test will stop automatically if the load reduces 20 % or the level of deformation reaches 12 % of the specimen height.

Appendix C, section C.1 gives further elaboration of the load rate and phases.
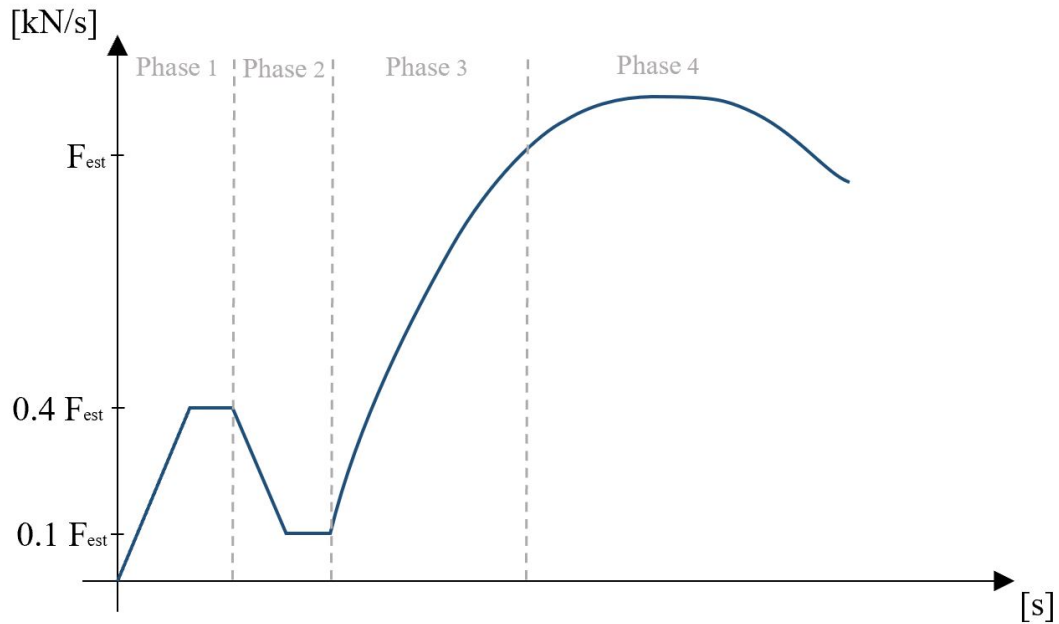
Figure 5.7: Phases

5.3.3 Moisture content

The moisture content is measured by Delmhorts RDM3 instrument. The measuring point is close to the screw area. The mean value shows moisture content of 12.3 %. For detailed moisture content per test specimen, see Appendix C, section C.5.

5.3.4 Setup torx test

The torx test is executed by connecting a torx bit to the load cell through a steel plate. The steel plate and torx bit used for the tests is shown in Figure 5.8. The torx bit and the screw head have to fit each other properly. During the test, the torx bit is replaced frequently due to fatigue and the risk of failure. For the measurement of the deformations, vertical sensors are used. The horizontal sensors are omitted since it is mainly the screw that is loaded, and there will not be any horizontal expansion. Otherwise, the test is performed similarly to the other load cases.

Figure 5.8: Steel plate used for Torx tests

The test setup of the torx tests is shown in Figure 5.9. Shorter torx bits performed better due to minor risk of buckling and biases. The torx bits used are bits developed by Rothoblaas and Dewalt.
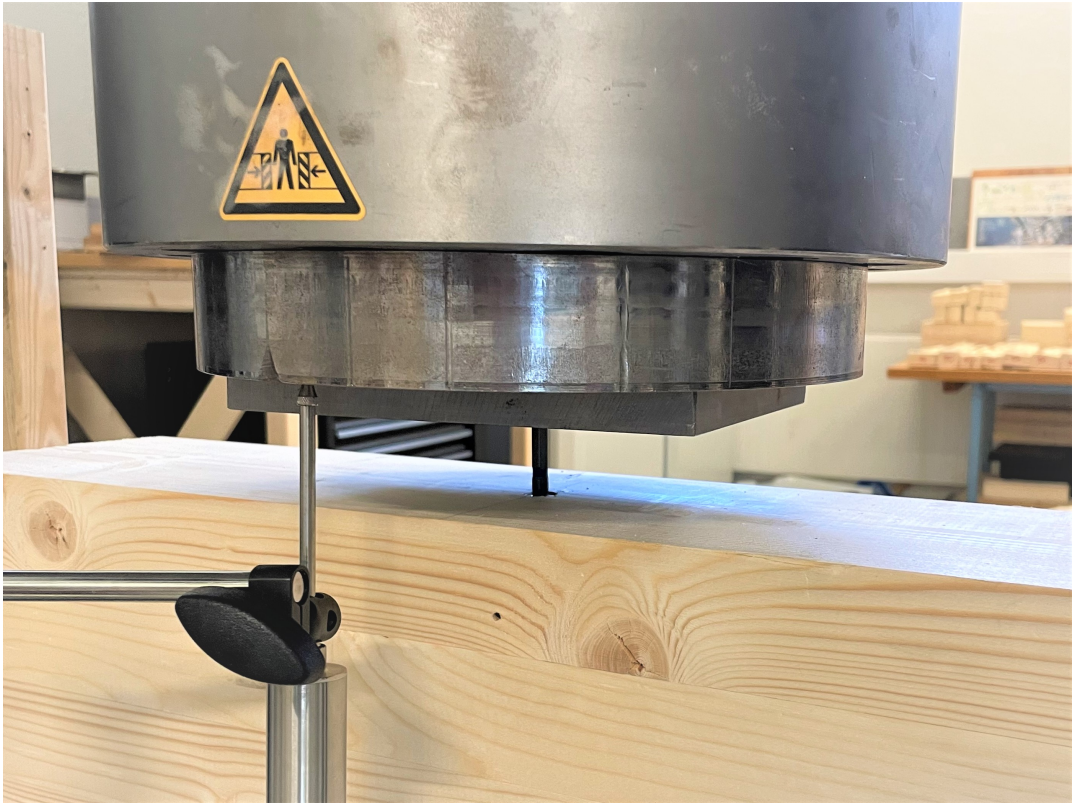
Figure 5.9: Setup of Torx test

6. Experimental results

6.1 Introduction of content

This chapter presents the experimental results. The results are separated and organized into load cases. Due to a greater number of configurations for load cases B and C, the results are differentiated into specimen height and number of screws. The increase of capacity is the relation between non-reinforced and reinforced members, given the achieved force at 1 % deformation. In the event of torx test, the results are separated into specimen height and type of screw head. The presentation of the results is shown in Table 6.1.

In cases where the configuration is executed more than once, the mean value is used in the tabulated results. In addition, the horizontal displacement, Δ_{hor}, is the mean value of the horizontal sensors on each long-side. The horizontal displacement is recorded at the tip of the screw and is the maximum displacement achieved during the tests.

Table 6.1: Result layout

Load case A		section 6.2
Specimen height 200 mm	Two screws	
Load case B		section 6.3
Specimen height 225 mm	Two screws	6.3.1
	Four and six screws	
Specimen height 540 mm	Two screws	6.3.2
	Four and six screws	
Load case C		section 6.4
Specimen height 225 mm	Two screws	6.4.1
	Four screws	
Specimen height 540 mm	Two screws	6.4.2
	Four screws	
Torx		section 6.5
Specimen height 225 mm	Cylindrical head	6.5.1
	Countersunk head	
Specimen height 540 mm	Cylindrical and countersunk head	6.5.2

6.2 Load case A

The experimental results of load case A are presented in Table 6.2. The capacity increases slightly with the use of reinforcement. The failure mode achieved is the failure of the timber.

Table 6.2: Results, Load case A

Test	No. tests	Failure mode	F_{max} [kN]	$F_{1\%,def}$ [kN]	Δ_{hor} [mm]	Increase
N200_A	2	B_1	-	88	-	-
Pe_8.2_160_A	2	A_2	104	96	9.39	9.1 %

Figure 6.1 shows the failure of the block test with reinforcement. From the side view, the screws are not straight after the failure is reached.

Figure 6.1: Failure WT-T 8.2x160

The load-displacement curve is shown in Figure 6.2. The yellow curves represent the non-reinforced specimens, while the blue and grey curves are the reinforced specimens. The curves are close to each other, but at 1 % deformation of specimen height, the reinforced specimen has a higher capacity than the non-reinforced.
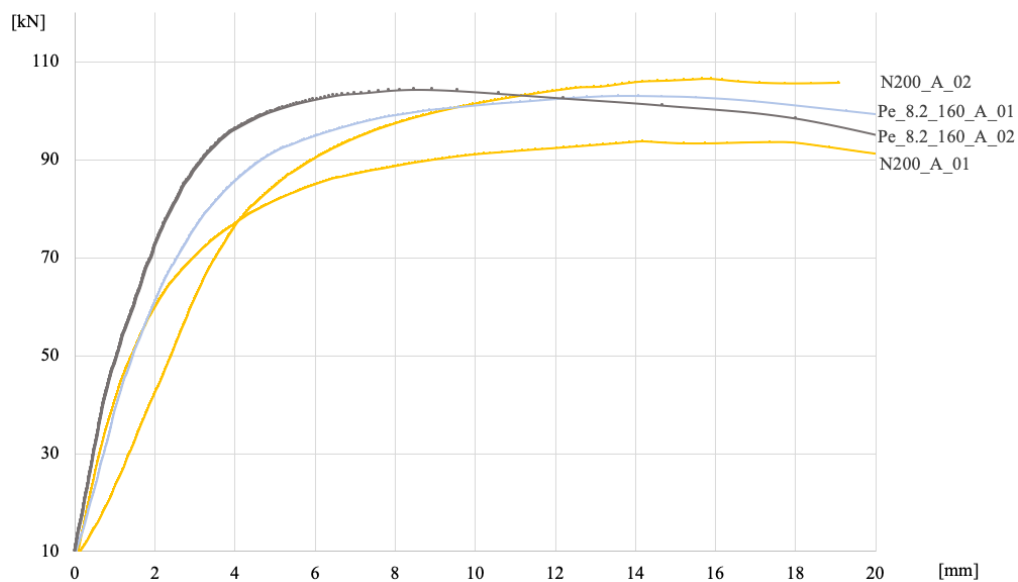
Figure 6.2: Load case A, Load-displacement diagram

6.3 Load case B

Load case B presents discrete support subjected to a uniformly distributed load.

6.3.1 Specimen height 225 mm

The test results according to load case B with specimen height 225 mm are presented in Table 6.3. The failure modes achieved are buckling and withdrawal.

Table 6.3: Results 225 mm, Load case B

Test	No. tests	Failure mode	F_{max} [kN]	$F_{1\%,def}$ [kN]	Δ_{hor} [mm]	Increase
N225_B	1	Timber	-	152	0.97	-
Pa_7.0_160_B	1	$A_1\{F_{w,k}\}$	174	172	0.71	13.2 %
Pe_7.0_160_B	1	$A_1\{F_{w,k}\}$	177	172	0.54	13.2 %
Pe_8.2_160_B	2	$A_1\{F_{w,k}\}$	189	174	0.74	14.5 %
Pe_8.0_180_B	1	$A_1\{F_{w,k}/F_{c,k}\}$	207	196	0.59	28.9 %
Pe_8.0_200_B	1	$A_1\{F_{c,k}\}$	213	205	0.42	34.9 %
S_7.0_160_B	1	$A_1\{F_{w,k}\}$	222	210	0.60	38.2 %
S_8.2_160_B	1	$A_1\{F_{w,k}\}$	191	189	0.73	24.3 %
S_8.0_160_B	1	$A_1\{F_{w,k}\}$	200	194	0.70	27.6 %
S_8.0_180_B	1	$A_1\{F_{w,k}\}$	226	217	0.92	42.8 %
S_8.0_200_B	1	$A_1\{F_{w,k}\}$	228	217	0.55	42.8 %
S6_7.0_160_B	1	$A_1\{F_{w,k}\}$	339	311	1.50	104.6 %

The horizontal displacement is below 1 mm for all cases, except for S6_7.0_160_B, where the horizontal displacement is 1.50 mm. The test configurations, Pa_7.0_160_B and Pe_7.0_160_B, achieved equal force at 1 % deformation. The difference between the configurations is the screw arrangement.

Figure 6.4 shows the failure modes achieved from the tests with different screws. The HT-T 8.0 x 200 mm screws achieved both buckling and withdrawal, which is shown in the figure.

Figure 6.3: Failure VGZ 7.0x160, WT-T 8.2x160, and HT-T 8.0x160, 8.0x180, 8.0x200, 8.0x200

The load-displacement curves are plotted in Figure 6.4 and Figure 6.5, with respectively two screws and, four and six screws. The curves of the reinforced specimens have a defined vertex, while the curve of the non-reinforced specimen increases continuously. The slope in the elastic range is more steep for the reinforced specimens compared to non-reinforced.
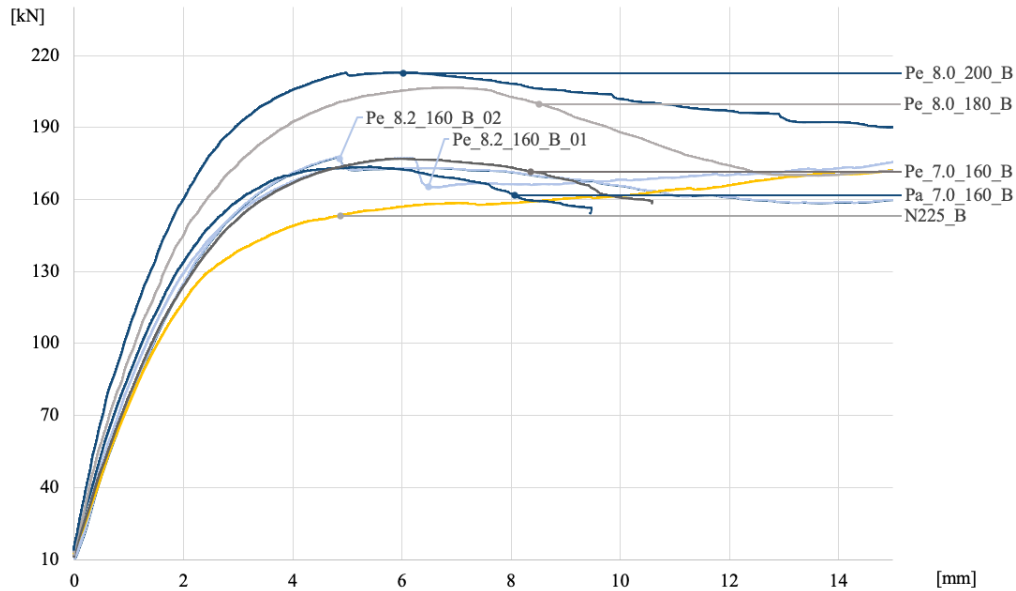
Figure 6.4: Load case B, diagram of non-reinforcement and two screws, 225 mm height

The configuration, S6_7.0_160_B, shows a great increase in capacity. However, the configuration has a greater number of screws, as well as increased contact area, 360 x 140 mm (length x width).
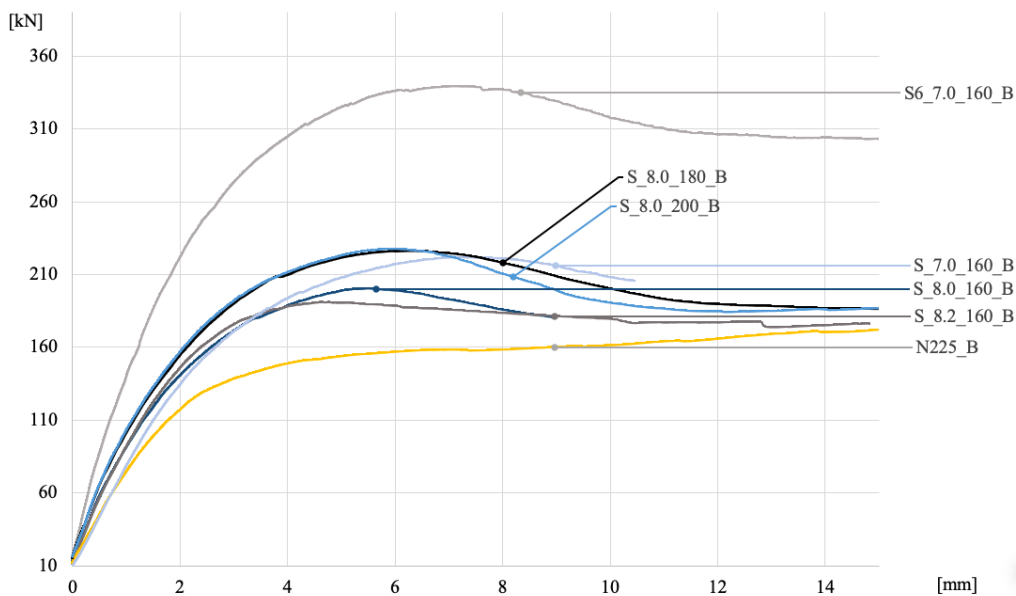
Figure 6.5: Load case B, diagram of non-reinforcement, four, and six screws, 225 mm height

6.3.2 Specimen height 540 mm

The test results of load case B with 540 mm specimen height are introduced in Table 6.4. The failure mode achieved for all configurations is buckling.

Table 6.4: Results 540 mm, Load case B

Test	No. tests	Failure mode	F_{max} [kN]	$F_{1\%,def}$ [kN]	Δ_{hor} [mm]	Increase
N540_B	1	Timber	-	165	0.47	-
Pe_8.0_300_B	1	$A_1\{F_{c,k}\}$	234	234	0.25	41.8 %
Pa_9.0_440_B	1	$A_1\{F_{c,k}\}$	231	230	0.47	39.4 %
Pe_9.0_440_B	2	$A_1\{F_{c,k}\}$	229	226	0.72	36.7 %
S_8.0_300_B	1	$A_1\{F_{c,k}\}$	256	256	0.67	55.2 %
S_8.0_340_B	1	$A_1\{F_{c,k}\}$	272	271	-	64.2 %
S_9.0_440_B	2	$A_1\{F_{c,k}\}$	296	292	0.83	77.0 %
S6_9.0_440_B	1	$A_1\{F_{c,k}\}$	457	455	1.47	175.8 %

The capacity increases with the number of screws. For the configuration S6_9.0_440_B, the horizontal displacement is greater than 1 mm; otherwise, the horizontal displacement is below 1 mm. The horizontal displacement for S_8.0_340_B is not reported.

Figure 6.6 presents the buckling behavior of the diverse screws.

Figure 6.6: Failure HT-T 8.0x300, 8.0x340 and VGZ 9.0x440

The load-displacement curves are plotted in Figure 6.7 and Figure 6.8, for two screws and, four and six screws, respectively. The curves have a defined apex before the load decreases with increasing deformation. In context with the non-reinforced (yellow curve), the capacities have increased substantially. The buckling behavior is similar for all screws in the event of six screws.
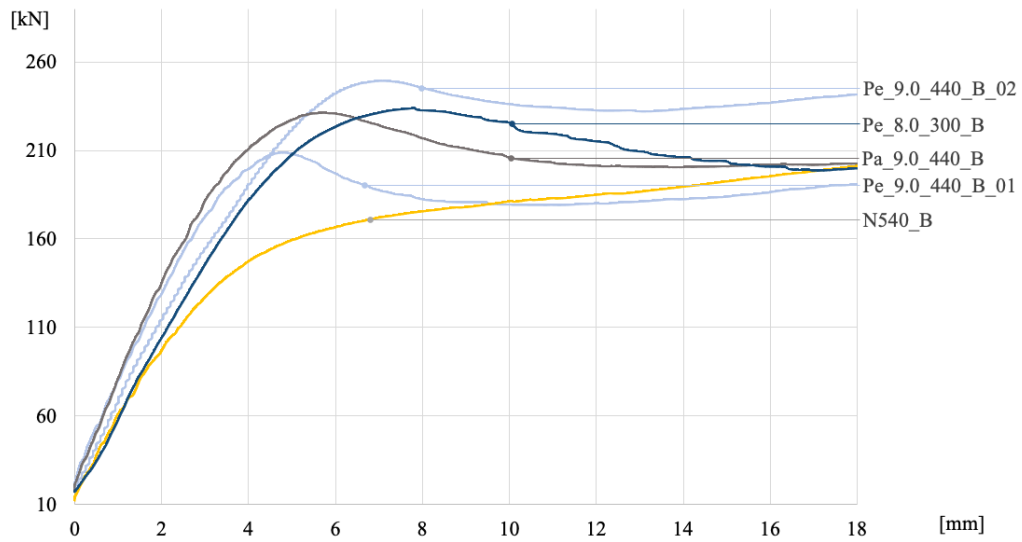
Figure 6.7: Load case B, diagram of non-reinforcement and two screws, 540 mm height
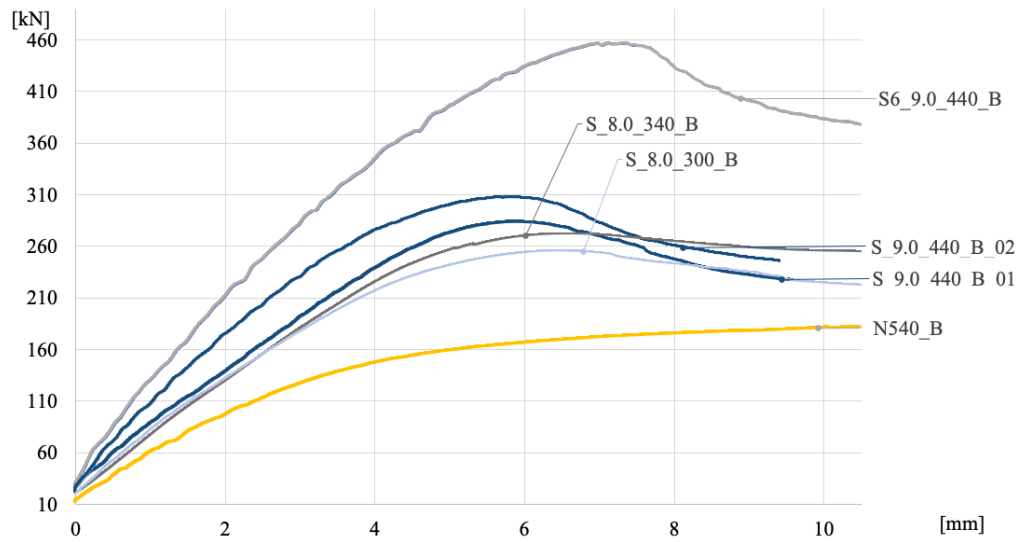
Figure 6.8: Load case B, diagram of non-reinforcement, four and six screws, 540 mm height

6.4   Load case C

Load case C presents discrete support with a concentrated load on the opposite side. On the non-reinforced side, a steel plate with dimensions 360 x 140 mm (length x width) is applied.

6.4.1   Specimen height 225 mm

Table 6.5 introduces the results of the specimens with a height 225 mm and load case C. All test configurations resulted in withdrawal as the failure mode, except the non-reinforced specimen.

Table 6.5: Results 225 mm, Load case C

Test	No. tests	Failure mode	F_{max} [kN]	$F_{1\%,def}$ [kN]	Δ_{hor} [mm]	Increase
N225_C	1	Timber	-	155	0.97	-
Pe_7.0_160_C	1	$A_1\{F_{w,k}\}$	188	173	1.45	11.6 %
Pe_8.2_160_C	1	$A_1\{F_{w,k}\}$	171	169	1.02	9.0 %
S_7.0_160_C	2	$A_1\{F_{w,k}\}$	220	192	1.69	23.9 %
S_8.2_160_C	1	$A_1\{F_{w,k}\}$	184	183	0.91	18.1 %
S_8.0_160_C	1	$A_1\{F_{w,k}\}$	220	191	2.05	23.2 %

The capacity of the test specimens increases with applying reinforcement. The horizontal displacement is approximately 1-2 mm for all cases. The configuration Pe_7.0_160_C received higher capacity compared to Pe_8.2_160_C.

The withdrawal failure of the diverse screws is shown in Figure 6.9.

Figure 6.9: Failure VGZ 7.0x160, WT-T 8.2x160 and HT-T 8.0x160

The load-displacement curves are shown in Figure 6.10 and Figure 6.11, respectively with two and four screws. The curves of reinforced specimens have a defined apex. In Figure 6.10 the slope at the elastic part for both reinforced and non-reinforced specimens is similar, but the course of the

non-reinforced curve decreases former. In the case of four screws, the curves have a more steep slope.
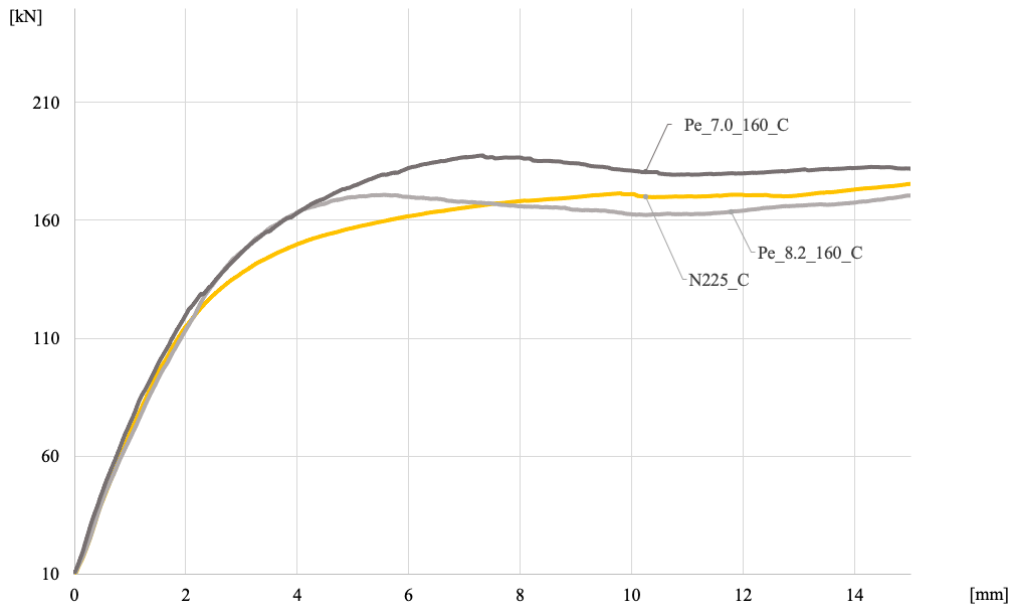
Figure 6.10: Load-displacement diagram with two screws, 225 mm height
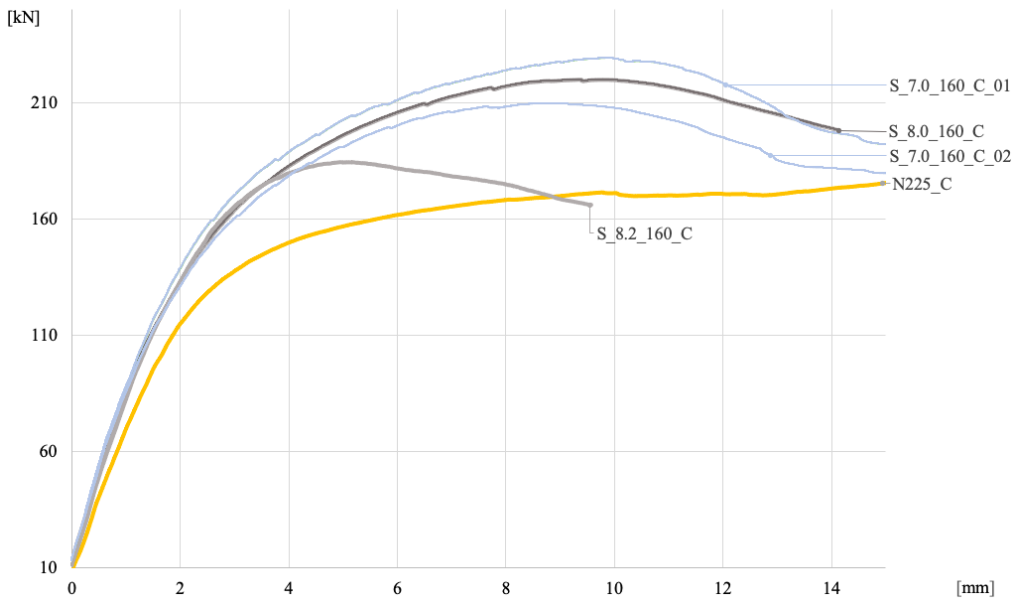
Figure 6.11: Load-displacement with four screws, 225 mm height

6.4.2 Specimen height 540 mm

Table 6.6 shows the test results of load case C with a specimen height of 540 mm. The failure mode achieved with two screws is buckling. In the case of four screws, the failure is due to the timber at the non-reinforced surface.

Table 6.6: Results 540 mm, Load case C

Test	No. tests	Failure mode	F_{max} [kN]	$F_{1\%,def}$ [kN]	Δ_{hor} [mm]	Increase
N540_C	1	Timber	-	182	1.30	-
Pe_9.0_440_C	2	$A_1\{F_{c,k}\}$	237	229	1.13	25.8 %
S_9.0_440_C	1	B_1	-	235	1.89	29.1 %

The capacity increases with the number of screws. The horizontal displacement is 1-2 mm for each configuration.

The buckling failure mode is shown in Figure 6.12.

Figure 6.12: Failure VGZ 9.0x440

The load-displacement curves of the specimens are shown in Figure 6.13 and Figure 6.14, with two and four screws, respectively. The slope of the reinforced curves are greater compared to the non-reinforced curves. S_9.0_440_C is omitted for further evaluation due to the failure of timber on the non-reinforced surface. Consequently, only one configuration represents specimen height 540 mm for load case C.
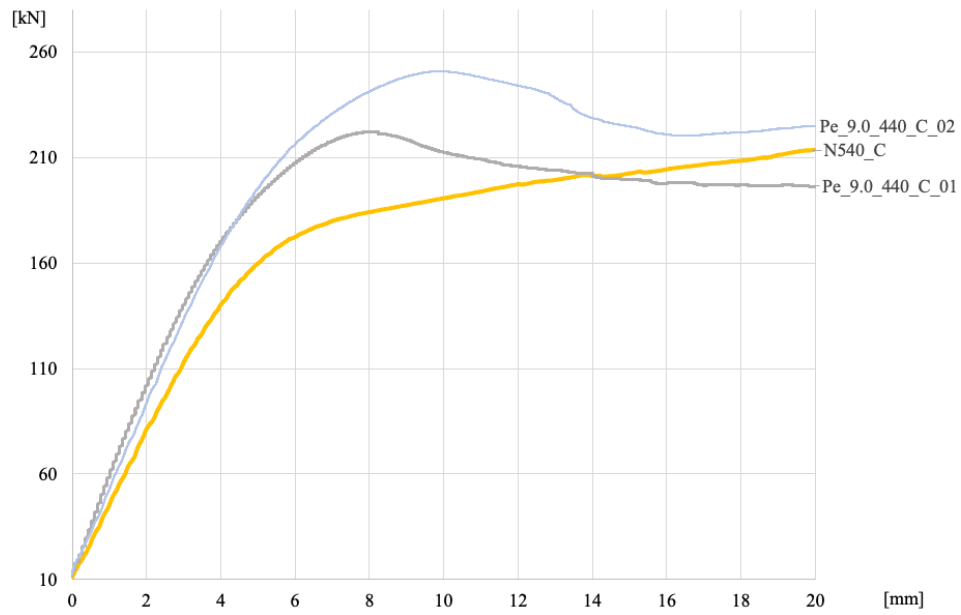
Figure 6.13: Load case C, diagram of non-reinforcement and two screws, 540 mm height
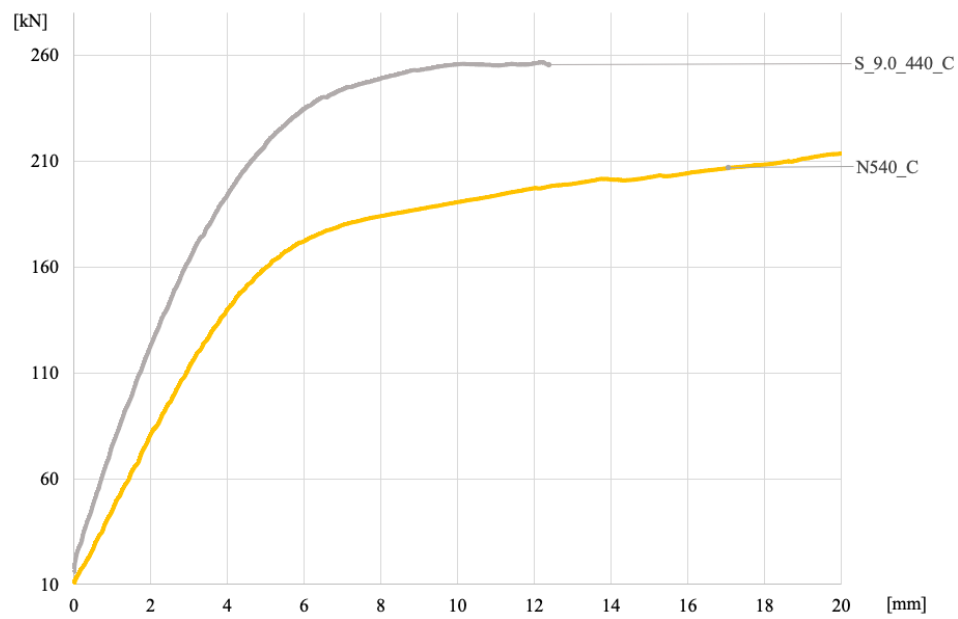
Figure 6.14: Load case C, diagram of non-reinforcement, four and, six screws, 540 mm height

6.5   Torx

The torx test is performed with a series of two per test configuration. The mean value of the results is applied. In contrast to the other load cases, the maximum force achieved during the tests is used. The load-displacement curves are based on measurements of both external sensor and sensor in the load cell, which results in a different representation of the curves. The sensor in the load cell is applied in the case of 160 mm and 440 mm lengths of the screw, reasoning some inaccuracies in the external sensor.

6.5.1   Specimen height 225 mm

Table 6.7 introduces the results of the torx tests with 225 mm specimen height. The failure modes of the screws are withdrawal and buckling.

Table 6.7: Results, torx test 225 mm

Test	No. tests	Failure mode	F_{max} [kN]
T_7.0_160	2	$A_1\{F_{w,k}\}$	21.9
T_8.2_160	2	$A_1\{F_{w,k}\}$	21.3
T_8.0_160	2	$A_1\{F_{c,k}\}$	28.3
T_8.0_180	2	$A_1\{F_{c,k}\}$	29.2
T_8.0_200	2	$A_1\{F_{c,k}\}$	27.5

The load increases with the length of the screw, except when the length of the screw is 200 mm. In this case, the capacity decreases.

Figure 6.15 shows the diverse screws and the failure modes.

Figure 6.15: Failure VGZ 7.0x160, WT-T 8.2x160, HT-T 8.0x160, 8.0x180, 8.0x200

Figure 6.16 displays the load-displacement curves. The diagram to the left shows the load-displacement curves for the cylindrical head, while the diagram to the right shows the curves for the countersunk head. In the event of a countersunk head, the diameter is similar for all configurations, while the screw length varies. The slope in the elastic range is similar for these configurations. All test configurations have a defined vertex.
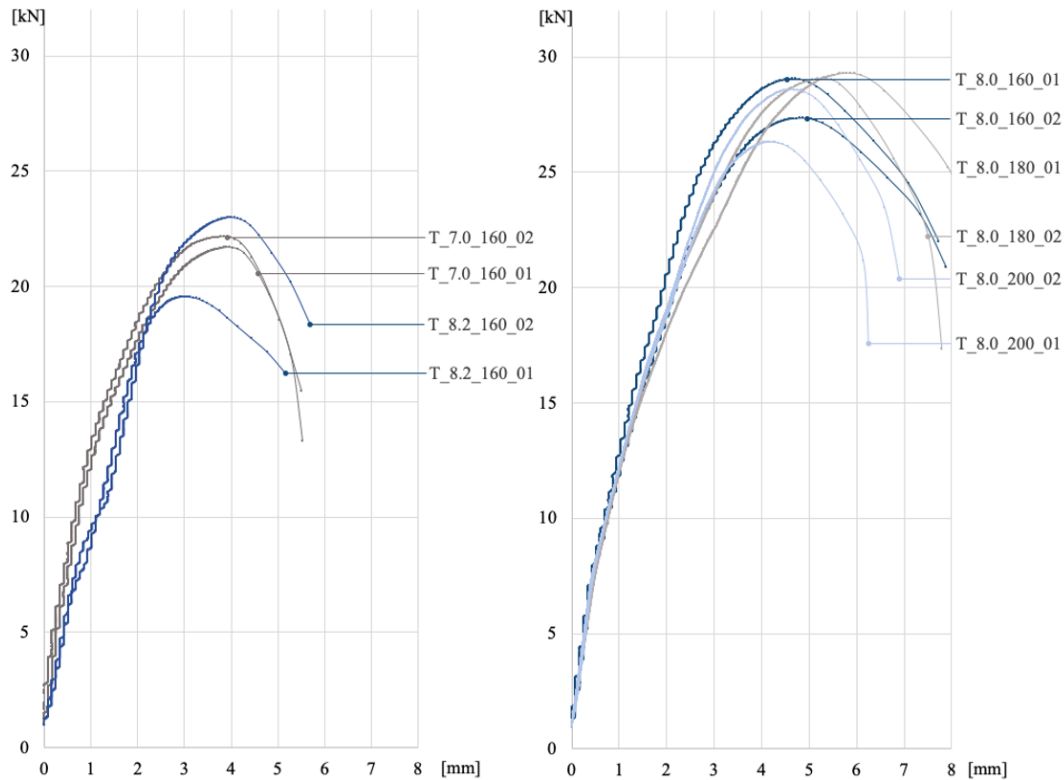
Figure 6.16: Load-displacement diagram Torx of 225 mm specimen

6.5.2   Specimen height 540 mm

Table 6.8 introduces the results of the torx tests with specimen height 540 mm. The failure mode achieved is buckling.

Table 6.8: Results, torx test 540 mm

Test	No. tests	Failure mode	F_{max} [kN]
T_8.0_300	2	$A_1\{F_{c,k}\}$	26.0
T_8.0_340	2	$A_1\{F_{c,k}\}$	28.5
T_9.0_440	2	$A_1\{F_{c,k}\}$	40.8

The load increases with the length and diameter of the screws. Figure 6.17 shows the buckling behavior of each screw.
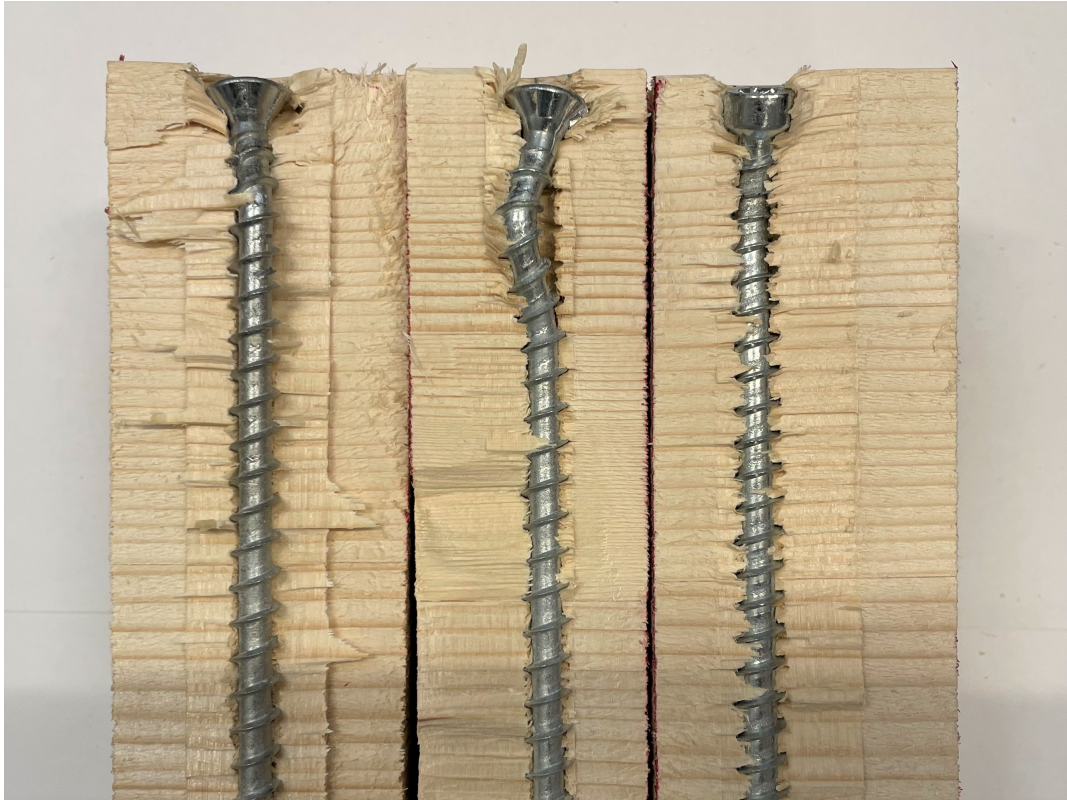
Figure 6.17: Buckling failure of 540 mm specimens, HT-T 8.0x300, 340 and VGZ 9.0x440

Figure 6.18 shows the load-displacement diagram. The curves have a clearly defined vertex. With the VGZ 9.0 screw, the capacity is greater, compared to the HT-T 8.0 screw. However, the failure is reached at a smaller displacement. The torx bit got a sizable horizontal deformation at the vertex of the curves of VGZ screws. The torx bit buckled in one of the cases when the screw failed.
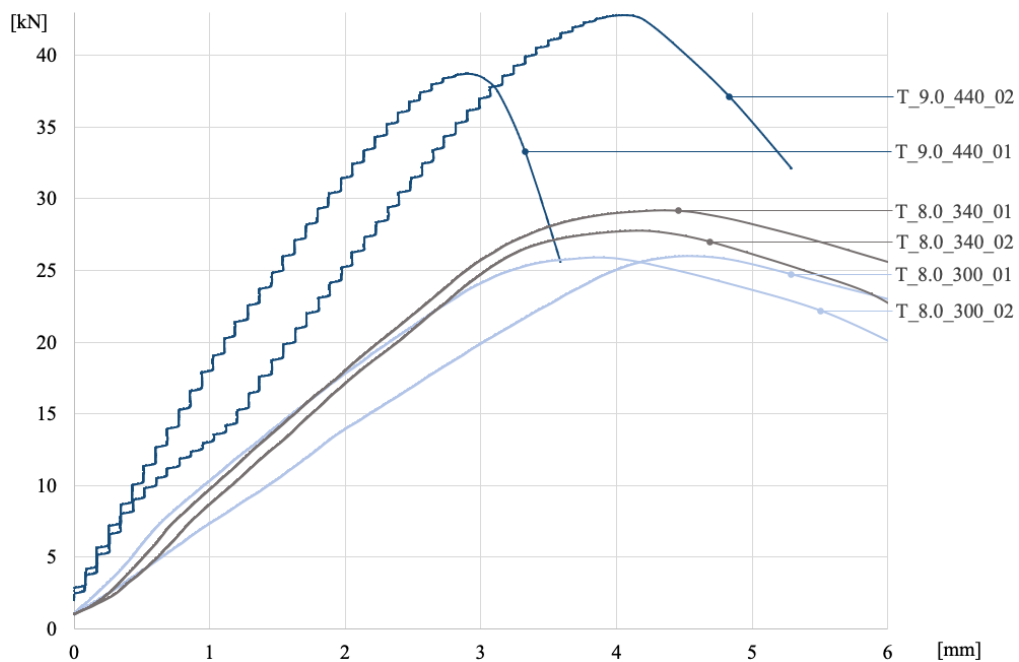
Figure 6.18: Load-displacement Torx of 540 mm specimen

6.6   Summary of results

In total, is have been accomplished 53 valid tests. However, the magnitude of variety in configurations is preferred on behalf of test repetitions. Throughout the tests, eight different screws have been utilized in four loading situations.

The load-displacement curves show that the initial load increases linearly in the elastic range. The slope of the curves is reduced when the load approaches the maximum load. After this point, the load decreases with increasing deformation. This range is connected to the failure of the screws and local crushing of timber. After the screws have failed, there is a slight increase in capacity after a certain point. The increase is related to the activation of the timber.

In the elastic range, the load-displacement curves have the same tendency, while when the plastic range is reached, the load-displacement curve is dependent on the failure mode.

Furthermore, Figure 6.19 shows the maximum horizontal expansion at the screw tip for each test. The horizontal expansion is below 2 mm for all cases, except load case A. Nevertheless, load case A does not represent a design situation. The maximum horizontal displacement is reached at 2 mm. However, this amount of expansion is not considered as a failure mode. The failure is clearly define by the screws.
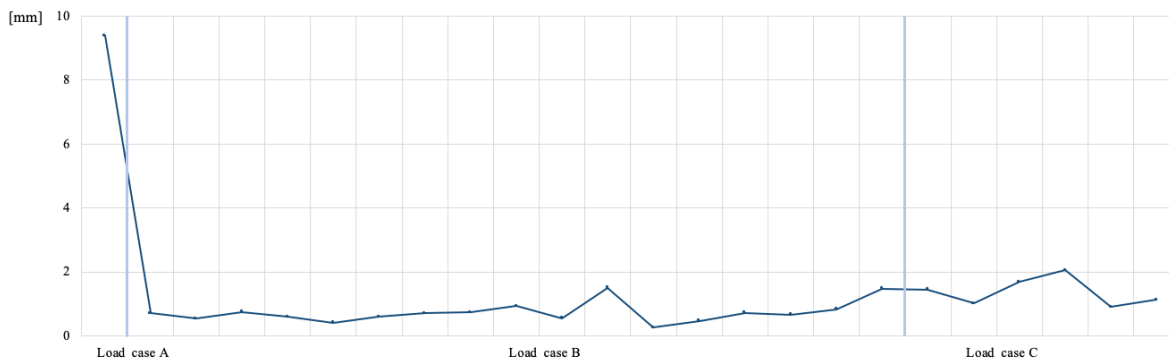
Figure 6.19: Horizontal expansion of the test specimen, divided into the different load cases

Appendix C, section C.5 shows the assembled data from the preformed test, i.e. $F_{1\% \, def}$, F_{max}, predictions, failure mode, moisture content and horizontal deformation.

7. Test evaluation and harmonization

The following section presents an evaluation of the tests in context with the design model, prEN 1995. The reliability and accuracy of the model are reflected. The load of comparison, $F_{1\%def}$ is the load at 1 % deformation of the member height, the reason being that the compressive strength $f_{c,90,k}$ is based on 1 % level of deformation. The predicted capacity according to the design models is referred to as abbreviations, as stated in Equation 3.9.

Furthermore, the second section addresses the feasibility of harmonizing the design model. The evaluations of harmonization are based on the experimental study and earlier investigations performed by other researchers.

7.1 Test evaluation

7.1.1 Load case A

Table 7.1 presents the test results and the design model of load case A. The test results confirm the predicted failure mode. Hence the failure mode is due to A_2. However, the predicted capacity is 63 kN, which is 34 % deviation. Based on the comparison, the prediction of the capacity is conservative.

Table 7.1: Evaluation, test results and design model of load case A

Name	Test results		Design model			Deviation $\{F_{1\%def}\}$	
	$F_{1\%def}$ [kN]	Failure	A_1 [kN]	A_2 [kN]	Failure	A_1	A_2
N200_A	88	-	-	63[a]	-	-	-
Pe_8.2_160_A	96	A_2	94	63	A_2	2 %	34 %

[a] Timber capacity for non-reinforced members.

Compared to the non-reinforced test specimen, the capacity of the reinforced specimen increases slightly. Theoretically, the effective spreading length of the specimens is not fully utilized due to the specimen's geometry, 180 x 140 x 200 mm (length x width x height). According to the decisive capacity, A_2, and corresponding spreading length, the capacity of non-reinforced and reinforced specimens is equal for load case A. However, the slight increase of the test results between the non-reinforced and reinforced test specimen may be due to imperfections in the timber.

7.1.2 Load case B

The test results do not sufficiently confirm the predicted failure modes, see Table 7.2. For the test specimens with a height of 225 mm, the failure mode is withdrawal or buckling, corresponding to A_1. In contrast, the predicted failure is A_2. Furthermore, according to the design model, the decisive capacity is significantly reduced compared to the test results. Since the failure mode achieved is due to screws in the tests, it is of interest to investigate A_1 in accordance with test results. The predicted capacity of A_1 is precise, with a deviation of 5.9 %, for specimens with a height 225 mm.

Table 7.2: Evaluation, test results and design model of load case B

Name	Test results		Design model			Deviation $\{F_{1\%def}\}$	
	$F_{1\%def}$ [kN]	Failure	A_1 [kN]	A_2 [kN]	Failure	A_1	A_2
Pa_7.0_160_B	172	$A_1\ \{F_{w,k}\}$	171	137	A_2	0.3 %	21 %
Pe_7.0_160_B	172	$A_1\ \{F_{w,k}\}$	171	112	A_2	0.3 %	35 %
Pe_8.0_180_B	196	$A_1\ \{F_{w,k}\}/\{F_{c,k}\}$	178	126	A_2	9 %	36 %
Pe_8.0_200_B	205	$A_1\ \{F_{c,k}\}$	178	140	A_2	13 %	32 %
Pe_8.2_160_B	174	$A_1\ \{F_{w,k}\}$	178	91	A_2	2 %	48 %
S_7.0_160_B	210	$A_1\ \{F_{w,k}\}$	196	137	A_2	7 %	35 %
S_8.0_160_B	194	$A_1\ \{F_{w,k}\}$	210	137	A_2	8 %	30 %
S_8.0_180_B	217	$A_1\ \{F_{w,k}\}$	209	151	A_2	4 %	31 %
S_8.0_200_B	217	$A_1\ \{F_{w,k}\}$	209	165	A_2	4 %	24 %
S_8.2_160_B	189	$A_1\ \{F_{w,k}\}$	209	116	A_2	10 %	39 %
S6_7.0_160_B	311	$A_1\ \{F_{w,k}\}$	331	161	A_2	6 %	48 %
Pa_9.0_440_B	230	$A_1\ \{F_{c,k}\}$	188	333	$A_1\ \{F_{c,k}\}$	18 %	45 %
Pe_8.0_300_B	234	$A_1\ \{F_{c,k}\}$	178	210	$A_1\ \{F_{c,k}\}$	24 %	10 %
Pe_9.0_440_B	226	$A_1\ \{F_{c,k}\}$	188	308	$A_1\ \{F_{c,k}\}$	17 %	37 %
S_8.0_300_B	256	$A_1\ \{F_{c,k}\}$	209	235	$A_1\ \{F_{c,k}\}$	18 %	8 %
S_8.0_340_B	271	$A_1\ \{F_{c,k}\}$	209	263	$A_1\ \{F_{c,k}\}$	23 %	3 %
S_9.0_440_B	292	$A_1\ \{F_{c,k}\}$	229	333	$A_1\ \{F_{c,k}\}$	22 %	14 %
S6_9.0_440_B	455	$A_1\ \{F_{c,k}\}$	380	350	A_2	17 %	23 %

In the configurations with a specimen height of 540 mm the predicted failure mode, A_1, is confirmed by the test results in almost all cases. Only S6_9.0_440_B, the predictions are in disagreement with the test results. The overall predicted capacities deviate by approximately 20 %, according to test results.

Pa (Parallel) and Pe (Perpendicular) are two configurations where the screws are placed based on the grain direction. According to the obtained test results, a distinction in capacities is not observed. However, the configuration Pa and Pe have only an impact on A_2, where the failure mode did not occur.

Subsection 5.1.1 presents the predicted failure mode of each screw. The predicted failure mode of the screws is buckling, except for the screw WT-T 8.2 x 160 mm where withdrawal is the failure mode. In contrast to the predictions, all screws with a length of 160 mm failed due to withdrawal. In the case of 2 x HT-T 8.0 x 180 mm screws, the tendency of the failure mechanism is withdrawal and buckling. Accordingly, 4 x HT-T 8.0 x 180 mm has an apparent withdrawal failure. Similarly with HT-T 8.0 x 200 mm, the failure mode changes with the number of screws. The change in failure mode may indicate a higher load concentration with two screws. However, with four screws, the load is more evenly distributed over the contact area.

The variation of capacities between the load configurations may be caused by imperfections in the timber. Since the number of tests performed per configurations is minor, the test results reflect the tendency of capacities. Figure 7.1 and Figure 7.2 describes the test results in correlation with the design model. The curves show that A_1 is in accordance with the test results. In the event of a specimen height 540 mm, the deviation corresponding to A_1 is greater. However, the distinction is steady for all configurations.
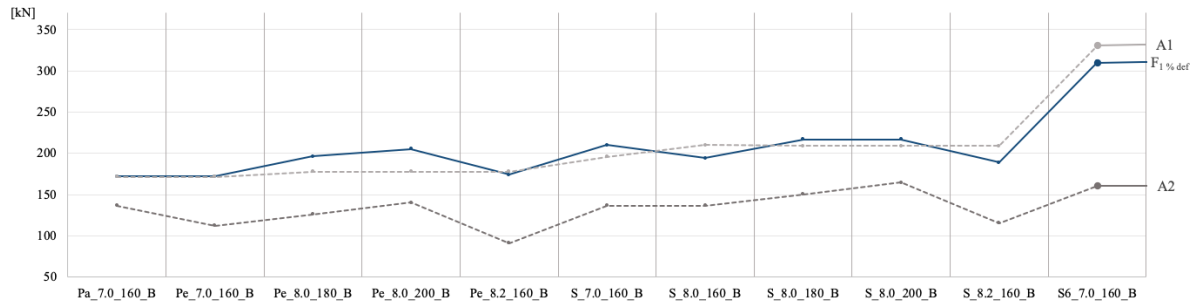
Figure 7.1: Load case B 225 mm specimen, comparison of design model and test result
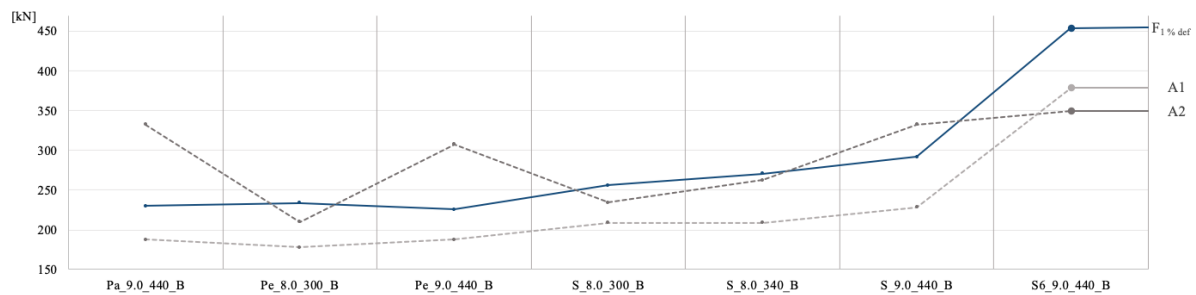
Figure 7.2: Load case B 540 mm specimen, comparison of design model and test result

7.1.3   Load case C

According to the tests, the predicted failure mode is not sufficiently confirmed. In the case of a specimen height 225 mm, the failure mode is withdrawal. Hence, this does not reflect the predictions. The deviation of the capacities, A_1 and A_2, in relation to test results is significant, 29 % and 35 %, respectively. The specimen height of 540 mm is the predicted failure mode corresponding to the test results. However, the predicted capacity has a significant deviation.

Table 7.3: Evaluation, test results and design model of load case C

Name	Test results		Design model			Deviation $\{F_{1\%def}\}$	
	$F_{1\%def}$ [kN]	Failure	A_1 [kN]	A_2 [kN]	Failure	A_1	A_2
Pe_7.0_160_C	173	$A_1 \{F_{w,k}\}$	108	112	$A_1 \{F_{c,k}\}$	37 %	35 %
Pe_8.2_160_C	169	$A_1 \{F_{w,k}\}$	115	91	A_2	32 %	46 %
S_7.0_160_C	192	$A_1 \{F_{w,k}\}$	133	137	$A_1 \{F_{c,k}\}$	31 %	29 %
S_8.0_160_C	191	$A_1 \{F_{w,k}\}$	147	137	A_2	23 %	29 %
S_8.2_160_C	183	$A_1 \{F_{w,k}\}$	146	116	A_2	20 %	37 %
Pe_9.0_440_C	229	$A_1 \{F_{c,k}\}$	125	308	$A_1 \{F_{c,k}\}$	46 %	34 %

Figure 7.3 describes the tendency of the test results in correlation with the design model. Both A_1 and A_2 have a constant deviation compared to the capacity achieved in the tests.
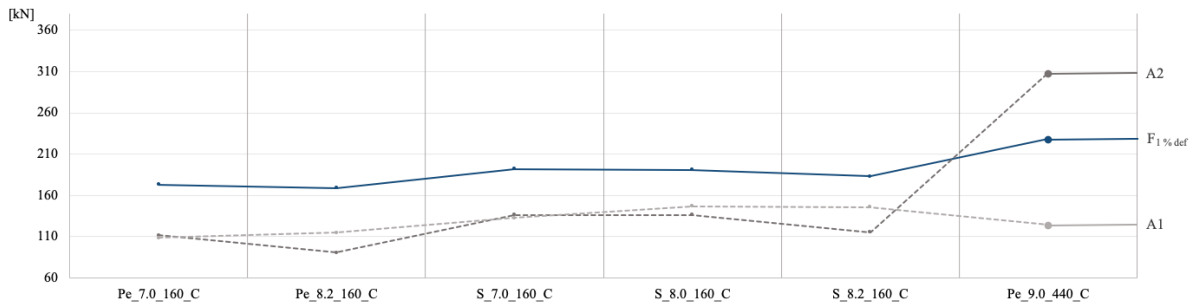
Figure 7.3: Load case C, comparison of design model and test result

7.1.4 Torx test

The purpose of the torx tests is to investigate the screw capacity without the timber contribution. Additionally, the torx tests can give an insight into how the load disperses to the screws and timber separately. The tests consider only the behavior of the screws. Consequently, only A_1 is evaluated. The model accounts for a small timber contribution due to the screw head, A_{11}, see Equation 3.9. The screw contribution, A_{12}, is given by the minimum of $F_{c,k}$ and $F_{w,k}$.

Table 7.4 displays the experimental and design results of the torx tests. Contrary to the previously reviewed tests, the maximum force achieved is applied, the reason being that the capacity of a screw is not based on 1 % deformation. The predicted failure mode corresponds to the test results, except VGZ 7.0 x 160 mm, where the failure mode is withdrawal. The decisive capacity of the design model is consistently lower compared to the test results. The mean deviation between the test results and the predicted capacity is 35 %.

Table 7.4: Evaluation, test results and design model of torx test

Name	Test results		Design model				Deviation $\{F_{max}\}$
	F_{max} [kN]	Failure	A_1 [kN]	$F_{c,k}$ [kN]	$F_{w,k}$ [kN]	A_{12}	A_1
T_7.0_160	21.9	$\{F_{w,k}\}$	13.4	12.2	17.1	$\{F_{c,k}\}$	39 %
T_8.2_160	21.3	$\{F_{w,k}\}$	16.8	17.0	15.4	$\{F_{w,k}\}$	21 %
T_8.0_160	28.3	$\{F_{c,k}\}$	18.3	15.4	18.7	$\{F_{c,k}\}$	35 %
T_8.0_180	29.2	$\{F_{c,k}\}$	18.3	15.4	21.0	$\{F_{c,k}\}$	37 %
T_8.0_200	27.5	$\{F_{c,k}\}$	18.3	15.4	23.4	$\{F_{c,k}\}$	33 %
T_8.0_300	26.0	$\{F_{c,k}\}$	18.3	15.4	35.1	$\{F_{c,k}\}$	30 %
T_8.0_340	28.5	$\{F_{c,k}\}$	18.3	15.4	39.7	$\{F_{c,k}\}$	34 %
T_9.0_440	40.8	$\{F_{c,k}\}$	22.1	20.4	55.6	$\{F_{c,k}\}$	46 %

The impact of the slenderness is considered by testing the HT-T screw with a constant diameter and different lengths. In all cases, the screw failed due to buckling. According to the design model, the buckling failure is dependent on the diameter of the screw and not the screw length. Hence, the predictions and the test results have a proper correlation. The failure modes in the torx tests for HT-T appears to be different compared to the load cases with these screws. The different behavior may be explained by the effect of the contact plate and the distribution of the load.

The screw capacities is presented in Figure 7.4. The tendency between F_{max} and the predictions is in agreement. Hence, the predictions are consistently lower. The timber contribution may increases the capacities slightly.
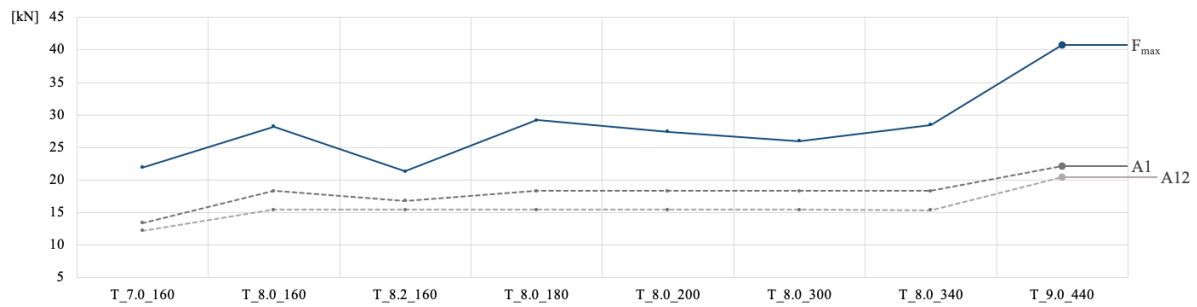
Figure 7.4: Torx test, comparison of design model and test result

7.1.5 Timber and screw contribution

The screw and timber contribution can be investigated separately by the torx test and the difference in the capacity between the test configurations. The timber contribution in the torx test is assumed to be negligible. The difference in capacity between the test configurations enlightens the increase in capacity due to the screws. These results can describe the accuracy of the timber (A_{11}) and screw contribution (A_{12}) in the design model.

The timber contribution is defined by the following Equation 7.1 and is calculated based on the screw capacity obtained by torx tests. However, this calculation is a rough approximation since the timber contribution in the torx tests is assumed neglected.

$$\text{Timber contribution} = \frac{(F_{1\%,def} - n \cdot F_{max})}{F_{1\%,def}} \tag{7.1}$$

Table 7.5 describes the timber contribution in load cases B and C with different screws. The columns named "*Timber*" are the contribution from the timber in Equation 7.1. The table shows a tendency of decreasing timber contribution with an increasing number of screws. This is confirmed in both the design model and test results. Through reducing the number of screws, more timber may be activated during the load application.

Table 7.5: Timber contribution of load cases B and C

Screw type	Test results					Design model			
	F_{max} {Torx}	$F_{1\%def}$ {2 screws}	$F_{1\%def}$ {4 screws}	Timber {2 screws}	Timber {4 screws}	A_{12}	A_{11}	Timber {2 screws}	Timber {4 screws}
VGZ 7.0x160 B	21.9	172	210	75 %	61 %	12.2	147	86 %	75 %
WT-T 8.2x160 B	21.3	174	189	77 %	55 %	15.4	147	83 %	70 %
HT-T 8.0x160 B	28.3	-	194	-	44 %	15.4	147	83 %	70 %
HT-T 8.0x180 B	29.2	196	217	72 %	48 %	15.4	147	83 %	70 %
HT-T 8.0x200 B	27.5	205	217	74 %	52 %	15.4	147	83 %	70 %
HT-T 8.0x300 B	26.0	234	256	78 %	59 %	15.4	147	83 %	70 %
HT-T 8.0x340 B	28.5	-	271	-	58 %	15.4	147	83 %	70 %
VGZ 9.0x440 B	40.8	228	292	65 %	45 %	20.4	147	78 %	64 %
VGZ 7.0x160 C	21.9	173	192	75 %	54 %	12.2	84	77 %	63 %
WT-T 8.2x160 C	21.3	169	183	75 %	53 %	15.4	84	73 %	58 %
HT-T 8.0x160 C	28.3	-	191	-	41 %	15.4	84	73 %	58 %

According to Table 7.5, the overall timber contribution from test results show a mean value of 74 % and 52 % with two and four screws, respectively. The timber contribution in the design model is 79 % and 66 %, with two and four screws. The design model predicts a greater timber contribution than the test results in load case B. In load case C, the number of performed tests is minor. However, the comparison of timber contribution between the design model and test results corresponds more.

Furthermore, even though load case C has a more accurate timber contribution compared to load case B, the capacities according to the test results in load cases B and C are close. The difference in predicted capacity between the load cases is the consideration of $k_{c,90}$.

Moreover, the difference in the capacity between the configurations with similar member height, load case, and load application area can be directly connected to the screws. This capacity is estimated by the difference in capacities between the test configurations. Equation 7.2 describes the model applied.

$$\text{Estimated capacity, one screw} = \frac{F_{1\%,def}\,(4\text{ screws}) - F_{1\%,def}\,(2\text{ screws})}{2} \tag{7.2}$$

Table 7.6 shows the estimated capacities of one screw for load cases B and C. The estimated capacities of the screws deviates from the test results of the torx tests. The deviation varies between 13 % and 78 %. By comparing the test results and the estimated capacity, the values do not coincides. The deviation in capacity may indicates a non-linear increase in capacity with the number of screws.

Table 7.6: Estimated values, screw capacity

Screw type	Test results			Estimated capacity	
	F_{max} {Torx}	$F_{1\%,def}$ {2 screws}	$F_{1\%,def}$ {4 screws}	A_{12}[a] [kN]	Deviation {F_{max}}
VGZ 7.0x160 B	21.9	172	210	19.0	13 %
WT-T 8.2x160 B	21.3	174	189	7.5	65 %
HT-T 8.0x180 B	29.2	196	217	10.5	64 %
HT-T 8.0x200 B	27.5	205	217	6.0	78 %
HT-T 8.0x300 B	26.0	234	256	11.0	58 %
VGZ 9.0x440 B	40.8	228	292	32.1	21 %
VGZ 7.0x160 C	21.9	173	192	9.5	57 %
WT-T 8.2x160 C	21.3	169	183	7.0	67 %
HT-T 8.0x160 B	28.3	-	194	-	-
HT-T 8.0x340 B	28.5	-	271	-	-

[a] Calculated according to Equation 7.2.

Figure 7.5 displays the estimated value per screw and the test results obtained by torx test. The figure emerges a greater capacity of the test results compared to the estimated capacity.
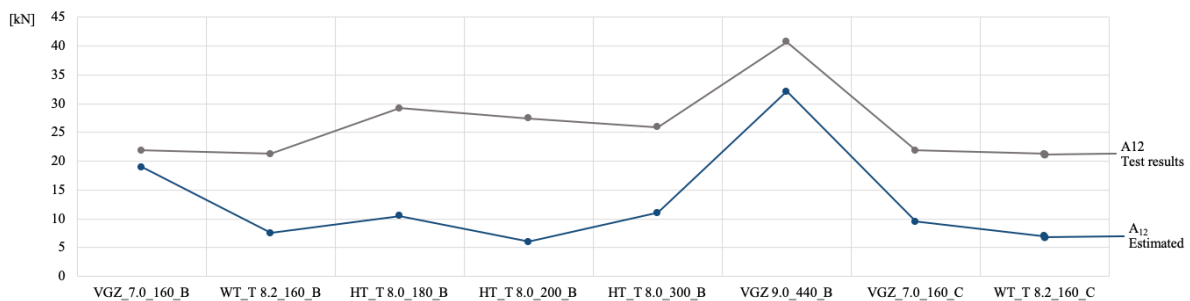
Figure 7.5: Estimated screw capacity and test result

7.1.6   Summary of evaluation

The evaluation of the test results presents a good correlation between the capacities of test results and A_1 for load case B. There is a greater deviation between the test results and the design model in load case C. The failure mode achieved for all tests is according to A_1 for load cases B and C. However, some of the predicted failure modes appear to be different from the results of the experimental campaign. In the event of shorter screws, the predicted failure mode is mostly buckling, while the achieved failure mode is withdrawal. In addition, there are some inaccuracies in the design model when considering the timber and screw contribution separately.

Figure 7.6 displays the obtained test results in accordance with the predicted capacity of A_1. The predicted capacity is presented as the grey line along the xy-axis. Furthermore, the test results are represented along the y-axis. Accordingly, the correlation is strong if the test results and the prediction coincides. In load case C, the capacity of the test results is higher for all configurations. Load case B shows a proper correlation between the test results and the design model. Nevertheless, the test results are higher for some configurations in load case B. The diagram shows that the test results are overall higher than the predictions.
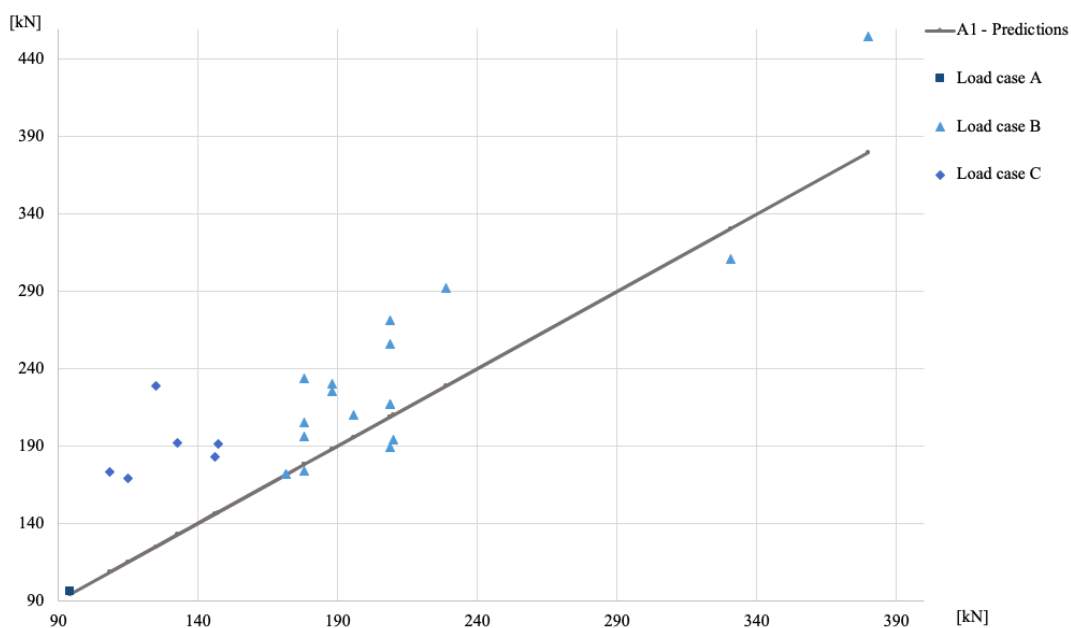
Figure 7.6: Predictions according A1 and test result

The test results for load cases B and C are within the same range of capacity. Table 7.7 presents the maximum force at 1 % deformation for both load cases. According to the table, the deviation between the capacity in the two load cases is small. However, the predicted capacity in the design model shows a great difference. The definition of the load arrangement factor, $k_{c,90}$, results in a jump in capacity. Accordingly, the timber contribution is 1.75 times higher in load case B compared to load case C. This does not reflect the test result.

Table 7.7: Comparison of test result for load case B and load case C

Load case B		Load case C		
Name	$F_{1\%def}$ [kN]	Name	$F_{1\%def}$ [kN]	Deviation [kN]
Pe_7.0_160_B	172	Pe_7.0_160_C	173	1
Pe_8.2_160_B	174	Pe_8.2_160_C	169	5
S_7.0_160_B	210	S_7.0_160_C	192	18
S_8.0_160_B	194	S_8.0_160_C	191	3
S_8.2_160_B	189	S_8.2_160_C	183	6
Pe_9.0_440_B	226	Pe_9.0_440_C	229	4

Figure 7.7 presents the test results in correlation with A_2. Similar to Figure 7.6 the prediction of A_2 is presented as the grey line. Both load cases B and C have a deviation between the test results and the predictions. However, the achieved failure mode is not according to A_2. Consequently, it can be assumed that the capacity of A_2 is higher than the test results for load cases B and C.
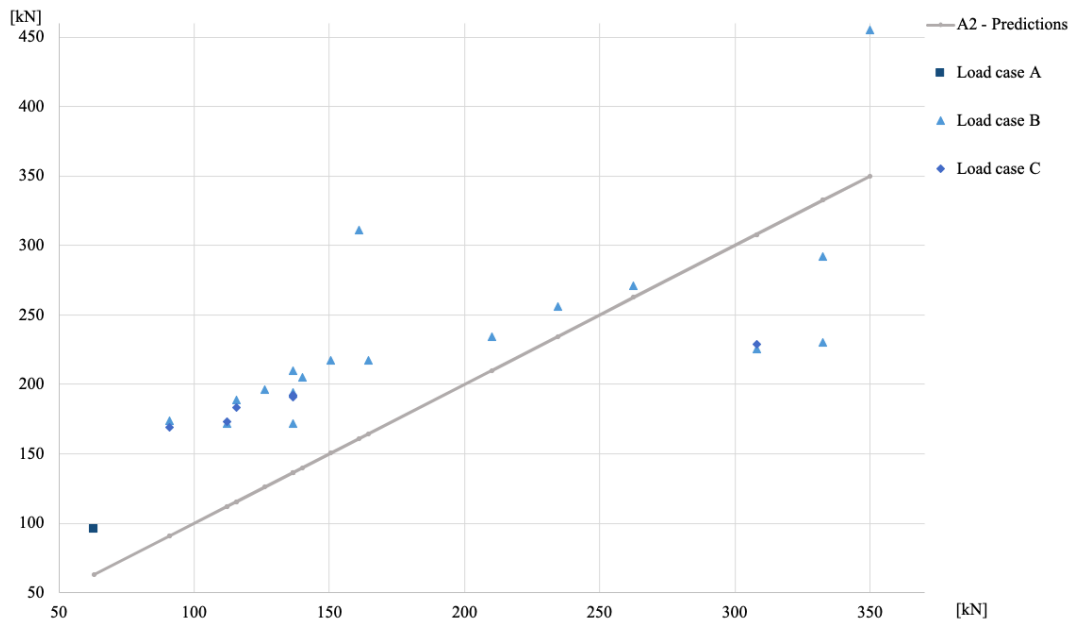
Figure 7.7: Predictions according A2 and test result

The capacities achieved by the design model have a deviation compared to the test results. However, the prediction of the capacity according to the design model is conservative. In some cases, the capacity is reduced significantly due to A_2. In section 3.4, earlier investigations is presented. The comparison between earlier investigation and prEN 1995 confirms the inaccuracy of A_2. Both the comparison with test performed by Reichegger and Nilsson shows that the capacity of A_2 is overly conservative. Additionally, the failure modes achieved in the tests performed by Reichegger supports the consideration of the accuracy concerning A_1. Further, an improvement of the design model is proposed, due to the great extent of reduction.

7.2 Harmonization of the design model

Based on the deviation between the test results and the design model, this section considers the possibility of harmonizing A_1 and A_2. The harmonization and decisions are made with a background in the experimental evaluation and earlier investigations performed by different researchers.

In the event of the harmonization, the two approaches for reinforced and non-reinforced members in prEN 1995 are considered. The determination of the CPG capacity of timber for non-reinforced and reinforced members is based on different theories. The design model for non-reinforcement, presented in section 2.6, describes $k_{c,90}$ as the dispersion of the load. In addition, the factor k_p considers an increase in capacity at different levels of deformation. The design model for reinforcement, section 3.2, describes $k_{c,90}$ as a coefficient accounting for risk of splitting and deformation. The background for the coefficient is the transition between the SLS and ULS.

The design model of non-reinforced members reflects the theory of plasticity. The capacity increases in the plastic range as a result of the timber structure and its properties. This is applicable for CPG due to the behavior of the fibers; instead of collapsing the fibers are crushed. The possibility of utilizing the increased capacity in the plastic range is not acceptable with steel since the material has a defined ultimate load. Consequently, it is not applicable to use the increase in capacity due to the deformation of reinforced members. In ULS the deformation applied according to non-reinforced members is equal 2.5 %. The reinforced members will not achieve a deformation at 2.5 %. According to the test results, failure occurs at approximately 1 % deformation. However, a k_p-factor equal to 1.0 is representative in the case of reinforced members.

Accordingly, $k_{c,90}$ applies in the design model of non-reinforced members to describe the spreading of the load at a certain depth, based on an effective height. In the case of reinforcement, the failure occurs near the contact area. The failure is either along the length of the screw or near the screw's head. A harmonization with $k_{c,90}$ corresponding to the non-reinforced design model will result in an arbitrary position of the failure plane for reinforced members. This position does not represent reality. Hence the design model of reinforced members, A_1, is incompatible with the design model of non-reinforced members.

Furthermore, based on the test evaluation, the current design model is conservative, and there is a potential to increase the capacity. The following section presents two proposals. These proposals are based on an evolution of the current design model.

7.2.1 Proposal 1

A_1 in prEN 1995 is evaluated based on; the strength and properties of timber, the load arrangement, and the screw contribution. The load arrangement factor, $k_{c,90}$, is determined by considering the load cases. Based on the experimental tests, the capacity of A_1 is considered unrelated to the load cases. Hence, $k_{c,90}$ considers equal for both load cases B and C. An adaption of $k_{c,90}$ equal 1.75 is adequate, referrer Equation 7.4.

A_2 is the decisive capacity for most configurations evaluated in section 7.1. The capacity is determined based on the timber strength and the effective spreading length due to the screw length. Failure corresponding to A_2 results in expansion of the timber and rift at the screw tips. The $k_{c,90}$ factor accounts for the risk of splitting by a transition of the capacity from SLS to ULS. Considering the failure mode, $k_{c,90}$ should be accounted for in A_2. In accordance with A_1, the considered capacity, A_2, is unaffected by the load cases. $k_{c,90}$ in A_2 is therefore equivalent as in A_1. Equation 7.3 shows the proposed adaption.

$$\text{Proposal } 1 = \min \begin{cases} k_{c,90} \cdot b_c \cdot l_{ef,1} \cdot f_{c,90,k} + n \cdot \min \{F_{w,k}, F_{c,k}\} \\ k_{c,90} \cdot b \cdot l_{ef,2} \cdot f_{c,90,k} \end{cases} \tag{7.3}$$

Where:

$$k_{c,90} = 1.75 \tag{7.4}$$

Table 7.8 presents the proposed design model in context with the executed tests and the failure according to the calculated predictions. In this context, there is a better correlation between the predicted failure mode and the failure of the tests. Additionally, the mean deviation between the prediction in the design model and the test result is reduced from 36 % to 8 % with respect to load case C. Nevertheless, some disagreement with the prediction of the failure mode occurs. However, the deviation between A_1 and A_2 in these configurations is minor. Appendix C, section C.6 shows the procedure of calculation.

Table 7.8: Evaluation, Proposal 1

Name	Design model, Proposal 1					Deviation $\{F_{1\% \, def}\}$	
	A_{11} [kN]	A_{12} [kN]	A_1 [kN]	A_2 [kN]	Failure	A_1	A_2
Pe_8.2_160_A	110	31	141	110	A_2	47 %	15 %
Pa_7.0_160_B	147	24	171	239	A_1	0.3 %	39 %
Pe_7.0_160_B	147	24	171	196	A_1	0.3 %	14 %
Pe_8.0_180_B	147	31	178	221	A_1	9 %	13 %
Pe_8.0_200_B	147	31	178	245	A_1	13 %	20 %
Pe_8.2_160_B	147	31	178	159	A_2	2 %	8 %
S_7.0_160_B	147	49	196	239	A_1	7 %	14 %
S_8.0_160_B	147	62	209	239	A_1	8 %	23 %
S_8.0_180_B	147	62	209	263	A_1	4 %	21 %
S_8.0_200_B	147	62	209	288	A_1	4 %	33 %
S_8.2_160_B	147	62	209	202	A_2	10 %	7 %
S6_7.0_160_B	257	73	330	282	A_2	6 %	9 %
Pa_9.0_440_B	147	41	188	582	A_1	18 %	153 %
Pe_8.0_300	147	31	178	368	A_1	24 %	57 %
Pe_9.0_440_B	147	41	188	539	A_1	17 %	139 %
S_8.0_300_B	147	62	209	410	A_1	18 %	60 %
S_8.0_340_B	147	62	209	459	A_1	23 %	70 %
S_9.0_440_B	147	82	229	582	A_1	22 %	99 %
S6_9.0_440_B	257	122	380	625	A_1	17 %	37 %
Pe_7.0_160_C	147	24	171	196	A_1	0.9 %	13 %
Pe_8.2_160_C	147	31	178	159	A_2	5 %	6 %
S_7.0_160_C	147	49	196	239	A_1	2 %	24 %
S_8.0_160_C	147	62	209	239	A_1	9 %	25 %
S_8.2_160_C	147	62	209	202	A_2	14 %	10 %
Pe_9.0_440_C	147	41	188	539	A_1	18 %	135 %

7.2.2 Proposal 2

Reviewing the failure mode and the literature of reinforced members, an additional modification is proposed of the design model. In accordance with proposal 1 the equation of A_1 is unchanged, however A_2 is evaluated considering the concentrated stress area located close to the tip of the screws. Line of reasoning of this approach is to give a new point of view by evolving the current equation of A_2.

In the study of Dietsch [22], the stress distribution in reinforced timber members is described in an numerical model. The study recognizes a considerable variation of stress along $l_{ef,2}$. A stress concentration appears at the tip of the screws. Given a new perspective of the effective spreading due to the concentrated stress a new proposal considering $l_{ef,3}$ is suggested.

The failure of A_2 is assumed to be caused by exceeding the timber capacity due to the load transition between the screws and the timber. In section 7.1 the contribution from the screw and timber is evaluated. Accordingly, the proposal is derived based on this load transition. Further, the procedure of the proposal is presented.

Equation 7.5 is the timber capacity, with no effect of the screws.

$$F_{c,90,k} = k_{c,90} \cdot l_{ef} \cdot b_c \cdot f_{c,90,k} \tag{7.5}$$

Further, Equation 7.6 and Equation 7.7 is a modification of Equation 7.5. A load transition factor c and the length $l_{ef,3}$ is introduced. The load transition factor accounts for the ratio of stress transferred to the screws. The effective spreading length, $l_{ef,3}$, is the length of the stress concentration at the tip of the screws. $k_{c,90}$ is considered equal to 1.75.

$$c_{screw} \cdot F_{c,90,k} = k_{c,90} \cdot l_{ef,3} \cdot b_c \cdot f_{c,90,k} \tag{7.6}$$

$$F_{c,90,k} = k_{c,90} \cdot l_{ef,3} \cdot b_c \cdot f_{c,90,k} \cdot \frac{1}{c_{screw}} \tag{7.7}$$

Where:

$$c = \frac{1}{c_{screw}} = \frac{1}{0.48} = 2.1 \tag{7.8}$$

$$l_{ef,3} = (n_0 - 1) \cdot a_1 + \min\{a_{3,c}, a_1\} + a_1 \tag{7.9}$$

$$k_{c,90} = 1.75 \tag{7.10}$$
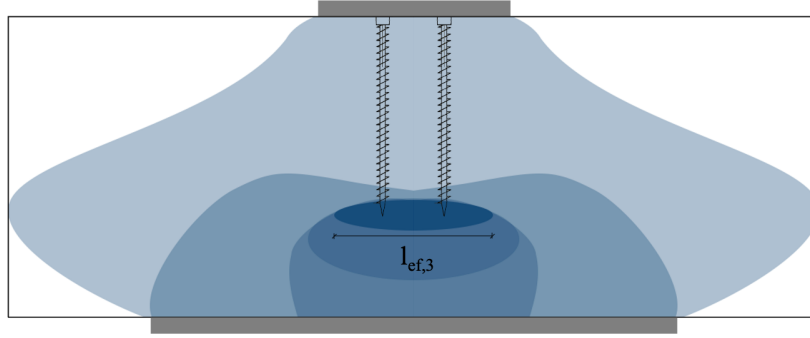
Figure 7.8: Description of $l_{ef,3}$ and illustration of the stress concentration, intermediate support

The modified effective length, $l_{ef,3}$, is calculated with respect to the intermediate distances between the screws, see Figure 7.8. Additionally, the stresses will disperse gradually outwards on both sides of the screw group. This is taken into account with the assumption that the concentrated stress will be limited to a distance of a_1 within the limit of the loaded edge. Equation 7.9 is the proposed formula for the effective length, both for intermediate and edge supports.

A load transition factor, c, corresponding to the screws contribution is implemented due to the load dispersion from the contact plate. According to subsection 7.1.5 the load is transferred by the contact plate to both the timber and the screw. In proportion to apply $l_{ef,3}$ the load transferred from the screw is essential. Therefore a factor c is implemented, which accounts for the redistribution of the load. The factor is based on the test results obtained by the torx test and Table 7.5. Given the table, the mean timber contribution is 74 % and 52 % for two and four screws, respectively. Consequently, the screw contribution is 26 % and 48 %. The maximum value is applied to determine the factor c, with the consideration of a conservative approach, see Equation 7.8.

Based on the derivation of A_1 and A_2, the second proposal for the design model is presented in Equation 7.11.

$$Proposal\ 2 = \min \begin{cases} k_{c,90} \cdot b_c \cdot l_{ef,1} \cdot f_{c,90,k} + n \cdot \min\{F_{w,k}, F_{c,k}\} \\ k_{c,90} \cdot b \cdot l_{ef,3} \cdot f_{c,90,k} \cdot c \end{cases} \tag{7.11}$$

Table 7.9 presents the proposed design model in context with the executed tests and the failure according to the predictions. The design model is accurate in most cases regarding the failure modes. For two load configurations the predictions deviate from the achieved failure mode, however the deviations is minor between the predictions of A_1 and A_2, where the difference is 8 kN. Appendix C, section C.7 shows the procedure of calculation.

Table 7.9: Evaluation, Proposal 2

Name	Design model, Proposal 2					Deviation $\{F_{1\% \, def}\}$	
	A_{11} [kN]	A_{12} [kN]	A_1 [kN]	A_2 [kN]	Failure	A_1	A_2
Pe_8.2_160_A	110	31	141	77	A_2	47 %	20 %
Pa_7.0_160_B	147	24	171	270	A_1	0.3 %	57 %
Pe_7.0_160_B	147	24	171	180	A_1	0.3 %	5 %
Pe_8.0_180_B	147	31	178	180	A_1	9 %	8 %
Pe_8.0_200_B	147	31	178	180	A_1	13 %	12 %
Pe_8.2_160_B	147	31	178	180	A_1	2 %	3 %
S_7.0_160_B	147	49	196	270	A_1	7 %	29 %
S_8.0_160_B	147	62	209	270	A_1	8 %	39 %
S_8.0_180_B	147	62	209	270	A_1	4 %	24 %
S_8.0_200_B	147	62	209	270	A_1	4 %	24 %
S_8.2_160_B	147	62	209	270	A_1	10 %	43 %
S6_7.0_160_B	257	73	330	360	A_1	6 %	16 %
Pa_9.0_440_B	147	41	188	270	A_1	18 %	17 %
Pe_8.0_300	147	31	178	180	A_1	24 %	23 %
Pe_9.0_440_B	147	41	188	180	A_2	17 %	20 %
S_8.0_300_B	147	62	209	270	A_1	18 %	6 %
S_8.0_340_B	147	62	209	270	A_1	23 %	0.3 %
S_9.0_440_B	147	82	229	270	A_1	22 %	7 %
S6_9.0_440_B	257	122	380	360	A_2	17 %	21 %
Pe_7.0_160_C	147	24	171	180	A_1	0.9 %	4 %
Pe_8.2_160_C	147	31	178	180	A_1	5 %	7 %
S_7.0_160_C	147	49	196	270	A_1	2 %	41 %
S_8.0_160_C	147	62	209	270	A_1	9 %	41 %
S_8.2_160_C	147	62	209	270	A_1	14 %	48 %
Pe_9.0_440_C	147	41	188	180	A_2	18 %	21 %

7.2.3 Sensitivity analysis

A sensitivity analysis is performed with respect to Proposal 1 and Proposal 2. The varying parameters and geometrical descriptions are consistent with the sensitivity study of reinforced members, presented in section 4.3. The analysis considers a symmetrical screw arrangement with four screws. Consequently, by adapting $k_{c,90}$ equal 1.75 for both load cases B and C, the load cases are identical in terms of the calculated capacities.

Figure 7.9 presents the performance corresponding to the first proposal. Figure 7.9 a) shows the minimum of A_1 and A_2, while Figure 7.9 b) shows the Equation 7.3 separated. Consequently, by increasing the length of the screw, the decisive capacity is A_1. Furthermore, for short screws, the decisive capacity corresponds to A_2. Therefore, the performance is according to the description of failure mode in section 3.3. According to Figure 7.9 b), A_2 increases linearly due to the length of the screw and is constant in relation to the diameter. The tendency of A_2 is equal to the design model in prEN 1995. However, the capacity is increased by introducing $k_{c,90}$. The complete procedure of the sensitivity analysis of Proposal 1 is given in Appendix B, section B.5.
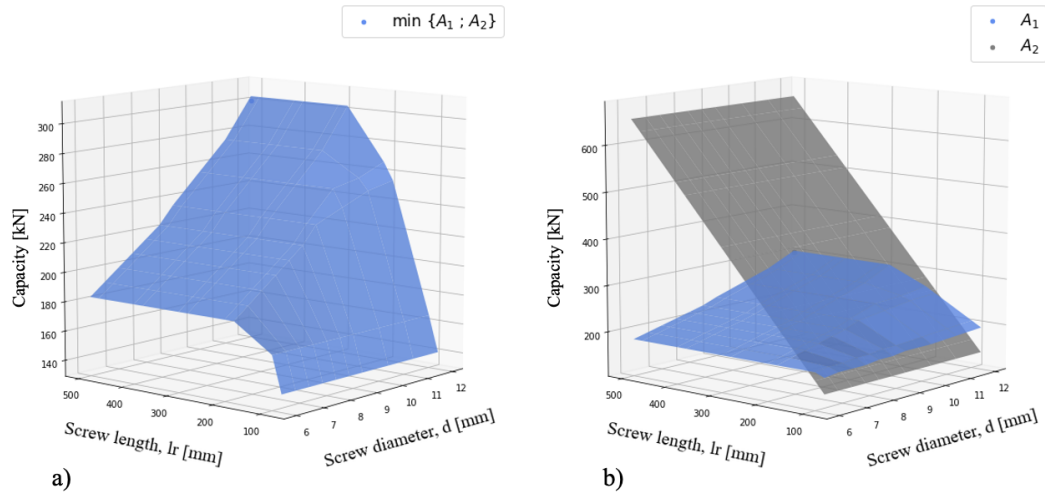
Figure 7.9: Sensitivity analysis, Proposal 1, load cases B and C

Figure 7.10 a) displays the performance corresponding to Proposal 2, and Figure 7.10 b) shows the Equation 7.11 separated. A_1 is unchanged compared to Proposal 1 (Note: the magnitude of the axis in Figure 7.9 b) and 7.10 b) is does not coincide). A_2 is dependent on the screw arrangement. Since the spacing and amount of screws are constant, the capacity is steady. The decisive capacity is due to A_2 if the diameter increases, otherwise A_1 is the decisive capacity. The complete procedure of the sensitivity analysis of Proposal 1 is given in Appendix B, section B.6
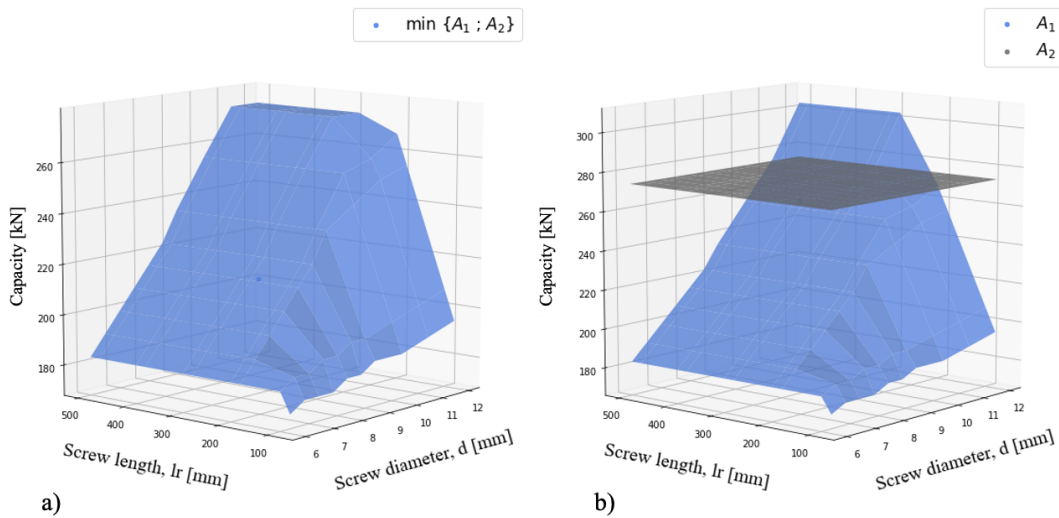
Figure 7.10: Sensitivity analysis, Proposal 2, load cases B and C

7.2.4 General comments to harmonization

Chapter 7 is a presentation of the design model and the influence of various parameters. Studying the experimental results against the design model, there is a potential to take advantages of greater capacities when designing timber members subjected to CPG with reinforcement. Through the work of evaluating the design model, experimental data have been applied. The harmonization is based on empirical evaluations. Nonetheless, the data derived in chapter 6 does not represent a great number of repetitive tests, whereby a variety of configurations have been preferred. Further studies are required to ascertain the reliability and robustness of proposals made in this work.
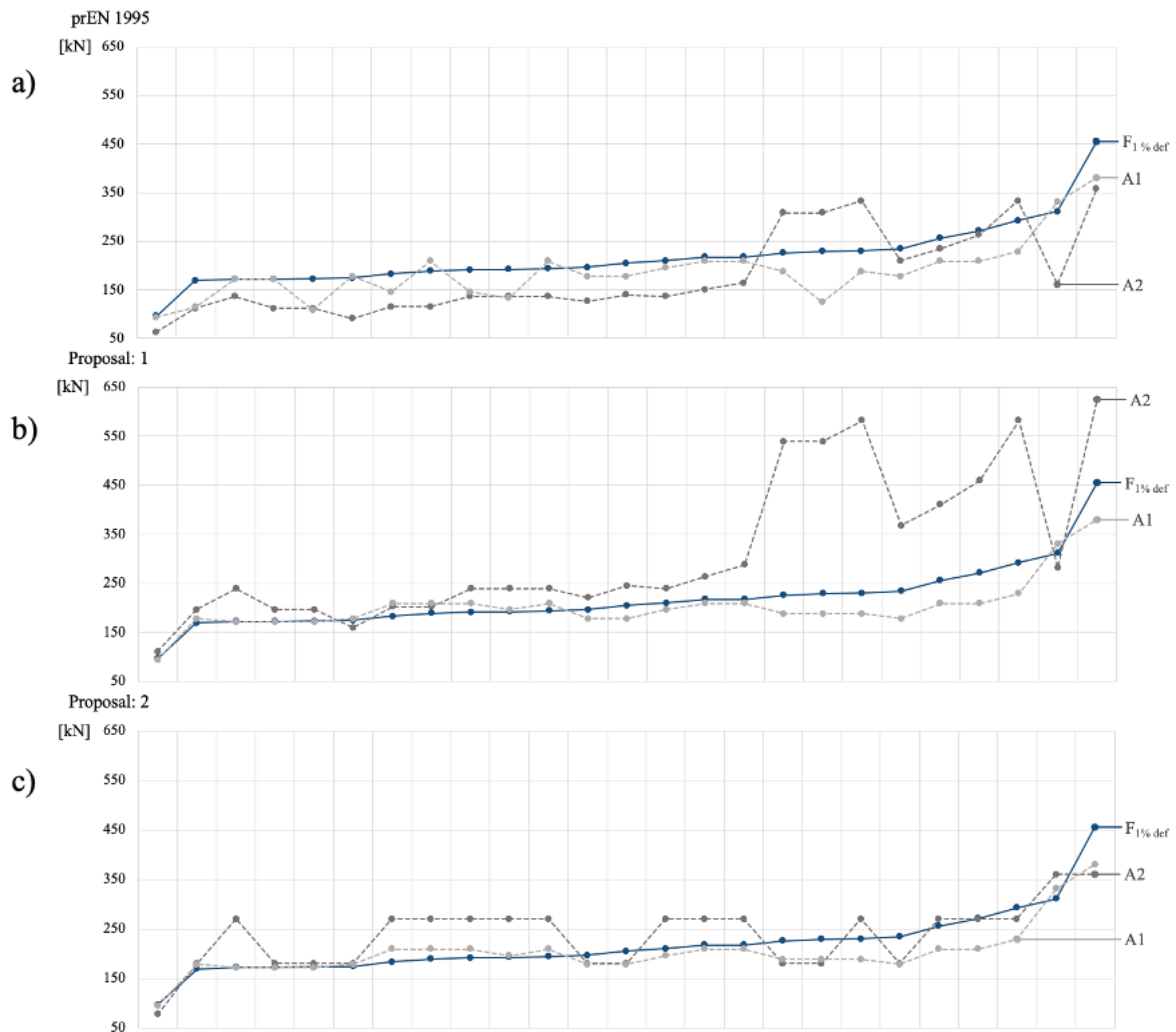
Figure 7.11: Test results and predictions of prEN 1995, Proposal 1 and Proposal 2

Figure 7.11 presents a) prEN 1995, b) Proposal 1 and, c) Proposal 2. Each diagram presents the accomplished tests results in relation with the design model, A_1 and A_2. The test result is presented in an increasing sequence and not sorted within the load cases.

Proposal 1 shows that A_1 is the decisive capacity in almost all cases. The tendency of the decisive capacity shows a proper correlation with the failure mode compared to prEN 1995. The overall adjustment in the proposal is more adequate in relations to the experimental results. The tendency of the graph A_2 display a jump in the predictions, this is due to the increase of the screw length.

Proposal 2 displays similar trend regarding the decisive capacity as Proposal 1. The design model is derived from the experimental tests. The tendency of the graph shows that the capacity of both A_1 and A_2 are approximately the same and reflects the test results. The capacity of A_2 is equal for some cases, due to the screw arrangement. The load transition factor, c, is determined from the ratio of the load distribution to the timber and the screws. Hence, factor is depending on the number of screws, screw arrangement and loading area. Consequently, the factor may not be applicable for other situations. To validate the factor, further investigation is required.

A_1 is equal for both proposals. In the presented evaluation the deviation regarding load case C in prEN 1995 is addressed. The overall adjustment of A_1 is more adequate in relation to the experimental results. The effect of longer beams is not accounted for in the conducted tests. Hence, bending may occur and affect the capacity at the support, which can cause a reduction in the bearing strength. The study of Karlsruhe has conducted tests according to load cases C and H. The preliminary study of load cases C and H performed in section 3.4 considering $k_{c,90}$ equal to 1.0. However, the investigations shows that the design model predicts a lower capacity compared to the test results. This supports the theory of consider $k_{c,90}$ equal to 1.75 instead of 1.0. In addition, the tests performed by Reichegger and Nilsson consider load case B. Accordingly, $k_{c,90}$ is equal to 1.75. The comparison of the tests of Reichegger and the design model shows a proper correlation. With background of the experimental study and preliminary investigation, the use of $k_{c,90}$ equal to 1.75 is adequate for both load cases B and C.

A_2 in the two proposals are based on a different consideration of the stress at the tip of the screws. In Proposal 1, the capacity of A_2 increases if the screw length or number of screws increases. However, in Proposal 2 the capacity increases if the number of screws or the distances between the screws increases. In both proposal of A_2, $k_{c,90}$ is considered equal to 1.75. Since A_2 of Proposal 1 increases linearly with the length of the screws, the difference in capacity between the A_1 and A_2 can be significant, compared with Proposal 2.

The failure of timber is not achieved in the experimental test for load cases B and C. The two proposal of A_2 can not be evaluated with the test results. Despite of not achieving the failure mode, the design model in prEN 1995 proposes A_2 as the decisive capacity. This implies that the capacity of A_2 should be increased.

8. Final remarks

8.1 Conclusion

The scope of this master thesis is to validate and strengthen the knowledge concerning the design model of reinforced glulam members subjected to CPG (compression perpendicular to the grain) in Eurocode 5. The work concerns an empirical assessment, and experimental campaign. The test specimens have varying geometry, load case, and screw arrangement. Furthermore, the predicted capacity and failure modes according to the design model are evaluated in relation with the test results. Established by the evaluation and the preliminary investigation, a harmonization of the design model is proposed. The experimental results show that using threaded screws as reinforcement, effectively increases the capacity of timber subjected to CPG. The following research questions are being answered throughout this work.

- What is the level of accuracy, reliability, and robustness of the design model for CPG of reinforced members in prEN 1995?

The experimental tests do not confirm the predictions regarding failure modes and capacities for all configurations. In the configurations where A_2 represents the decisive capacity, the predictions do not correspond with the tests. According to A_1, the predicted capacities coincide with the test results for load case B. However, in load case C, the predicted capacity is consistently lower, but the tendency corresponds to the test results. The overall predicted failure mode of A_1 is mainly confirmed, except for the shorter screws. Despite some inaccuracies in A_1, the model is reliable and accurate. Evaluating the complete design model, A_1 and A_2, concludes that the model is overly conservative.

- Is it possible to harmonize the proposed approaches for reinforced and non-reinforced members subjected to CPG?

The design models of non-reinforced and reinforced members are based on diverse theories regarding k_p and $k_{c,90}$. The material behavior factor, k_p, defines the allowable deformation, given an increase of capacity with the level of deformation. In ULS, members are designed to enable 2.5 % deformation. However, failure appears at approximately 1 % deformation for reinforced members. Additionally, for non-reinforced members $k_{c,90}$, describes the load dispersion due to the member height and support conditions. The failure plane of the non-reinforced and reinforced members do not coincide. This causes an arbitrary position of the failure plane for reinforced members. Hence, k_p and $k_{c,90}$, according to the design model of non-reinforcement, are not applicable for reinforced members. Due to the incompatibility of the harmonization, two proposals are presented with an empirical assessment, to bridge the gap of the predicted capacity.

Proposal 1 is a modification of the design model in prEN 1995. The load arrangement factor, $k_{c,90}$, is introduced in A_2. In the event of load cases B and C, A_1 and A_2 consider $k_{c,90}$ equal to 1.75. The predictions correspond to the experimental tests. However, the difference in capacity between A_1 and A_2 can be significant regarding longer screws. The predictions of A_2 are not confirmed by experimental tests since the failure mode is not observed for load cases B and C.

Proposal 2 is a modification of the design model in prEN 1995. The load arrangement factor, $k_{c,90}$, is introduced in A_2. $k_{c,90}$ considers equal to 1.75 for load cases B and C in both A_1 and A_2. In addition, a load transition factor, c, and the effective length of stress concentration, $l_{ef,3}$, are introduced in A_2. The load transition factor is evolved based on the torx tests. The predictions according to Proposal 2 confirm mostly the experimental results. For some situations, the predicted failure mode is not correct. However, the tendency of the capacities for both A_1 and A_2 is within the range of the test results. Experimental tests do not confirm the prediction of A_2 since the failure mode did not occur for load cases B and C.

Finally, this thesis strengthens the scientific data regarding reinforced members subjected to CPG. The study confirms that there is a potential to evolve the design model in prEN 1995. The predictions according to the model do not correspond to the experimental results for all configurations. Accordingly, Proposal 2 enlightens another aspect of the stress consideration at the tip of the screws. There is potential of adapting Proposal 2 in Eurocode 5.

8.2   Further work

In the work of validating the design model in prEN 1995, the following recommendations are made:

- In addition to this study, other design situations should be investigated. An extension of the study will lead a deeper knowledge of the reliability regarding the design model. Other factors, such as the effect of different load cases, geometries and configurations, can lead to other results than the ones obtained. Longer beams may reveal the effect of bending, which can results in reduced bearing capacity. The failure according to A_2 is not observed, except for load case A. A detailed investigation of A_2 is recommended.

- The study is not confirmed by numerical analysis. A detailed numerical analysis should be carried out to confirm the experimental study and the sensitivity analysis.

Bibliography

[1] G. Glasø, 'Fleretasjes trehus,' *Fokus på tre*, no. 32, Jan. 2011. [Online]. Available: https://www.treteknisk.no/publikasjoner/fokus-pa-tre/32--fleretasjes-trehus.

[2] L. Bugge, 'Bruk av tre i offentlige bygg,' Feb. 2016. [Online]. Available: https://d21dbafykfdck9.cloudfront.net/1481729588/bruk-av-tre-i-offentlige-bygg.pdf.

[3] S. Leknes and S. A. Løkken, 'Befolkningsframskrivinger for kommunene, 2020-2050,' *Tall som forteller*, no. 27, Aug. 2020. [Online]. Available: https://www.ssb.no/befolkning/artikler-og-publikasjoner/_attachment/429172?_ts=173fc97ddf0.

[4] *Timber structures - Glued laminated timber and glued solid timber - Requirements*. NS-EN 14080:2013+NA:2016, Dec. 2016.

[5] I. Bejtka, 'Verstärkung von bauteilen aus holz mit vollgewindeschrauben,' Band 2 der Reihe Karlsruher Berichte zum Ingenieurholzbau, Doctoral Thesis, Fakultät für Bauingenieur-, Geo- und Umweltwissenschaften, Universität Fridericiana zu Karlsruhe, Karlsruhe, Germany, 2005. DOI: 10.5445/KSP/1000003354.

[6] S. Hicks, 'Second generation of the structural eurocodes,' Presented at Conference: Institution of Civil Engineers East & West Midlands webinar, Jul. 2020. DOI: 10.13140/RG.2.2.13415.47524.

[7] J. Porteous and A. Kermani, "*Bearing (Perpendicular to the grain),*" *in Structural timber design to Eurocode 5*, 2nd ed. West Sussex, United Kingdom, 2013, Section 4.5.3.

[8] A. Harte, 'Chapter 60: Timber engineering: An introduction,' *ICE manual of Construction Materials*, pp. 707–715, Jan. 2009. [Online]. Available: https://www.icevirtuallibrary.com/doi/abs/10.1680/mocm.35973.0707.

[9] B. Kucera, 'Treets oppbygning og vedanatomi,' vol. 1, pp. 1–60, 1998. [Online]. Available: https://nmbu.brage.unit.no/nmbu-xmlui/handle/11250/2598521.

[10] K. Persson, 'Micromechanical modelling of wood and fibre properties,' Doctoral Thesis, Department of Mechanics and Materials, LTH, Lund University, Lund, Sweden, 2000. DOI: 10.13140/RG.2.1.1389.7685.

[11] Swedish Wood, "*Structural properties of sawn timber and engineered wood products*", *Design of timber structures*, vol. 1, 2nd ed. Swedish Forest Industries Federation, Stockholm, Sweden, 2016, Chapter 2, pages 26–67.

[12] Forening, Norske Limtreprodusenters, "*Rette bjelker og søyler*", *Limtreboka*, vol. 2. Norske Limtreprodusenters Forening, Norway, 2015, Chapter 4, pages 67–70.

[13] Rice University, "*Elasticity and Plasticity*", *University Physics*, vol. 1. OpenStax, Houston,TX, USA, Sep. 2016, Section 12.4, pages 597–598.

[14] *Timber structures - Structural timber and glued laminated timber - Determination of some physical and mechanical properties*. NS-EN 408:2010+A1:2012, Oct. 2012.

[15] A. Leijten, S. Franke, P. Quenneville and R. Gupta, 'Bearing strength capacity of continuous supported timber beams: Unified approach for test methods and structural design codes,' *Journal of Structural Engineering*, vol. 138, no. 2, pp. 266–272, Feb. 2012. DOI: 10.1061/ (ASCE)ST.1943-541X.0000454.

[16] A. Leijten, 'The bearing strength capacity perpendicular to grain of norway spruce – evaluation of three structural timber design models,' *Construction and Building Materials*, vol. 105, pp. 528–535, Feb. 2016. DOI: 10.1016/j.conbuildmat.2015.12.170.

[17] E. Suenson, 'Zulässiger druck auf querholz,' *Holz als Roh-und Werkstoff*, vol. 1, no. 6, pp. 213–216, 1938. DOI: 10.1007/BF02612242.

[18] M. Reichegger, 'Compressione ortogonale alle fibre negli elementi strutturali lignei secondo le nuove proposte di normative,' Master thesis, Facoltà di Ingegneria, Università degli Studi di Trento, Trento, Italy, Oct. 2004.

[19] *Eurocode 5: Design of timber structures - Part 1-1: General - Common rules and rules for buildings*. NS-EN 1995-1-1:2004+A1:2008+NA:2010, Jul. 2010.

[20] *Eurocode 5: Consolidated draft prEN 1995-1-1*. prEN 1995-1-1:20XX, Nov. 2021.

[21] I. Bejtka and H. J. Blaß, 'Reinforcements perpendicular to the grain using self-tapping screws,' in *Proceedings, 8th World Conference on Timber Engineering*, Lahti, Finland, 2004.

[22] P. Dietsch, S. Rodemeier and H. Blaß, 'Transmission of perpendicular to grain forces using self-tapping screws,' in *International Conference on Timber Engineering Research*, Tacoma, USA, 2019.

[23] K. Nilsson, 'Skruvarmering som förstärkning i trä vid belastning vinkelrätt fiberriktningen: En försöksstudie,' Master thesis, Avdelningen för Konstruktionsteknik, LTH, Lund Universitet, Lund, Sweden, 2002.

[24] P. Niebuhr and M. Sieder, 'Comparison of design models for timber in compression perpendicular to grain,' *CEN*, no. CEN/TC 250/SC 5/PT 3 /N 26, Jan. 2019.

[25] *Timber structures - Joints made with mechanical fasteners - General principles for the determination of strength and deformation characteristics*. NS-ISO 6891:1983, May 1991.

A. Extract

A.1 Compression perpendicular to the grain

8.1.6 Compression perpendicular to grain

8.1.6.1 General

(1) The compressive stresses perpendicular to grain $\sigma_{c,90,d}$ shall satisfy Formula 8.4:

$$\sigma_{c,90,d} \leq k_p k_{c,90} f_{c,90,d} \qquad (8.4)$$

with

$$\sigma_{c,90,d} = \frac{F_{c,90,d}}{A} \qquad (8.5)$$

where

k_p is the factor taking into account the material behaviour and degree of compressive deformation perpendicular to grain, see Table 8.1;

$k_{c,90}$ is the load arrangement factor in accordance with 8.1.6.1(3);

$f_{c,90,d}$ is the design compressive strength perpendicular to grain;

$F_{c,90,d}$ is the design compressive force perpendicular to grain;

A is the area of the applied force perpendicular to grain.

(2) The value of $k_{c,90}$ and k_p shall be taken as 1,0 or be calculated according to Formula 8.6 and taken from Table 8.1, respectively.

(3) The value of the load arrangement factor $k_{c,90}$ shall be taken as:

$$k_{c,90} = \sqrt{\frac{l_{ef}}{l_c}} \leq 4,0 \qquad (8.6)$$

where

l_{ef} is the effective spreading length of the compressive stress;

l_c is the contact length of the applied force.

(4) The effective spreading length of the compressive stress l_{ef} should be calculated using a stress spreading gradient of 45°.

NOTE 1   The spreading gradient of the compressive stresse perpendicular to grain (width direction) can be neglected. This does not apply for CLT, see 8.1.6.1(9) .

NOTE 2   The effective spreading length, l_{ef} is governed by the effective depth, h_{ef}, which is the penetration depth of the compressive stresses perpendicular to grain.

NOTE 3   In the case of LVL-C loaded flatwise, the effective spreading length of the compressive stress perpendicular to the grain, lef can be calculated using a stress spreading gradient of 45°.

(5) For a member on a continuous support loaded by concentrated forces perpendicular to grain on the opposite face (see Figure 8.2 and Figure 8.3), the load arrangement factor $k_{c,90}$ should be calculated with an effective spreading length of the compressive stress, l_{ef} in accordance with 8.1.6.1(4) and an effective depth, h_{ef} determined as:

$$h_{ef} = \min\{h; 280 \text{ mm}\} \qquad (8.7)$$

where

h_{ef} is the effective depth;

h is the member depth.

A.1 Compression perpendicular to the grain
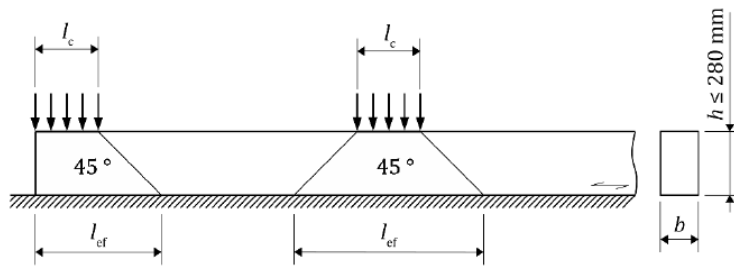
a) Continuously supported member with depth $h \leq 280$ mm
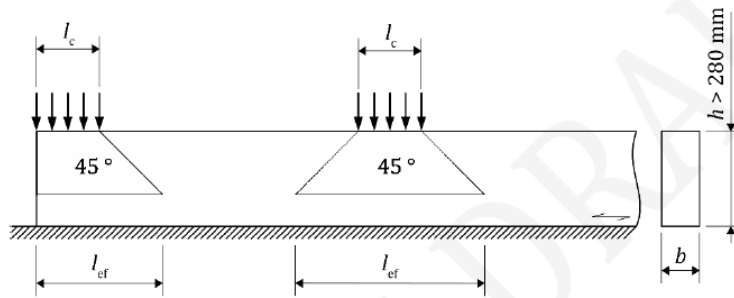
b) Continuously supported member with depth $h > 280$ mm

Figure 8.2 — Effective spreading length of a continuously supported members
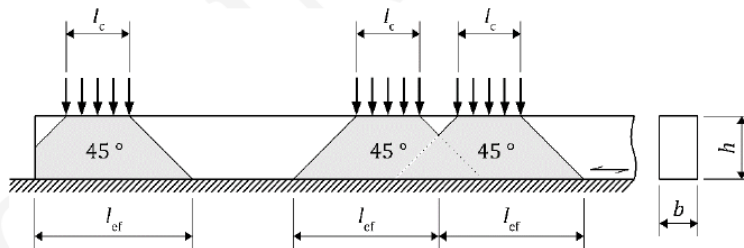
Figure 8.3 — Effective spreading length of a continuously supported member with compressive forces perpendicular to grain either closely spaced or near the end of the member with $h \leq 280$ mm

81

A.1 Compression perpendicular to the grain

(6) For members on local supports loaded by distributed and / or concentrated compressive forces perpendicular to grain, (see Figure 8.2 and Figure 8.3), the load arrangement $k_{c,90}$ should be calculated using an effective spreading length of the compressive stress, l_{ef} in accordance with 8.1.6.1(4) and an effective depth, h_{ef} determined as:

$$h_{ef} = \min\{0{,}4\,h;\,140\text{ mm}\} \tag{8.8}$$

where

h_{ef} is the effective depth;

h is the member depth.
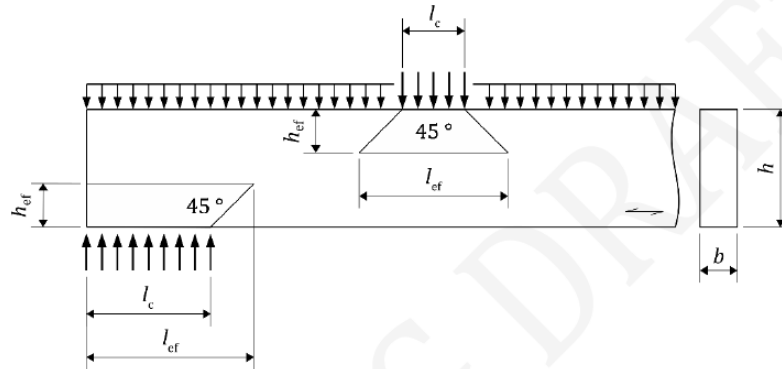
Figure 8.4 — Effective spreading length of a locally supported member loaded by distributed and / or concentrated compressive forces perpendicular to grain
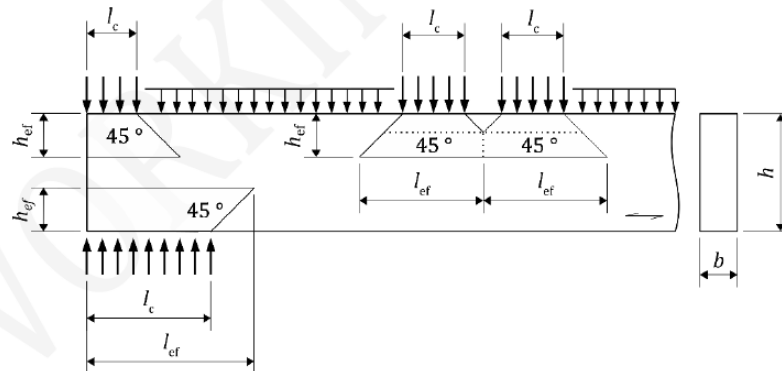
Figure 8.5 — Effective spreading length of a locally supported member loaded with distributed and / or concentrated compressive forces perpendicular to grain either closely spaced or near the end of the member

(7) For other shapes of the loaded area than square (for instance round washers) the effective spreading length l_{ef} and contact length of the applied force l_c in Formula 8.6 may be replaced by the effective spreading area and the area of the applied load, respectively.

A.1 Compression perpendicular to the grain

Table 8.1 — Values for k_p

Type of timber product	Case A [a]		Case B [b]		Case C [c]	
	Deformation[d]	k_p	Deformation[d]	k_p	Deformation[d]	k_p
ST and ST-d, GLT , BGLT, FST, GST and CLT	2,5 %	1,4	10 %	2,1	20 %	2,7
Softwood LVL [e] loaded edgewise	1,5 %	1,0	-	-	-	-
Softwood LVL [e] loaded flatwise	2,5 %	1,3	for $h \geq 46$ mm 7 %	1,9	for 20 mm $\leq h < 46$ mm (30 - 0,5h) %	2,5
Hardwood LVL [e] loaded edgewise	1,5 %	1,0	3,5 %	1,2	-	-
Hardwood LVL [e] loaded flatwise	2 %	1,3	5 %	1,6	-	-

NOTE 1   Table 8.1 refers to ultimate limit state design situations. For the calculation of deformations in serviceability limit state design situations see 9.4.

NOTE 2   The deformation percentages in Table 8.1 are approximate magnitude values.

[a] Case A applies when deformations result in member or system instability or cause unacceptable damage to other components, e.g. for ST where $h > 5b$; where h is the member depth and b the width. The deformation percentages indicate the on-set of yielding.

NOTE 3   The depth to width ratio restriction is to prevent premature rolling shear failure.

[b] Case B applies when deformation has no significant effect on member or system stability.

NOTE 4   Higher values of k_p can apply provided the lateral deformation at the loaded area is prevented. An example is the use of joist hangers with external flanges provided they fit well and are able to withstand the lateral stresses.

[c] Case C applies when deformation has no significant effect on member stability and failure of the member does not lead to failure of the whole structure or parts of it.

NOTE 5   Examples of such cases include members that are continuously supported and for which the width $b \geq h$, or plate or beam supports where local indentation will not lead to failure of the whole structure or parts of it, e.g. due to force redistribution to adjacent members.

[d] is the ratio of the total deformation and the depth, h or effective depth, h_{ef}, respectively.

A.2 Reinforcement

8.1.6.2 Reinforcement

(1) 8.1.6.2 applies for

— members made from ST, FST, GST, GLT, BGLT and LVL-P in flatwise bending from softwoods;
— with reinforcements to carry compressive stresses perpendicular to grain;
— either by fully threaded screws or rods with wood screw thread.

The screws or rods with wood screw thread should be

— applicable for the respective timber product and service class of the reinforced timber member;
— evenly distributed over the reinforced contact area;
— applied at an angle between screw or rod axis and grain direction of $45° \leq \varepsilon \leq 90°$;
— applied at an angle between screw or rod axis and contact surface of $90°$;
— applied with its heads flush to the contact area.

The contact area should

— have adequate stiffness (e.g. a steel plate of adequate thickness) and evenness to prevent penetration of the screw or rod heads into the contact member
— ensure adequate rotational capacity where necessary, to provide an equal distribution of the compressive force over all screws or rods;

The contact width at the tip of the reinforcement should be equal to the member width b, see Figure 8.7 c).

For such reinforcements the characteristic resistance of the reinforced contact area $F_{c,90,k}$ should be taken as the minimum value calculated according to Formula 8.12:

$$F_{c,90,Rk} = \min \begin{cases} k_{c,90} \; b_c \; l_{ef,1} \; f_{c,90,k} + n \; \min\{F_{w,k}; \; F_{c,k}\} \\ b \; l_{ef,2} \; f_{c,90,k} \end{cases} \tag{8.12}$$

with

$$l_{ef,1} = l_c + \min\{30 \text{ mm}; l_e; l_s/2; l_c\} \qquad \text{for end supports, see [Figure 8.7 a)]} \tag{8.13}$$

$$l_{ef,1} = l_c + \min\{30 \text{ mm}; l_s/2; l_c\} \qquad \text{for intermediate supports, see [Figure 8.7 b)]} \tag{8.14}$$

$$l_{ef,2} = l_r + (n_0 - 1) \, a_1 + \min\{l_{ad}; \, a_{3,c}\} \quad \text{for end supports, see [Figure 8.7 a)]} \tag{8.15}$$

$$l_{ef,2} = 2 \, l_r + (n_0 - 1) \, a_1 \qquad \text{for intermediate supports, see [Figure 8.7 b)]} \tag{8.16}$$

where

$k_{c,90}$ is the factor that takes into account the load arrangement;

b_c is the width of the contact area, see Figure 8.7 c);

A.2 Reinforcement

$l_{ef,1}$ is the effective contact length parallel to grain in the plane defined by the contact area, see Figure 8.7 a) and b) and Formulae 8.13 and 8.14; For $\alpha < 90°$, $l_{ef} = l$;

$f_{c,90,k}$ is the characteristic compressive strength perpendicular to grain;

n is the product ($n_0 \cdot n_{90}$), i.e. the number of fully threaded screws or rods applied for reinforcement, see Figure 8.7;

$F_{w,k}$ is the characteristic withdrawal capacity at the given angle to the grain according to 11.2.5 or a European Technical Assessment based on EAD 130118-01-0603;

$F_{c,k}$ is the characteristic resistance of a screw in axial compression according to 11.2.5;

b is the member width, see Figure 8.7 c1) and c2);

$l_{ef,2}$ is the effective distribution length parallel to grain in the plane defined by the screw or rod tips, see Figure 8.7;

l_c is the length of the contact area, see Figure 8.7 a) and b);

l_e is the clear spacing parallel to grain between the end of the member and the contact area, see Figure 8.7 a);

l_s is the clear spacing parallel to grain between the contact area and the concentrated load, see Figure 8.7 a);

l_r is the penetration length of the threaded part of the screw or rod in the timber member, see Figure 8.7;

n_0 is the number of fully threaded screws or rods arranged in a row parallel to grain;

a_1 is the spacing parallel to grain, see Figure 8.7;

$a_{3,c}$ is the distance between the screw or rod and the member end, see Figure 8.7.

n_{90} is the number of fully threaded screws or rods arranged in a row perpendicular to grain.

NOTE   For simplicity, the characteristic withdrawal capacity is used for the axial resistance of the fastener under compression.

The value of $k_{c,90}$ should be taken as 1,0 unless the following conditions apply. For members on discrete supports loaded by distributed loads and/or by concentrated loads at clear distance from the support $l_s \geq 2h$, see Figure 8.7 a), the value of $k_{c,90}$ should be taken as:

— $k_{c,90} = 1,5$ for ST, GST and FST from softwood
— $k_{c,90} = 1,75$ dor GL and BGL softwood, provided that $l_c \leq 400$ mm

NOTE   A series of point loads acting at close centres (e.g. joists of rafters at centres < 610 mm) can be regarded as a distributed load.

(2) Minimum spacings and end and edge distances should be taken from Table 11.16 or a European Technical Assessment based on EAD 130118-01-0603.

(3) The contact material (e.g. steel plate) should be designed for the load introduced by the screw head. The thickness of steel plates t may be assumed adequate, if Formula 8.17 is satisfied:

$$t \geq \max\left\{5,0; 1,45\sqrt{\frac{F_{c,\alpha,Ed}}{f_{y,d}}}\right\} \tag{8.17}$$

where

A.2 Reinforcement

t is the thickness of the steel plate, in mm;

$F_{c,\alpha,Ed}$ is the design compressive force in one screw or rod, in N;

$f_{y,d}$ is the design yield strength of the steel plate, in N/mm² (determined with γ_{M0} according to EN 1993-1-1, 6.1).

a) Discrete end support with reinforcement

b) Intermediate support with reinforcement

c) Discrete support with reinforcement

d) Overlapping reinforcement
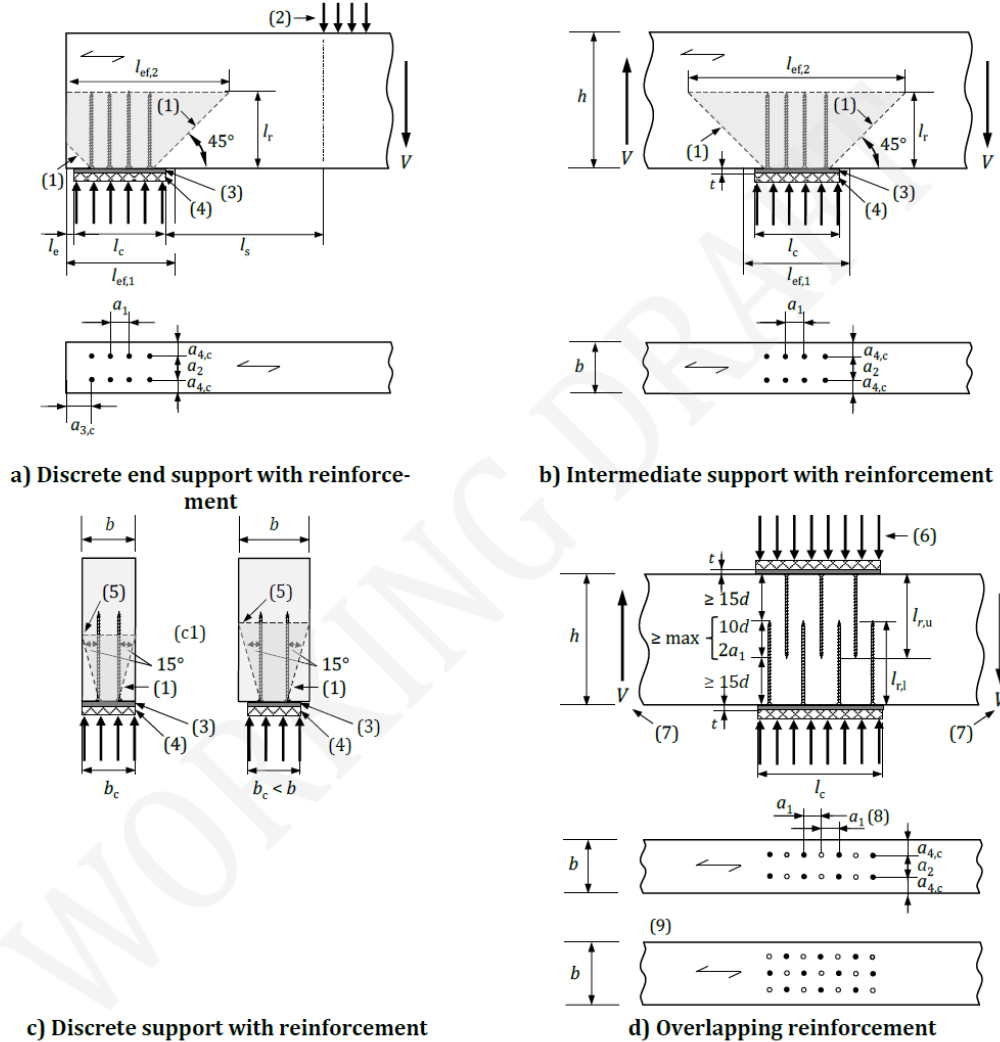
Key

(1)   Load distribution

(2)   Concentrated load

(3)   Stiff bearing material (e.g. steel plate)

(4)   E.g. elastomeric bearing (optional)

(5)   Plane of fully activated member width b, see 8.2.2(1)

(6)   Compression load to be transferred through the member

(7)   Section forces in the member

(8)   Recommended spacing parallel to the grain a1,max = 5 d

(9)   Alternative arrangement

Figure 8.7 — Reinforcement by means of fully threaded screws or threaded rods in areas of concentrated compressive stresses perpendicular to grain

A.3 Withdrawal resistance

11.2.3 Withdrawal resistance

(1) The characteristic withdrawal resistance of a fastener $F_{w,k}$ should be taken from:

$$F_{w,k} = \begin{cases} \pi\, d\, l_w\, f_{w,k} & \text{for smooth and ring shank nails, screws and bonded in rods} \\ 2 d l_w\, f_{w,k} & \text{for staples} \end{cases} \tag{11.4}$$

where

l_w	is the anchorage depth according to Figure 11.2;
$f_{w,k}$	is the characteristic withdrawal strength parameter taken from Table 11.2;
d	is the diameter of the fastener.

NOTE   The tensile failure of screws (steel) and timber failure around the screw are brittle, i.e. with small ultimate deformation and therefore have a limited possibility for stress redistribution.

(2) Only the profiled part of ring shanked nails and the length of the coated part of staples should be considered capable of transmitting axial load.

(3) For smooth nails and staples that are installed in timber at or near the fibre saturation point, which is likely to dry out in service, values of the withdrawal resistance, $F_{w,k}$ should be multiplied by 1/3.

(4) Smooth nails and uncoated staples should only be assigned a withdrawal resistance for instantaneous, short-term and medium-term load-durations. Smooth nails in hardwood LVL should not be assigned any withdrawal resistance.

(5) Coated staples should only be assigned a withdrawal resistance for permanent and long-term load-duration by using $k_{mod} = 0,3$.

(6) Staples should only be used in SC 1 and 2.

(7) The anchorage length of the thread l_w should be used to determine the withdrawal resistance of screws and rods with wood screw thread. The point length of a screw l_p is the length from the tip to the first fully developed thread with outer diameter d. The tip length l_p may be assumed as $l_p = 1,0\, d$.

Key	
d	Diameter of fastener, in mm
d_1	Thread diameter of the screw or rods with wood screw thread, in mm
k_{mat}	Material parameter for the number of laminations
l_w	Anchorage length, in mm;
l_{w2}	Anchorage lenth of the pointed end part, see Figure 11.2, in mm
n_p	Number of penetrated layers
θ	Angle between the staple crown and the grain direction, in degree
α	Force to grain angle or grain direction of the face ply
ρ_k	Characteristic density, in kg/m^3

A.3 Withdrawal resistance

Table 11.2 — Characteristic withdrawal strength $f_{w,k}$

Material	Limits	$f_{w,k}$	
		Ring shank nails $2,5 \text{ mm} \leq d \leq 6,0 \text{ mm}$	(1)
ST, PL, CL and LVL, not predrilled	for $l_w \geq 6d$	$f_{w,k} = 2 \left(\frac{\rho_k}{350}\right)^{1,25}$ see 11.1.2(5)	(2)
	for $3d \leq l_{w2} < 6d$	$f_{w,k} = 2 \left(\frac{\rho_k}{350}\right)^{1,25} \left(\frac{l_{w2}}{3d} - 1\right)$	(3)
SWP	not predrilled	$f_{w,k} = 0,117 d^{0,6} l_w \rho_k^{0,8}$	(4)
		Screws and rods with woodscrew thread $3,5 \text{ mm} \leq d \leq 20 \text{ mm}$ and $0,55d \leq d_1 \leq 0,76d$	(5)
ST, PL, CL and LVL	$l_w \geq 5d$ $\rho_k \leq 700 \text{ kg/m}^3$ $d \geq 8 \text{ mm for CLT}$	$f_{w,k} = 8,2 \, k_w k_{mat} \, d^{-0,33} \left(\frac{\rho_k}{350}\right)^{k_\rho} \text{N/mm}^2$	(6)
		For materials not mentioned specifically $k_w = k_{mat} = 1,0$ $k_w = \begin{cases} 1,0 & \text{for } 30° \leq \varepsilon \leq 90° \\ 1 - 0,01(30 - \varepsilon) & \text{for } 0° \leq \varepsilon < 30° \end{cases}$ for CLT	(7)
		$k_{mat} = \begin{cases} 1,00 & \text{for } n_p = 1 \\ 1,06 & \text{for } n_p \geq 2 \\ 1,10 & \text{for } n_p \geq 3 \\ 1,13 & \text{for } n_p \geq 5 \\ 1,15 & \text{for } n_p \geq 7 \end{cases}$ for PL and CL	(8)
		$k_\rho = \begin{cases} 1,10 & \text{for softwoods and } 15° \leq \varepsilon \leq 90° \\ 1,25 - 0,05d & \text{for softwoods and } 0° \leq \varepsilon < 15° \\ 1,6 & \text{for hardwoods and } 0° \leq \varepsilon \leq 90° \end{cases}$	(9)
PLY	$l_w \geq 2,5d$ $\rho_k \geq 350 \text{ kg/m}^3$	$f_{w,k} = 4,0 \text{ N/mm}^2$	(10)
		Staples $1,5 \text{ mm} \leq d \leq 3,1 \text{ mm}$	(11)
ST, PL, CL and LVL	$l_w \geq 12d$	$f_{w,k} = k_w \begin{cases} 4,9 \left(\frac{\rho_k}{350}\right)^2 \text{ N/mm}^2 \text{ for } \Theta \geq 30^0 \end{cases}$	(12)
		$\begin{cases} 2,45 \left(\frac{\rho_k}{350}\right)^2 \text{ N/mm}^2 \text{ for } \Theta < 30^0 \end{cases}$	(13)
		$k_w = \begin{cases} 1,0 & \text{for resin coated} \\ 0,5 & \text{for non-coated} \end{cases}$	(14)
	$8d \leq l_{w2} < 12d$	$k_w = \left(\frac{t_{w2}}{4d} - 2\right) \begin{cases} 1,0 & \text{for resin coated} \\ 0,5 & \text{for uncoated} \end{cases}$	(15)

A.4 Compression resistance

11.2.5 Compression resistance

(1) The characteristic compression resistance $F_{c,k}$ of a dowel-type fastener should be taken from the respective declaration of performance. For axially loaded screws in members from ST, FJT, GST, GL, BGL, and LVL, GLVL in flatwise bending from softwood, the characteristic compression resistance $F_{c,k}$ may alternatively be determined by:

$$F_{c,k} = 1{,}18\, k_c N_{pl,k} \tag{11.5a}$$

$$N_{pl,k} = \pi \frac{d_1^2}{4} f_{y,k} \tag{11.5b}$$

where

k_c is the factor for the buckling of screws and is given in Table 11.3a;

$N_{pl,k}$ is the characteristic yield capacity of the screw;

$f_{y,k}$ is the characteristic yield strength of the screw.

NOTE   A more detailed approach to determine the characteristic load-carrying capacity of the screw in axial compression is given in Annex O.

Table 11.3a — Reduction factors k_c for buckling of screws ($\rho_k \geq 350$ kg/m³)

	Angle α between screw axis and grain	
Characteristic value of yield strength of steel	$\alpha = 90°$	$\alpha = 0°$
$f_{y,k} = 1000$ N/mm²	$k_c = 0{,}6$	$k_c = 0{,}5$
$f_{y,k} = 800$ N/mm² [a]	$k_c = 0{,}65$	$k_c = 0{,}55$
$f_{y,k} = 500$ N/mm² [b]	$k_c = 0{,}75$	$k_c = 0{,}65$

NOTE   for characteristic values of yield strength of steel in between the specified values, k_c can be determined by linear interpolation. For angles α between the specified values, k_c can be determined by linear interpolation.

[a]   e.g. hot dip galvanized steel

[b]   e.g. stainless steel

A.4 Compression resistance

<div align="center">

Annex O
(informative)

Characteristic load-carrying capacity of screws in axial compression

</div>

O.1   Use of this Informative Annex

This Informative Annex provides additional guidance to that given in 10.7.2(8) for the determination of load-carrying capacity of screws in axial compression.

NOTE   The status of this Informative Annex is given in the National Annex. If the National Annex is silent on the use of this Informative Annex, it can be used.

O.2   Scope and field of application

(1) This Informative Annex covers the determination of load-carrying capacity of screws in axial compression.

(2) For screws in accordance with EN 14592 with

— 6 mm ≤ d ≤ 12 mm

— 0,55 ≤ d_1/d ≤ 0,76

where

d is the outer thread diameter;

d_1 is the inner thread diameter.

The characteristic compression resistance (pushing-in or buckling), $F_{c,\alpha,Rk}$, should be taken according to Formula 0.1 as:

$$F_{c,\alpha,Rk} = \min\{F_{ax,\alpha,Rk}; F_{b,Rk}\} \tag{0.1}$$

where

$F_{ax,\alpha,Rk}$ is the characteristic withdrawal capacity according to Formula 11.15 respectively;

$$F_{b,Rk} = 1{,}18 \, k_c \, N_{pl,k} \quad \text{is the characteristic load} - \text{capacity of the screw in axial compression} \tag{0.2}$$

with

$$k_c = \begin{cases} 1 & \text{for } \bar{\lambda}_k \le 0{,}2 \\ \dfrac{1}{\left(k+\sqrt{k^2-\bar{\lambda}_k^2}\right)} & \text{for } \bar{\lambda}_k > 0{,}2 \end{cases} \tag{0.3}$$

$$k = 0{,}5\left[1 + 0{,}49\left(\bar{\lambda}_k - 0{,}2\right) + \bar{\lambda}_k^2\right] \tag{0.4}$$

$$\bar{\lambda}_k = \sqrt{\dfrac{N_{pl,k}}{N_{ki,k}}} \qquad \text{is the relative slenderness ratio of the screw;} \tag{0.5}$$

A.4 Compression resistance

where

$$N_{\mathrm{pl,k}} = \pi \, \frac{d_1^2}{4} \, f_{\mathrm{y,k}} \qquad \text{is the characteristic yield capacity of the screw;} \qquad (0.6)$$

d_1 is the inner thread diameter;

$f_{\mathrm{y,k}}$ is the characteristic yield strength of the screw;

and

$$N_{\mathrm{ki,k}} = \sqrt{c_{\mathrm{h}} \, E_{\mathrm{S}} \, I_{\mathrm{S}}} \; \text{is the characteristic ideal elastic buckling load, in N;} \qquad (0.7)$$

$$c_{\mathrm{h}} = (0{,}19 + 0{,}012 \, d) \, \rho_{\mathrm{k}} \left(\frac{90° + \alpha}{180°} \right) \qquad \text{is the elastic foundation of the screw, in N/mm}^2, \text{ for solid timber}$$
$$\text{and glued laminated timber of softwood;} \qquad (0.8)$$

ρ_{k} is the characteristic density of the wood-based member, in kg/m^3;

α is the angle between screw axis and grain direction of the wood;

$$E_{\mathrm{S}} \, I_{\mathrm{S}} = 210\,000 \, \frac{\pi \, d_1^4}{64} \quad \text{is the bending stiffness of the screw.}$$

91

A.5 Reinforcement, Model of Karlsrhue

$$R_{90,k} = \min \begin{Bmatrix} n \cdot R_{S,k} + l_{ef} \cdot t \cdot k_{c,90} \cdot f_{c,90,k} \\ A_{ef}(z) \cdot f_{c,90,k} \end{Bmatrix} \tag{51}$$

Mit dem charakteristischen Wert der axialen Tragfähigkeit $R_{S,k}$ einer Vollgewinde-schraube:

$$R_{S,k} = \min \begin{Bmatrix} R_{ax,k} = d \cdot l_S \cdot f_{ax,k} \\ R_{c,k} = \kappa_c \cdot N_{pl,k} \end{Bmatrix} \tag{52}$$

Der Abminderungsbeiwert κ_c für die Berechnung der Grenztragfähigkeit der Schraube beim Ausknicken $R_{c,k}$ wird in Anlehnung an DIN 18800 wie folgt berechnet:

$$\kappa_c = 1 \qquad \text{für} \qquad \overline{\lambda}_k \leq 0{,}2 \tag{53}$$

$$\kappa_c = \frac{1}{k + \sqrt{k^2 - \overline{\lambda}_k^2}} \qquad \text{für} \qquad \overline{\lambda}_k > 0{,}2$$

mit

$$k = 0{,}5 \cdot \left[1 + 0{,}49 \cdot \left(\overline{\lambda}_k - 0{,}2 \right) + \overline{\lambda}_k^2 \right] \tag{54}$$

Der charakteristische Wert des bezogenen Schlankheitsgrades bei Druckbeanspru-chung beträgt:

$$\overline{\lambda}_k = \sqrt{\frac{N_{pl,k}}{N_{ki,G/E,k}}} \tag{55}$$

Für selbstbohrende Vollgewindeschrauben mit einem Kerndurchmesser von 70% des Gewindeaußendurchmessers gilt:

$$N_{pl,k} = \pi \cdot \frac{(0{,}7 \cdot d)^2}{4} \cdot f_{y,k} \tag{56}$$

Weitere Angaben:

n	Anzahl der selbstbohrenden Vollgewindeschrauben
l_{ef}	Länge der Lasteinleitung. Für die Ermittlung der wirksamen Länge an der Stelle der Lasteinleitung darf die Länge l_{ef} zu beiden Seiten in Faser-richtung um $\Delta l = \min[30\ \text{mm} ; l_{ef}]$ erweitert werden.

t	Breite der Lasteinleitung
$k_{c,90}$	Querdruckbeiwert nach Blaß et al. (2002) mit $k_{c,90} \in [1,0 \ ; \ 1,75]$
$f_{c,90,k}$	charakteristischer Wert der Querdruckfestigkeit
$A_{ef}(z)$	Wirksame querdruckbeanspruchte Fläche an der Stelle der Schrauben-spitze ($z = l_S$) nach Abschnitt 3.3.5 in Abhängigkeit von der Art der Last-einleitung (direkt und indirekt) und in Abhängigkeit von der Art der Last-ausbreitung (einseitig und beidseitig)
d	Schraubennenndurchmesser
l_S	Schraubenlänge oder Länge des Gewindebereiches
$f_{ax,k}$	charakteristischer Wert des Ausziehparameters nach Abschnitt 3.3.2.
$f_{y,k}$	charakteristischer Wert der Streckgrenze des Schraubenmaterials. Für gehärtete Holzschrauben kann für den Wert der Streckgrenze f_y die 0,2%-Dehngrenze $f_{0,2\%}$ zugrunde gelegt werden. Die 0,2%-Dehngrenze $f_{0,2\%}$ wird in Anlehnung an DIN EN 10002, Teil 1 ermittelt.
$N_{ki,G/E,k}$	charakteristischer Wert der Verzweigungslast für den Fall einer gelenki-gen Lagerung des Schraubenkopfes ($N_{ki,G,k}$) sowie für den Fall einer drehsteifen Lagerung des Schraubenkopfes ($N_{ki,E,k}$). Die charakteristi-schen Werte der Verzweigungslasten sind in Bild 3-11 und in Bild 3-12 sowie in Tabelle 3-4 und Tabelle 3-5 dargestellt.

Tabelle 3-4　Verzweigungslasten $N_{ki,G,k}$

$N_{ki,G,k}$ in [kN]		ρ_k = 310 kg/m³ Durchmesser in [mm]					ρ_k = 380 kg/m³ Durchmesser in [mm]				
		4	6	8	10	12	4	6	8	10	12
Schraubenlänge l_S in [mm]	20	3,99	4,51	4,95	5,37	5,79	4,85	5,52	6,06	6,58	7,10
	40	7,50	12,5	14,5	15,9	17,3	8,38	14,9	17,6	19,5	21,1
	60	7,44	16,4	24,2	28,3	31,2	8,30	18,4	28,7	34,3	38,1
	80	7,41	16,5	28,5	39,0	45,4	8,24	18,5	32,2	45,9	54,7
	100		16,6	29,0	43,9	56,9		18,6	32,5	49,7	66,7
	120			29,4	44,9	62,4			33,0	50,6	71,1
	140			29,7	45,7	64,2			33,2	51,4	72,5
	160	7,25			46,4	65,4	8,06	18,6		52,1	73,9
	180		16,7		46,8	66,5				52,4	75,0
	200			29,8		67,4			33,3		75,8
	220				47,1	68,1				52,7	76,4
	>240					68,6					76,9

$N_{ki,G,k}$ in [kN]		ρ_k = 410 kg/m³ Durchmesser in [mm]					ρ_k = 450 kg/m³ Durchmesser in [mm]				
		4	6	8	10	12	4	6	8	10	12
Schraubenlänge l_S in [mm]	20	5,22	5,95	6,54	7,10	7,66	5,70	6,53	7,18	7,79	8,40
	40	8,73	16,0	19,0	21,0	22,8	9,16	17,3	20,7	23,0	25,0
	60	8,64	19,2	30,5	36,8	41,0	9,08	20,2	32,7	40,1	44,8
	80	8,58	19,2	33,6	48,7	58,6	9,00	20,2	35,4	52,1	63,7
	100		19,3	34,0	52,1	70,6		20,3	35,8	55,0	75,4
	120			34,4	52,9	74,5			36,2	55,8	78,8
	140			34,6	53,7	75,9			36,4	56,7	80,2
	160	8,38			54,3	77,3	8,80	20,3		57,2	81,6
	180		19,3		54,7	78,4				57,6	82,7
	200			34,7		79,2			36,5		83,5
	220				55,0	79,7				57,8	84,0
	>240					80,2					84,4

Hinweis: Zwischenwerte dürfen linear interpoliert werden

Tabelle 3-5   Verzweigungslasten $N_{ki,E,k}$

$N_{ki,E,k}$ in [kN]	ρ_k = 310 kg/m³ Durchmesser in [mm]					ρ_k = 380 kg/m³ Durchmesser in [mm]				
Schraubenlänge l_S in [mm]	4	6	8	10	12	4	6	8	10	12
20	13,3	16,9	18,5	20,0	21,6	14,5	20,7	22,6	24,6	26,5
40	16,2	24,5	36,1	39,1	42,2	19,1	28,2	44,2	47,9	51,7
60	17,2	31,9	41,1	56,4	62,7	19,3	38,0	48,4	64,4	76,9
80	17,2	36,6	51,2	61,7	76,5	19,1	41,2	61,4	73,3	89,1
100		36,9	60,7	73,9	85,7		41,7	69,5	88,9	102
120			62,1	86,8	99,8			70,5	102	120
140			63,7	92,2	115			72,3	105	137
160	15,6			94,5	126	17,3			108	145
180		36,1		97,2	130		40,0		111	149
200			64,8		134			73,0		154
220				99,1	137				112	157
>240					140					159

$N_{ki,E,k}$ in [kN]	ρ_k = 410 kg/m³ Durchmesser in [mm]					ρ_k = 450 kg/m³ Durchmesser in [mm]				
Schraubenlänge l_S in [mm]	4	6	8	10	12	4	6	8	10	12
20	15,0	22,4	24,4	26,5	28,6	15,7	24,6	26,8	29,1	31,3
40	20,3	29,8	47,7	51,7	55,8	21,7	32,0	50,8	56,8	61,2
60	20,1	40,5	51,5	67,8	82,9	21,2	43,7	55,6	72,3	91,0
80	19,8	43,0	65,6	78,2	94,5	20,8	45,3	71,2	84,8	102
100		43,6	72,8	95,2	110		46,0	77,0	103	119
120			74,0	108	129			78,4	115	140
140			75,7	111	146			80,0	117	157
160	17,9			114	153	18,8			121	163
180		41,6		116	157		43,7		123	167
200			76,2		162			80,3		172
220				117	165				124	175
>240					167					177

Hinweis: Zwischenwerte dürfen linear interpoliert werden

A.5 Reinforcement, Model of Karlsrhue

Die beste Korrelation zwischen den Versuchsergebnissen und den rechnerisch ermittelten Traglasten wird mit einem Korrelationskoeffizienten R von R = 0,953 mit Gleichung (6) erreicht (siehe Bild 3-4). Darüber hinaus ist das Verhältnis zwischen den Versuchsergebnissen und den berechneten Werten für alle untersuchten Werte des Ausziehwiderstandes konstant.

$$R_{ax} = d \cdot l_S \cdot f_{ax,neu} \tag{6}$$

$$f_{ax,neu} = 0{,}61 \cdot \frac{\rho^{0,79}}{d^{0,47} \cdot l_S^{0,09}} \quad \text{in} \quad \frac{N}{mm^2} \tag{7}$$
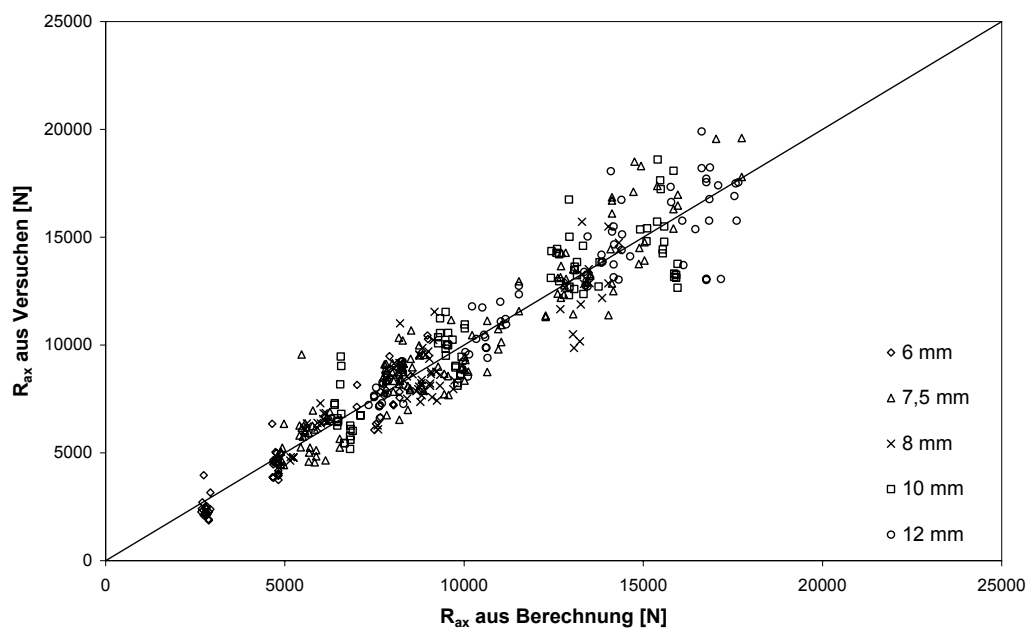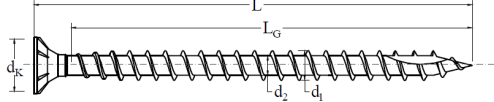
Bild 3-4   Ausziehwiderstand R_{ax} aus Versuchen über den nach Gleichung (6) berechneten Ausziehwiderstand R_{ax}

A.6 Screw properties, ETA
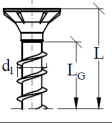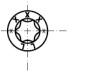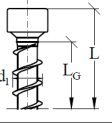
Rotho Blaas screws

rothoblaas

CARBON STEEL
FULL THREAD
Ø 7.0 mm

L
L_G

d_K d_2 d_1

Alternative names:

VGZ/GWZ
VGS/GWS

Alternative head types:

Headstamps (supplier head mark and specific lenght) optional.

countersunk head with or without milling ribs under head	cylindrical head
"CS"	**"CY"**
d_k	d_k
d_1 L L_G	d_1 L L_G

d_1	7.00		d_1	7.00
d_K	13.00 ±0.65		d_K	9.50 ±0.60

Alternative thread tip types:

"RBN" with or without cutting edge	d_2 d_1
"RBN2" with or without cutting edge	d_2 d_1

	d_1	d_2
"RBN"	7.00 ±0.35	4.60 ±0.30
"RBN2"	7.00 ±0.35	4.60 ±0.30

Lenghts and Thread Lenghts

d_1	L		L_G	
	min	max	min	max
7.00	60.0	400.0	50.0	390.0
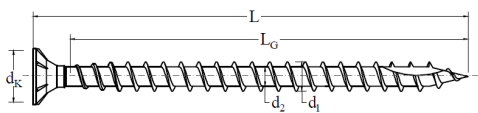
Tolerance (L and L_G): according to EAD 130118-01-0603.
Intermediate lengths (L) are possible.
Intermediate thread lengths (L_G) are possible.

All dimensions in [mm].

A.6 Screw properties, ETA

CARBON STEEL
FULL THREAD
Ø 9.0 mm

Alternative names:

VGZ/GWZ
VGS/GWS

Alternative head types:

Headstamps (supplier head mark and specific lenght) optional.

countersunk head with or without milling ribs under head	cylindrical head
"CS"	**"CY"**
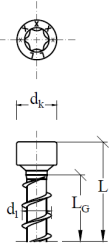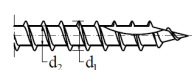
d_1	9.00
d_K	16.00 ±0.80

d_1	9.00
d_K	11.50 ±0.60
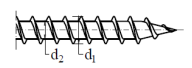
Alternative thread tip types:

"RBN" with or without cutting edge	
"RBN2" with or without cutting edge	

	d_1	d_2
"RBN"	9.00 ±0.45	5.90 ±0.30
"RBN2"	9.00 ±0.45	5.90 ±0.30

Lenghts and Thread Lenghts

d_1	L		L_G	
	min	max	min	max
9.00	100.0	520.0	90.0	510.0

Tolerance (L and L_G): according to EAD 130118-01-0603.
Intermediate lengths (L) are possible.
Intermediate thread lengths (L_G) are possible.

All dimensions in [mm].

A.6 Screw properties, ETA

Head types for d = 8.0 mm, all materials

⌀14,8
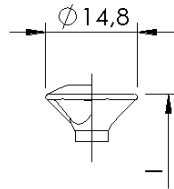
Flat countersunk head 90° with
and without raised head, with
and without milling pockets
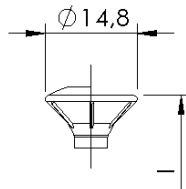
⌀14,8

Flat countersunk head 90° with
and without raised head, with
and without milling ribs

⌀14,8
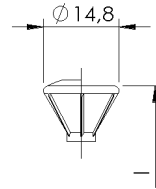
Flat countersunk head 60° /
75°, with or without raised
head, with or without milling
ribs

⌀13
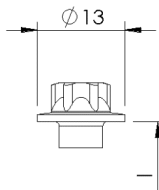
External hexagon head
with and without washer

⌀19
SW 13

Hexagon head with and
without washer

⌀18

Raised flange head

⌀22,5
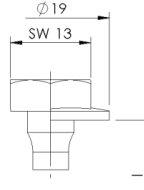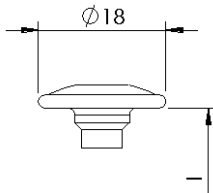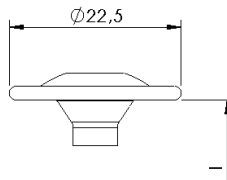
Raised flange head with
big washer

⌀18,4
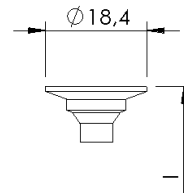
Flat flange head with and
without milling ribs

⌀12

Cylindrical head

⌀12
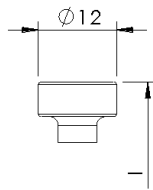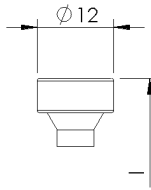
Cylindrical head with counter-
sinking

HECO-TOPIX-plus self-tapping screws
d = 8.0 mm, steel

Annex A

A.6 Screw properties, ETA

Secondary thread for d = 8.0 mm, steel
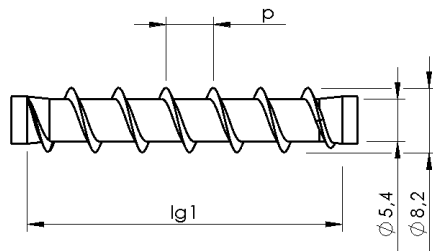
Secondary thread

Thread types for d = 8.0 mm, steel
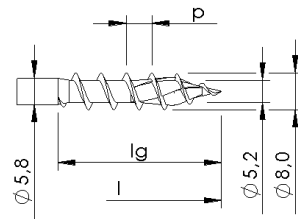
With and without thread variation,
with milling ribs
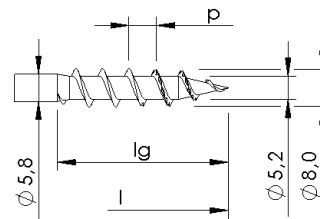
With and without thread variation,
with toothed tip
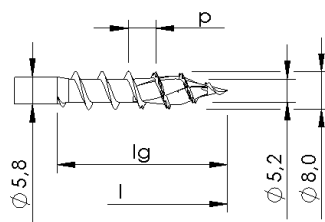
With and without thread variation,
with toothed tip and milling ribs

HECO-TOPIX-plus self-tapping screws
d = 8.0 mm, steel

Annex A

A.6 Screw properties, ETA

WT-T-8,2 x L

160 mm ≤ L ≤ 330 mm
65 mm ≤ s_{spann} ≤ 135 mm
65 mm ≤ s_g ≤ 135 mm

Tolerances	
Length	± 5%
Diameter	± 5%

Alternative screw tip for screws WT-T-8,2

SFS Self-tapping Screws WT	Annex 5.2
Self-tapping screws WT-T-8,2 Dimensions	
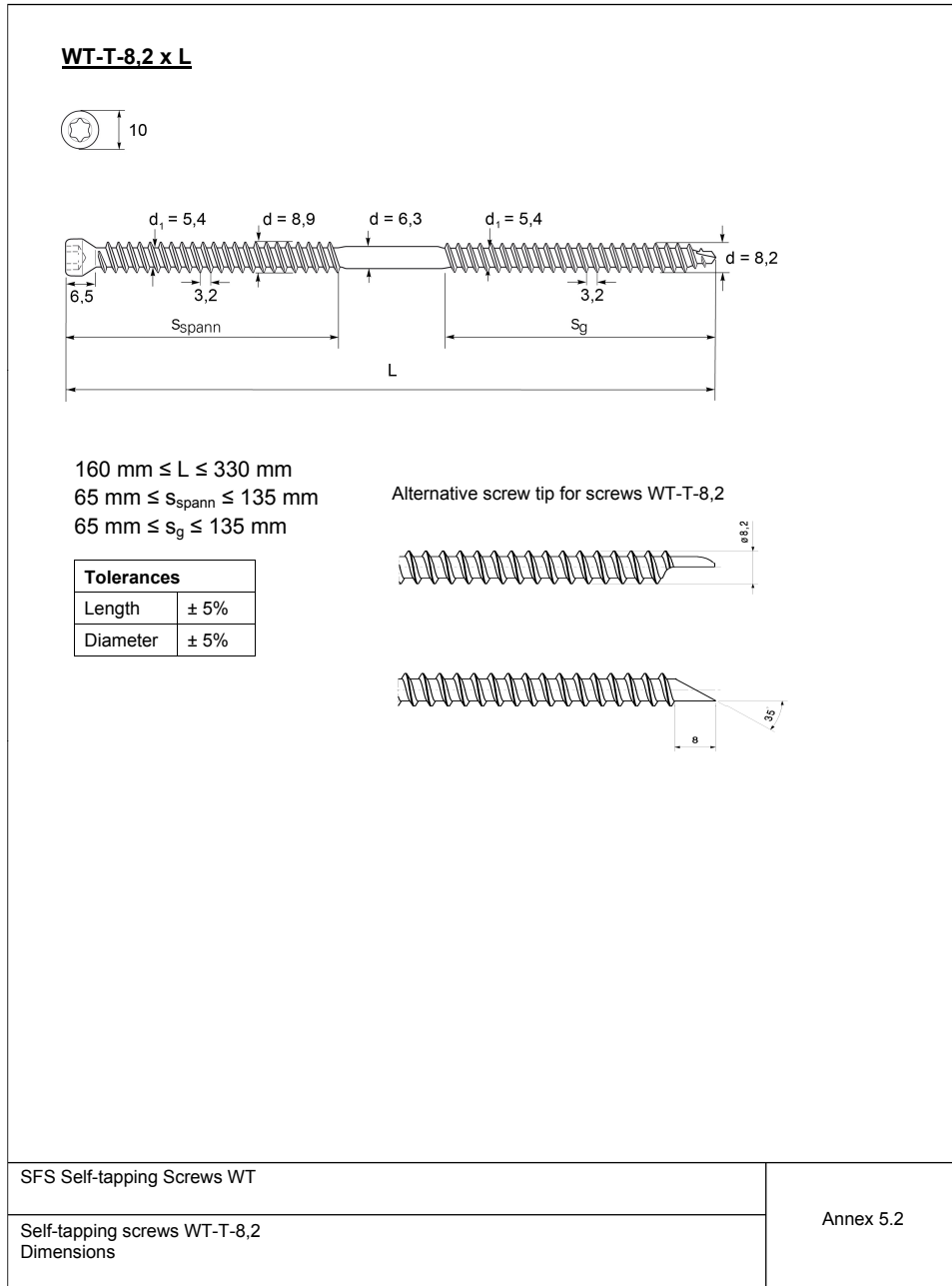
B. Sensitivity plots

B.1 Load case B, non-reinforcement

```python
# -*- coding: utf-8 -*-
"""
Created on Thu Feb 17 2022

@author: Kari Ryen Thunberg
@author: Eldbjørg Aaraas Hånde
"""


'-------------------------------------------------------------------------------'
' COMPRESSION PERPENDICULAR TO THE GRAIN'
'-------------------------------------------------------------------------------'
' Imports '
'-------------------------------------------------------------------------------'
import numpy as np
import matplotlib.pyplot as plt
csfont = {'fontname':'Times New Roman'}


'-------------------------------------------------------------------------------'
' Constant inputs'
'-------------------------------------------------------------------------------'
"""
Material:          GL30c
Support condition: Continuous support
Load: position:    Loaded midspan, load case B
Deformation:       1.0 % , 2.5% and 10%
Approach:          Eq.8.4 According to consolidated draft prEN1995-1-1
(November 2021)

                   Eq.6.1 According to CEN-WG3-N0023 CPG resistamce
                   Eq.6.7 According to CEN-WG3-N0023 CPG deformation

"""

fc90k = 2.5                                # N/mm2   - Characteristic
compressive resistance
b     = 140                                # mm      - Members depth
l     = 1000                               # mm      - Members length
E     = 300                                # N/mm2   - E-modulus
kpa   = 1.4                                #         - 2.5 % Deformation
kpb   = 2.1                                #         - 10 % Deformation


'-------------------------------------------------------------------------------'
' Input '
'-------------------------------------------------------------------------------'

lc = [20,50,90,150,180,200,220,250,280,300]      # mm    - Effective contact
length
h1 = [20,100,200,300,400,500,600,700,800,1200]  # mm    - Member height


'-------------------------------------------------------------------------------'
' Matrices '
'-------------------------------------------------------------------------------'

h_ef = [0,0,0,0,0,0,0,0,0,0]
```

B.1 Load case B, non-reinforcement

```python
kc90 = np.zeros((10,10))
l_ef = np.zeros((10,10))
F1 = np.zeros((10,10))
F2 = np.zeros((10,10))
F3 = np.zeros((10,10))
wA = np.zeros((10,10))
wB = np.zeros((10,10))
wO = np.zeros((10,10))
pA = np.zeros((10,10))
pB = np.zeros((10,10))
pO = np.zeros((10,10))


'----------------------------------------------------------------------------'
' CALCULATIONS '
'----------------------------------------------------------------------------'
'List format for the various lengths, including kc90'
'----------------------------------------------------------------------------'

for l in range(len(lc)):
    for h in range(len(h1)):
        h_ef[l]  = min(h1[l], 2*140)                    #h_ef acc. new standard
        h#_ef[l] = h1[l]                                #h_ef acc. Eq. 6.1 Leijten
        l_ef[l,h]  = lc[h] + 2*h_ef[l]
        kc90[l,h]  = min((l_ef[l,h]/lc[h])**0.5,4)

'----------------------------------------------------------------------------'
'Design models'
'----------------------------------------------------------------------------'

def CPG(lc, kp, F):
    for h in range(len(h_ef)):
        for l in range(len(lc)):
            F[l,h] += ((kp * kc90[l,h] * fc90k * b * lc[h])/1000)
    return F

def deformation(Fc90k, w, p):
    for h in range(len(h_ef)):
        for l in range(len(lc)):
            w[l,h] = ((h_ef[l] * Fc90k[l,h]*1.35 *10**3)/ (2*b*E))*((1 / lc[h])
+ (1/ l_ef[l,h]))
            p[l,h] = (w[l,h]/h1[l])*100
    return w, p


'----------------------------------------------------------------------------'
' OUTPUT '
'----------------------------------------------------------------------------'
np.set_printoptions(precision=1)

A_Fc90k = CPG(lc, kpa, F1)
B_Fc90k = CPG(lc, kpb, F2)
O_Fc90k = CPG(lc, 1.0, F3)
```

B.1 Load case B, non-reinforcement

```
A_w, A_p= deformation(A_Fc90k, wA, pA)
B_w, B_p = deformation(B_Fc90k, wB, pB)
O_w, O_p = deformation(O_Fc90k, wO, pO)


'-----------------------------------------------------------------------------'
' PLOT'
'-----------------------------------------------------------------------------'
'CPG resistance'
'-----------------------------------------------------------------------------'


fig = plt.figure(figsize=(10,8))
ax  = plt.axes(projection ='3d')
ax.grid()

x,y = np.meshgrid(lc, h1)

ax.plot_surface(x,y,O_Fc90k, color = 'royalblue', alpha = 0.8 )
ax.scatter(250,200,100, color = 'royalblue', alpha =1 , label="1.0 %
deformation ")

ax.plot_surface(x,y,A_Fc90k, color = 'grey', alpha = 0.8 )
ax.scatter(250,200,100, color = 'grey', alpha =1 , label="2.5 % deformation ")

ax.plot_surface(x,y,B_Fc90k, color = 'cornflowerblue', alpha = 0.8 )
ax.scatter(250,200,100, color = 'cornflowerblue', alpha =1 , label="10 %
deformation ")


ax.view_init(10, 220)

ax.set_ylabel('Height, h [mm]', labelpad=20,**csfont, fontsize = 18)
ax.set_xlabel('Contact length, lc [mm]', labelpad=20, **csfont, fontsize = 18)
ax.set_zlabel('Resistance [kN]', labelpad=10, **csfont, fontsize = 18)

plt.legend( fontsize= 'x-large')
plt.show()

'-----------------------------------------------------------------------------'
'CPG Deformation'
'-----------------------------------------------------------------------------'


fig = plt.figure(figsize=(10,8))
ax  = plt.axes(projection ='3d')
ax.grid()
x,y = np.meshgrid(lc, h1)

ax.plot_surface(x,y,O_p, color = 'royalblue', alpha = 0.8 )
ax.scatter(250,200,1.5, color = 'royalblue', alpha =1 , label="1.0 %
deformation ")

ax.plot_surface(x,y,A_p, color = 'grey', alpha = 0.8 )
ax.scatter(250,200,1.5, color = 'grey', alpha =1 , label="2.5 % deformation ")
```

B.1 Load case B, non-reinforcement

```
ax.plot_surface(x,y,B_p, color = 'cornflowerblue', alpha = 0.8 )
ax.scatter(250,200,1.5, color = 'cornflowerblue', alpha =1 , label="10 %
deformation ")


ax.view_init(10, 240)

ax.set_ylabel('Height, h [mm]', labelpad=20, **csfont, fontsize = 18)
ax.set_xlabel('Contact length, lc [mm]', labelpad=20, **csfont, fontsize = 18)
ax.set_zlabel('w/h 100%', labelpad=10, **csfont, fontsize = 18)

plt.legend( fontsize= 'x-large')
plt.show()
```

B.2 Load case C non-reinforcement

```python
# -*- coding: utf-8 -*-
"""
Created on Thu Feb 17 12:56:50 2022

@author: Kari Ryen Thunberg
@author: Eldbjørg Aaraas Hånde
"""


'--------------------------------------------------------------------------'
' COMPRESSION PERPENDICULAR TO THE GRAIN'
'--------------------------------------------------------------------------'
' Imports '
'--------------------------------------------------------------------------'
import numpy as np
import matplotlib.pyplot as plt
csfont = {'fontname':'Times New Roman'}


'--------------------------------------------------------------------------'
' Constant inputs'
'--------------------------------------------------------------------------'
"""

Material:          GL30c
Support condition: Discrete support
Load: position:    Loaded midspan, load case B
Deformation:       1.0 % , 2.5% and 10%
Approach:          Eq.8.4 According to consolidated draft prEN1995-1-1
(November 2021)

                   Eq.6.1 According to CEN-WG3-N0023 CPG resistamce
                   Eq.6.7 According to CEN-WG3-N0023 CPG deformation

"""


fc90k = 2.5                              # N/mm2 -  Characteristic
compressive resistance
b     = 140                              # mm    -  Members depth **UNIT
LENGTH**
l     = 1000                             # mm    -  Members length
E     = 300                              # N/mm2 -  E-modulus
kpa   = 1.4                              #       -  2.5 % Deformation
kpb   = 2.1                              #       -  10 % Deformation

'--------------------------------------------------------------------------'
' Input '
'--------------------------------------------------------------------------'

lc = [20,50,90,150,180,200,220,250,280,300]    # mm   - Effective contact
length
h1 = [20,100,200,300,400,500,600,700,800,1200]  # mm   - Member height


'--------------------------------------------------------------------------'
' Matrices '
'--------------------------------------------------------------------------'
```

B.2 Load case C non-reinforcement

```
h_ef = [0,0,0,0,0,0,0,0,0,0]

kc90 = np.zeros((10,10))
l_ef = np.zeros((10,10))
F1 = np.zeros((10,10))
F2 = np.zeros((10,10))
F3 = np.zeros((10,10))
wA = np.zeros((10,10))
wB = np.zeros((10,10))
wO = np.zeros((10,10))
pA = np.zeros((10,10))
pB = np.zeros((10,10))
pO = np.zeros((10,10))


'---------------------------------------------------------------------------'
' CALCULATIONS '
'---------------------------------------------------------------------------'
'List format for the various lengths, including kc90'
'---------------------------------------------------------------------------'

for l in range(len(lc)):
    for h in range(len(h1)):
        h_ef[l]  = min(h1[l]*0.4, 140)                      #h_ef acc. prEN1995-1-1
(November 2021)
        #h_ef[l]  = h1[l]                                   #h_ef acc. Eq. 6.1
Leijten
        l_ef[l,h]  = lc[h] + 2*h_ef[l]
        kc90[l,h]  = min((l_ef[l,h]/lc[h])**0.5,4)

'---------------------------------------------------------------------------'
'Design models'
'---------------------------------------------------------------------------'

def CPG(lc, kp, F):
    for h in range(len(h_ef)):
        for l in range(len(lc)):
            F[l,h] += ((kp * kc90[l,h] * fc90k * b * lc[h])/1000)
    return F

def deformation(Fc90k, w, p):
    for h in range(len(h_ef)):
        for l in range(len(lc)):
            w[l,h] = ((h_ef[l] * Fc90k[l,h]*1.35 *10**3)/ (2*b*E))*((1 / lc[h])
+ (1/ l_ef[l,h]))
            p[l,h] = (w[l,h]/h1[l])*100
    return w, p


'---------------------------------------------------------------------------'
' OUTPUT '
'---------------------------------------------------------------------------'
np.set_printoptions(precision=1)
```

B.2 Load case C non-reinforcement

```
A_Fc90k = CPG(lc, kpa, F1)
B_Fc90k = CPG(lc, kpb, F2)
O_Fc90k = CPG(lc, 1.0, F3)

A_w, A_p= deformation(A_Fc90k, wA, pA)
B_w, B_p = deformation(B_Fc90k, wB, pB)
O_w, O_p = deformation(O_Fc90k, wO, pO)

'-----------------------------------------------------------------------------'
' PLOT'
'-----------------------------------------------------------------------------'
'CPG resistance'
'-----------------------------------------------------------------------------'


fig = plt.figure(figsize=(10,8))
ax  = plt.axes(projection ='3d')
ax.grid()

x,y = np.meshgrid(lc, h1)

ax.plot_surface(x,y,A_Fc90k, color = 'grey', alpha = 0.8 )
ax.scatter(250,200,100, color = 'grey', alpha =1 , label="2.5 % deformation ")

ax.view_init(10, 220)

ax.set_ylabel('Height, h [mm]', labelpad=20,**csfont, fontsize = 18)
ax.set_xlabel('Contact length, lc [mm]', labelpad=20, **csfont, fontsize = 18)
ax.set_zlabel('Resistance [kN]', labelpad=10, **csfont, fontsize = 18)

plt.legend( fontsize= 'x-large')
plt.show()

'-----------------------------------------------------------------------------'
'CPG Deformation'
'-----------------------------------------------------------------------------'


fig = plt.figure(figsize=(10,8))
ax  = plt.axes(projection ='3d')
ax.grid()
x,y = np.meshgrid(lc, h1)

ax.plot_surface(x,y,O_p, color = 'royalblue', alpha = 0.8 )
ax.scatter(250,200,1.5, color = 'royalblue', alpha =1 , label="1.0 %
deformation ")

ax.plot_surface(x,y,A_p, color = 'grey', alpha = 0.8 )
ax.scatter(250,200,1.5, color = 'grey', alpha =1 , label="2.5 % deformation ")

ax.plot_surface(x,y,B_p, color = 'cornflowerblue', alpha = 0.8 )
ax.scatter(250,200,1.5, color = 'cornflowerblue', alpha =1 , label="10 %
deformation ")
```

B.2 Load case C non-reinforcement

```
ax.view_init(10, 240)

ax.set_ylabel('Height, h [mm]', labelpad=20, **csfont, fontsize = 18)
ax.set_xlabel('Contact length, lc [mm]', labelpad=20, **csfont, fontsize = 18)
ax.set_zlabel('w/h 100%', labelpad=10, **csfont, fontsize = 18)

plt.legend( fontsize= 'x-large')
plt.show()
```

```
# -*- coding: utf-8 -*-
"""
Created on Fri Feb 11 2022

@author: Kari Ryen Thunberg
@author: Eldbjørg Aaraas Hånde
"""

' COMPRESSION PERPENDICULAR TO THE GRAIN'

' Imports '
'------------------------------------------------------------------------------'
import numpy as np
import matplotlib.pyplot as plt
csfont = {'fontname':'Times New Roman'}


'------------------------------------------------------------------------------'
'Properties'
'------------------------------------------------------------------------------'
"""
Material:         GL30c
Support condition: Continuous support
Load: position:   Load case B
Screw:            VGZ
"""


fc90k  = 2.5                                # N/mm2 - Characteristic
compressive resistance
p_k    = 390                                # kg/m3 - Density

h1    = 540                                 # mm    - Members depth
bc    = 140
ls    = 0                                   # mm    - Length from support to
consentrated load
le    = 1000                                # mm    - Length from support to
end of member
a1    = 70                                  # mm    - Spacing parallel to
grain
a3c   = 1070                                # mm    - Distance from edge to
screw parallel to the grain

f_yk = 1000                                 # N/mm2 - Characteristic yield
strength of screw
#d1   = 4.6                                 # mm    - Inner diameter of
threaded screw
lc    = 180                                 # mm    - Outer diameter of
threaded screw/bolt
n0    = 2                                   #       - Number of screws in a
row parallel to the grain
n     = 4                                   #       - Total number of
screws/bolts
```

B.3 Load case B, reinforcement

```
kc    = 0.6                                 # NB      Only valid for these
properties
kc90_A = 1.75


'----------------------------------------------------------------------------'
' Input '
'----------------------------------------------------------------------------'

d  = ([6, 6.5, 7, 7.5, 8, 8.5, 9, 10, 11, 12 ])              # mm    -
Diameter
lr = ([80 ,100, 180, 200, 280, 300, 380, 400, 480, 500])     # mm    -
Penetration length


'----------------------------------------------------------------------------'


l_ef1 =         ([0,0,0,0,0,0,0,0,0,0])              # mm Effective
contact width varies
l_ef2 =         ([0,0,0,0,0,0,0,0,0,0])              # mm Effective
contact width varies
h_ef  =         ([0,0,0,0,0,0,0,0,0,0])              # mm Effective
contact higth varies


'----------------------------------------------------------------------------'
' CALCULATIONS '
'----------------------------------------------------------------------------'
"Characteristic yield capacity"
'----------------------------------------------------------------------------'
fw_k  = ([0,0,0,0,0,0,0,0,0,0])
Fc_k  = ([0,0,0,0,0,0,0,0,0,0])
Npl_k = ([0,0,0,0,0,0,0,0,0,0])
Fw_k  = np.zeros((10,10))
Fk    = np.zeros((10,10))


for i in range(len(d)):
    Npl_k[i] = (np.pi * (0.7*d[i])**2 )/4 *f_yk  *10**-3    # kN
    Fc_k[i]  = 1.18*kc*Npl_k[i]                             # kN
    fw_k[i] = 8.2*1*1*d[i]**(-0.33)*(p_k/350)**1.1

    for l in range(len(lr)):
        Fw_k[i,l] = np.pi*d[i]*lr[l]*fw_k[i]/1000
        Fk[i,l] = min(Fc_k[i] , Fw_k[i,l])


'----------------------------------------------------------------------------'
'List format for the various lengths, including kc90'


#prEN1995:
l_ef1 = lc + min(30, le, lc) + min(30, lc)
```

B.3 Load case B, reinforcement

```python
for l in range(len(lr)):
    l_ef2[l]  = lr[l] + (n0-1)*a1 + min(lr[l], a3c)
```

```python
'----------------------------------------------------------------------------'
F1 = np.zeros((10,10))
F2 = np.zeros((10,10))
F3 = np.zeros((10,10))
F4 = np.zeros((10,10))
F5 = np.zeros((10,10))
FA = np.zeros((10,10))
FB = np.zeros((10,10))


'----------------------------------------------------------------------------'
'Design models'
'----------------------------------------------------------------------------'


def A1_CPG(lef,F):
    for l in range(len(d)):
        for h in range(len(lr)):
            F[h,l] += ((kc90_A * bc * lef * fc90k)/1000 + (n * Fk[l,h]))
    return F

def A2_CPG(lef,F):
    for l in range(len(d)):
        for h in range(len(lr)):
            F[l,h] += (bc * lef[l] * fc90k)/1000
    return F


'----------------------------------------------------------------------------'
' OUTPUT '
'----------------------------------------------------------------------------'

A1_Fc90k = A1_CPG(l_ef1, F1)
A2_Fc90k = A2_CPG(l_ef2, F2)

for l in range(len(d)):
    for h in range(len(lr)):
        FA[l,h] = min(A1_Fc90k[l,h], A2_Fc90k[l,h])


'----------------------------------------------------------------------------'

'----------------------------------------------------------------------------'
' PLOT, Min {A_1 ; A2}'
'----------------------------------------------------------------------------'
```

B.3 Load case B, reinforcement

```python
fig = plt.figure(figsize=(10,10))
ax  = plt.axes(projection ='3d')
ax.grid()
x,y = np.meshgrid(d,lr)

ax.plot_surface(x,y,FA, color ='cornflowerblue', alpha = 0.8 )
ax.scatter(12,500,50, color = 'cornflowerblue', alpha =1 , label="min {$A_1$ ;
$A_2$}")

ax.view_init(10, 220)

ax.set_xlabel('Screw diameter, d [mm]', labelpad=20,**csfont, fontsize = 20)
ax.set_ylabel('Screw length, lr [mm]', labelpad=20,**csfont, fontsize = 20)
ax.set_zlabel('Resistance [kN]', labelpad=10,**csfont, fontsize = 20)


plt.legend( fontsize= 'xx-large')
plt.show()




'-----------------------------------------------------------------------------'
' PLOT, A1 & A2'
'-----------------------------------------------------------------------------'

fig = plt.figure(figsize=(10,10))
ax  = plt.axes(projection ='3d')
ax.grid()

x,y = np.meshgrid(d,lr)
ax.plot_surface(x,y,A1_Fc90k, color ='cornflowerblue', alpha = 0.8)
ax.scatter(12,500,50, color = 'cornflowerblue', alpha =1 , label="$A_1$")

ax.plot_surface(x,y,A2_Fc90k, color = 'grey', alpha = 0.8 )
ax.scatter(12,500,50, color = 'grey', alpha =1 , label="$A_2$")

ax.view_init(10, 220)

ax.set_xlabel('Screw diameter, d [mm]', labelpad=20,**csfont, fontsize = 20)
ax.set_ylabel('Screw length, lr [mm]', labelpad=20,**csfont, fontsize = 20)
ax.set_zlabel('Resistance [kN]', labelpad=20, **csfont, fontsize = 20)


plt.legend( fontsize= 'xx-large')
plt.show()
```

B.4 Load case C, reinforcement

```
# -*- coding: utf-8 -*-
"""
Created on Fri Feb 11 2022

@author: Kari Ryen Thunberg
@author: Eldbjørg Aaraas Hånde
"""

' COMPRESSION PERPENDICULAR TO THE GRAIN'

' Imports '
'-------------------------------------------------------------------------------'
import numpy as np
import matplotlib.pyplot as plt
csfont = {'fontname':'Times New Roman'}


'-------------------------------------------------------------------------------'
' Constant inputs'
'-------------------------------------------------------------------------------'
"""
Material:          GL30c
Support condition: Discrete support
Load: position:    Load case C
Screw:             VGZ
"""


fc90k  = 2.5                            # N/mm2 -  Characteristic
compressive resistance
p_k    = 390                            # kg/m3 -  Density

h1     = 540                            # mm    -  Members depth
bc     = 140
ls     = 0                              # mm    -  Length from support to
consentrated load
le     = 1000                           # mm    -  Length from support to
end of member
a1     = 70                             # mm    -  Spacing parallel to
grain
a3c    = 1070                           # mm    -  Distance from edge to
screw parallel to the grain

f_yk = 1000                             # N/mm2 -  Characteristic yield
strength of screw
#d1    = 4.6                            # mm    -  Inner diameter of
threaded screw
lc     = 180                            # mm    -  Outer diameter of
threaded screw/bolt
n0     = 2                              #       -  Number of screws in a
row parallel to the grain
n      = 4                              #       -  Total number of
screws/bolts
```

116

B.4 Load case C, reinforcement

```
kc    = 0.6                              # NB        Only valid for these
properties
kc90_A = 1.0


'-----------------------------------------------------------------------------'
' Input '
'-----------------------------------------------------------------------------'

d  = ([6, 6.5, 7, 7.5, 8, 8.5, 9, 10, 11, 12])             # mm    -
Diameter screw
lr = ([80 ,100, 160, 200, 280, 300, 380, 400, 480, 500])   # mm    -
Penetration length


'-----------------------------------------------------------------------------'


l_ef1 =        ([0,0,0,0,0,0,0,0,0,0])             # mm Effective
contact width varies
l_ef2 =        ([0,0,0,0,0,0,0,0,0,0])             # mm Effective
contact width varies
kc90  =        ([0,0,0,0,0,0,0,0,0,0])
h_ef  =        ([0,0,0,0,0,0,0,0,0,0])             # mm Effective
contact higth varies

'-----------------------------------------------------------------------------'
' CALCULATIONS '
'-----------------------------------------------------------------------------'
"Characteristic yield capacity"
'-----------------------------------------------------------------------------'


fw_k  = ([0,0,0,0,0,0,0,0,0,0])
Npl_k = ([0,0,0,0,0,0,0,0,0,0])
Fw_k  = np.zeros((10,10))
Fc_k  = np.zeros((10,10))
Fk    = np.zeros((10,10))


for i in range(len(d)):
    Npl_k[i] = (np.pi * (0.7*d[i])**2 )/4 *f_yk  *10**-3    # kN
    fw_k[i] = 8.2*1*1*d[i]**(-0.33)*(p_k/350)**1.1

    for l in range(len(lr)):
        Fc_k[l,i]  = 1.18*kc*Npl_k[i]
        Fw_k[l,i] = np.pi*d[i]*lr[l]*fw_k[i]/1000
        Fk[l,i] = min(Fc_k[l,i] , Fw_k[l,i])


#%%
'-----------------------------------------------------------------------------'
'List format for the various lengths, including kc90'
```

B.4 Load case C, reinforcement

```python
#prEN1995:
l_ef1 = lc + min(30, le, lc) + min(30, lc)

for l in range(len(lr)):
    l_ef2[l]  = lr[l] + (n0-1)*a1 + min(lr[l], a3c)




'------------------------------------------------------------------------'


F1 = np.zeros((10,10))
F2 = np.zeros((10,10))
F3 = np.zeros((10,10))
F4 = np.zeros((10,10))
F5 = np.zeros((10,10))
FA = np.zeros((10,10))
FB = np.zeros((10,10))

'------------------------------------------------------------------------'
'Design models'
'------------------------------------------------------------------------'


def A1_CPG(lef,F):
    for l in range(len(d)):
        for h in range(len(lr)):
            F[l,h] += ((kc90_A * bc * lef * fc90k)/1000 + (n * Fk[l,h]))
    return F

def A2_CPG(lef,F):
    for l in range(len(d)):
        for h in range(len(lr)):
            F[l,h] += (bc * lef[l] * fc90k)/1000
    return F

def B1_CPG(kp,F):
    for l in range(len(d)):
        for h in range(len(lr)):
            F[h,l] += ((kp * bc * lc * kc90 * fc90k)/1000 + (n * Fk[l,h]))
    return F



'------------------------------------------------------------------------'
' OUTPUT '
'------------------------------------------------------------------------'

A1_Fc90k = A1_CPG(l_ef1, F1)
A2_Fc90k = A2_CPG(l_ef2, F2)

for l in range(len(d)):
    for h in range(len(lr)):
        FA[l,h] = min(A1_Fc90k[l,h], A2_Fc90k[l,h])
```

B.4 Load case C, reinforcement

```
'------------------------------------------------------------------------'

'------------------------------------------------------------------------'
' PLOT, Min {A_1 ; A2}'
'------------------------------------------------------------------------'


fig = plt.figure(figsize=(10,10))
ax  = plt.axes(projection ='3d')
ax.grid()


x,y = np.meshgrid(d,lr)

ax.plot_surface(x,y,FA, color ='cornflowerblue', alpha = 0.8 )
ax.scatter(12,500,50, color = 'cornflowerblue', alpha =1 , label="min {$A_1$ ;
$A_2$}")


ax.view_init(10, 200)

ax.set_xlabel('Screw diameter, d [mm]', labelpad=20,**csfont, fontsize = 20)
ax.set_ylabel('Screw length, lr [mm]', labelpad=20,**csfont, fontsize = 20)
ax.set_zlabel('Resistance [kN]', labelpad=10,**csfont, fontsize = 20)


plt.legend( fontsize= 'xx-large')
plt.show()



    '------------------------------------------------------------------------'
    ' PLOT, A1 & A2'
    '------------------------------------------------------------------------'

fig = plt.figure(figsize=(10,10))
ax  = plt.axes(projection ='3d')
ax.grid()

x,y = np.meshgrid(d,lr)
ax.plot_surface(x,y,A1_Fc90k, color ='cornflowerblue', alpha = 0.8)
ax.scatter(12,500,50, color = 'cornflowerblue', alpha =1 , label="$A_1$")

ax.plot_surface(x,y,A2_Fc90k, color = 'grey', alpha = 0.8 )
ax.scatter(12,500,50, color = 'grey', alpha =1 , label="$A_2$")

ax.view_init(10, 220)

ax.set_xlabel('Screw diameter, d [mm]', labelpad=20,**csfont, fontsize = 20)
ax.set_ylabel('Screw length, lr [mm]', labelpad=20,**csfont, fontsize = 20)
ax.set_zlabel('Resistance [kN]', labelpad=20, **csfont, fontsize = 20)
```

B.4 Load case C, reinforcement

```python
plt.legend( fontsize= 'xx-large')
plt.show()


'---------------------------------------------------------------------------'
' PLOT, Fk'
'---------------------------------------------------------------------------'

fig = plt.figure(figsize=(10,10))
ax  = plt.axes(projection ='3d')
ax.grid()

x,y = np.meshgrid(d,lr)
ax.plot_surface(x,y,Fk, color ='cornflowerblue', alpha = 0.8)
ax.scatter(12,500,50, color = 'cornflowerblue', alpha =1 , label="$F_k$")

ax.view_init(10, 220)
ax.set_xlabel('Screw diameter, d [mm]', labelpad=20,**csfont, fontsize = 20)
ax.set_ylabel('Screw length, lr [mm]', labelpad=20,**csfont, fontsize = 20)
ax.set_zlabel('Resistance [kN]', labelpad=20, **csfont, fontsize = 20)


plt.legend( fontsize= 'xx-large')
plt.show()



'---------------------------------------------------------------------------'
' PLOT, Fwk, Fck'
'---------------------------------------------------------------------------'


fig = plt.figure(figsize=(10,10))
ax  = plt.axes(projection ='3d')
ax.grid()

x,y = np.meshgrid(d,lr)


ax.plot_surface(x,y,Fw_k, color ='grey', alpha = 0.8)
ax.scatter(12,500,50, color = 'grey', alpha =1 , label="$F_wk$")

ax.plot_surface(x,y,Fc_k, color = 'cornflowerblue', alpha = 0.8 )
ax.scatter(12,500,50, color = 'cornflowerblue', alpha =1 , label="$F_ck$")

ax.view_init(10, 220)
ax.set_xlabel('Screw diameter, d [mm]', labelpad=20,**csfont, fontsize = 20)
ax.set_ylabel('Screw length, lr [mm]', labelpad=20,**csfont, fontsize = 20)
ax.set_zlabel('Resistance [kN]', labelpad=20, **csfont, fontsize = 20)


plt.legend( fontsize= 'xx-large')
```

B.4 Load case C, reinforcement

```
plt.show()
```

```
# -*- coding: utf-8 -*-
"""
Created on Fri Feb 11 13:36:41 2022

@author: Kari Ryen Thunberg
@author: Eldbjørg Aaraas Hånde
"""


' COMPRESSION PERPENDICULAR TO THE GRAIN'

' Imports '
'------------------------------------------------------------------------------'
import numpy as np
import matplotlib.pyplot as plt
csfont = {'fontname':'Times New Roman'}
'------------------------------------------------------------------------------'
' Constant inputs'
'------------------------------------------------------------------------------'
"""
Material:          GL30c
Support condition: Continuous support
Load: position:    Load case B/C
Screw:             VGZ
"""


fc90k = 2.5                            # N/mm2 -  Characteristic compressive
resistance
p_k   = 390                            # kg/m3 -  Density

h1    = 540                            # mm    -  Members depth
bc    = 140
ls    = 0                              # mm    -  Length from support to
consentrated load
le    = 4000                           # mm    -  Length from support to end
of member
a1    = 70                             # mm    -  Spacing parallel to grain
a3c   = 4000                           # mm    -  Distance from edge to
screw parallel to the grain

f_yk = 1000                            # N/mm2 -  Characteristic yield
strength of screw
#d1 = 4.6                              # mm    -  Inner diameter of threaded
screw
lc   = 180                             # mm    -  Outer diameter of threaded
screw/bolt
n0   = 2                               #       -  Number of screws in a row
parallel to the grain
n    = 4                               #       -  Total number of
screws/bolts

kc   = 0.6                             # NB       Only valid for these
properties
kc90_A = 1.75
```

B.5 Proposal 1

```
'--------------------------------------------------------------------------'
' Input '
'--------------------------------------------------------------------------'

d  = ([6, 6.5, 7, 7.5, 8, 8.5, 9, 10, 11, 12 ])
lr = ([80 ,100, 180, 200, 280, 300, 380, 400, 480, 500])          # mm    -
Penetration length


'--------------------------------------------------------------------------'

l_ef1 =          ([0,0,0,0,0,0,0,0,0,0])                 # mm Effective contact
width varies
l_ef2 =          ([0,0,0,0,0,0,0,0,0,0])                 # mm Effective contact
width varies
kc90  =          ([0,0,0,0,0,0,0,0,0,0])



'--------------------------------------------------------------------------'
' CALCULATIONS '
'--------------------------------------------------------------------------'
"Characteristic yield capacity"
'--------------------------------------------------------------------------'
Fw_k  = np.zeros((10,10))
fw_k  = ([0,0,0,0,0,0,0,0,0,0])
Fc_k  = ([0,0,0,0,0,0,0,0,0,0])
Fk    = np.zeros((10,10))
Npl_k = ([0,0,0,0,0,0,0,0,0,0])

for i in range(len(d)):
    Npl_k[i] = (np.pi * (0.7*d[i])**2 )/4 *f_yk  *10**-3    # kN
    Fc_k[i]  = 1.18*kc*Npl_k[i]                             # kN
    fw_k[i]  = 8.2*1*1*d[i]**(-0.33)*(p_k/350)**1.1

    for l in range(len(lr)):
        #Fc_k[i]  = 1.18*kc*Npl_k[i]
        Fw_k[i,l] = np.pi*d[i]*lr[l]*fw_k[i]/1000
        Fk[i,l] = min(Fc_k[i] , Fw_k[i,l])


'--------------------------------------------------------------------------'
'List format for the various lengths, including kc90'


#prEN1995:
l_ef1 = lc + min(30, le, lc) + min(30, lc)

for l in range(len(lr)):
    l_ef2[l]  = lr[l] + (n0-1)*a1 + min(lr[l], a3c)
```

B.5 Proposal 1

```
'-------------------------------------------------------------------------'
F1 = np.zeros((10,10))
F2 = np.zeros((10,10))
F3 = np.zeros((10,10))
F4 = np.zeros((10,10))
F5 = np.zeros((10,10))
FA = np.zeros((10,10))
FB = np.zeros((10,10))


'-------------------------------------------------------------------------'
'Design models'
'-------------------------------------------------------------------------'


def A1_CPG(lef,F):
    for l in range(len(d)):
        for h in range(len(lr)):
            F[h,l] += ((kc90_A * bc * lef * fc90k)/1000 + (n * Fk[l,h]))
    return F

def A2_CPG(lef,F):
    for l in range(len(d)):
        for h in range(len(lr)):
            F[l,h] += (kc90_A * bc * lef[l] * fc90k)/1000
    return F



'-------------------------------------------------------------------------'
' OUTPUT '
'-------------------------------------------------------------------------'


A1_Fc90k = A1_CPG(l_ef1, F1)
A2_Fc90k = A2_CPG(l_ef2, F2)

for l in range(len(d)):
    for h in range(len(lr)):
        FA[l,h] = min(A1_Fc90k[l,h], A2_Fc90k[l,h])




'-------------------------------------------------------------------------'

'-------------------------------------------------------------------------'
' PLOT, Min {A_1 ; A2}'
'       Min {B1 ; B2}'
'-------------------------------------------------------------------------'


fig = plt.figure(figsize=(10,10))
ax  = plt.axes(projection ='3d')
ax.grid()


x,y = np.meshgrid(d,lr)
```

```python
ax.plot_surface(x,y,FA, color ='cornflowerblue', alpha = 0.8 )
ax.scatter(12,500,300, color = 'cornflowerblue', alpha =1 , label="min {$A_1$ ;
$A_2$}")


ax.view_init(10, 220)

ax.set_xlabel('Screw diameter, d [mm]', labelpad=20,**csfont, fontsize = 20)
ax.set_ylabel('Screw length, lr [mm]', labelpad=20,**csfont, fontsize = 20)
ax.set_zlabel('Resistance [kN]', labelpad=10,**csfont, fontsize = 20)


plt.legend( fontsize= 'xx-large')
plt.show()



'-------------------------------------------------------------------------------'
' PLOT, A1 & A2'
'-------------------------------------------------------------------------------'

fig = plt.figure(figsize=(10,10))
ax  = plt.axes(projection ='3d')
ax.grid()

x,y = np.meshgrid(d,lr)
ax.plot_surface(x,y,A1_Fc90k, color ='cornflowerblue', alpha = 0.8)
ax.scatter(12,500,300, color = 'cornflowerblue', alpha =1 , label="$A_1$")

ax.view_init(10, 220)

ax.set_xlabel('Screw diameter, d [mm]', labelpad=20,**csfont, fontsize = 20)
ax.set_ylabel('Screw length, lr [mm]', labelpad=20,**csfont, fontsize = 20)
ax.set_zlabel('Resistance [kN]', labelpad=20, **csfont, fontsize = 20)


plt.legend( fontsize= 'xx-large')
plt.show()
```

```python
# -*- coding: utf-8 -*-
"""
Created on Fri Feb 11 13:36:41 2022

@author: Kari Ryen Thunberg
@author: Eldbjørg Aaraas Hånde
"""


' COMPRESSION PERPENDICULAR TO THE GRAIN'

' Imports '
'--------------------------------------------------------------------------------'
import numpy as np
import matplotlib.pyplot as plt
csfont = {'fontname':'Times New Roman'}



'--------------------------------------------------------------------------------'
' Constant inputs'
'--------------------------------------------------------------------------------'
"""
Material:          GL30c
Support condition: Continuous support
Load: position:    Load case B/C
Screw:             VGZ
"""


fc90k = 2.5                              # N/mm2 -  Characteristic compressive
resistance
p_k   = 390                              # kg/m3 -  Density

h1    = 540                              # mm    -  Members depth
bc    = 140
ls    = 0                                # mm    -  Length from support to
consentrated load
le    = 1000                             # mm    -  Length from support to end
of member
a1    = 70                               # mm    -  Spacing parallel to grain
a3c   = 1070                             # mm    -  Distance from edge to
screw parallel to the grain

f_yk  = 1000                             # N/mm2 -  Characteristic yield
strength of screw
#d1   = 4.6                              # mm    -  Inner diameter of threaded
screw
lc    = 180                              # mm    -  Outer diameter of threaded
screw/bolt
n0    = 2                                #       -  Number of screws in a row
parallel to the grain
n     = 4                                #       -  Total number of
screws/bolts

kc    = 0.6                              #          Only valid for these
```

B.6 Proposal 2

```
properties
kc90_A = 1.75
c     =  2.13                              #            Four screws
l_ef3= (n0-1)*a1 + 2*a1


'----------------------------------------------------------------------'
' Input '
'----------------------------------------------------------------------'

d  = ([6, 6.5, 7, 7.5, 8, 8.5, 9, 10, 11, 12 ])
lr = ([80 ,100, 180, 200, 280, 300, 380, 400, 480, 500])         # mm    -
Penetration length


'----------------------------------------------------------------------'

l_ef1 =        ([0,0,0,0,0,0,0,0,0,0])                   # mm Effective contact
width varies
l_ef2 =        ([0,0,0,0,0,0,0,0,0,0])                   # mm Effective contact
width varies
kc90 =         ([0,0,0,0,0,0,0,0,0,0])


'----------------------------------------------------------------------'
' CALCULATIONS '
'----------------------------------------------------------------------'
"Characteristic yield capacity"
'----------------------------------------------------------------------'
Fw_k  = np.zeros((10,10))
fw_k  = ([0,0,0,0,0,0,0,0,0,0])
Fc_k  = ([0,0,0,0,0,0,0,0,0,0])
Fk    = np.zeros((10,10))
Npl_k = ([0,0,0,0,0,0,0,0,0,0])

for i in range(len(d)):
    Npl_k[i] = (np.pi * (0.7*d[i])**2 )/4 *f_yk  *10**-3    # kN
    Fc_k[i]  = 1.18*kc*Npl_k[i]                             # kN
    fw_k[i] = 8.2*1*1*d[i]**(-0.33)*(p_k/350)**1.1

    for l in range(len(lr)):
        #Fc_k[i]  = 1.18*kc*Npl_k[i]
        Fw_k[i,l] = np.pi*d[i]*lr[l]*fw_k[i]/1000
        Fk[i,l] = min(Fc_k[i] , Fw_k[i,l])



'----------------------------------------------------------------------'
'List format for the various lengths, including kc90'


#prEN1995:
```

127

B.6 Proposal 2

```python
l_ef1 = lc + min(30, le, lc) + min(30, lc)

for l in range(len(lr)):
    l_ef2[l]  = lr[l] + (n0-1)*a1 + min(lr[l], a3c)



'------------------------------------------------------------------------------'
F1 = np.zeros((10,10))
F2 = np.zeros((10,10))
F3 = np.zeros((10,10))
F4 = np.zeros((10,10))
F5 = np.zeros((10,10))
FA = np.zeros((10,10))
FB = np.zeros((10,10))
'------------------------------------------------------------------------------'
'Design models'
'------------------------------------------------------------------------------'


def A1_CPG(lef,F):
    for l in range(len(d)):
        for h in range(len(lr)):
            F[h,l] += ((kc90_A * bc * lef * fc90k)/1000 + (n * Fk[l,h]))
    return F

def A2_CPG(lc,F):
    for l in range(len(d)):
        for h in range(len(lr)):
            #F[l,h] += (c * kc90_A * bc * lef[l] * fc90k)/1000
             F[l,h] += (c * kc90_A * bc * lc * fc90k)/1000 #40 +30 + 30
    return F


'------------------------------------------------------------------------------'
' OUTPUT '
'------------------------------------------------------------------------------'

A1_Fc90k = A1_CPG(l_ef1, F1)
A2_Fc90k = A2_CPG(l_ef3, F2)

for l in range(len(d)):
    for h in range(len(lr)):
        FA[l,h] = min(A1_Fc90k[l,h], A2_Fc90k[l,h])




'------------------------------------------------------------------------------'

'------------------------------------------------------------------------------'
' PLOT, Min {A_1 ; A2}'

'------------------------------------------------------------------------------'
```

B.6 Proposal 2

```python
fig = plt.figure(figsize=(10,10))
ax  = plt.axes(projection ='3d')
ax.grid()


x,y = np.meshgrid(d,lr)

ax.plot_surface(x,y,FA, color ='cornflowerblue', alpha = 0.8 )
ax.scatter(12,500,200, color = 'cornflowerblue', alpha =1 , label="min {$A_1$ ;
$A_2$}")


ax.view_init(10, 220)

ax.set_xlabel('Screw diameter, d [mm]', labelpad=20,**csfont, fontsize = 20)
ax.set_ylabel('Screw length, lr [mm]', labelpad=20,**csfont, fontsize = 20)
ax.set_zlabel('Resistance [kN]', labelpad=10,**csfont, fontsize = 20)



plt.legend( fontsize= 'xx-large')
plt.show()



'------------------------------------------------------------------------------'
' PLOT, A1 & A2'
'------------------------------------------------------------------------------'

fig = plt.figure(figsize=(10,10))
ax  = plt.axes(projection ='3d')
ax.grid()

x,y = np.meshgrid(d,lr)
ax.plot_surface(x,y,A1_Fc90k, color ='cornflowerblue', alpha = 0.8)
ax.scatter(12,500,250, color = 'cornflowerblue', alpha =1 , label="$A_1$")

ax.plot_surface(x,y,A2_Fc90k, color = 'grey', alpha = 0.8 )
ax.scatter(12,500,250, color = 'grey', alpha =1 , label="$A_2$")

ax.view_init(10, 220)

ax.set_xlabel('Screw diameter, d [mm]', labelpad=20,**csfont, fontsize = 20)
ax.set_ylabel('Screw length, lr [mm]', labelpad=20,**csfont, fontsize = 20)
ax.set_zlabel('Resistance [kN]', labelpad=20, **csfont, fontsize = 20)


plt.legend( fontsize= 'xx-large')
plt.show()
```
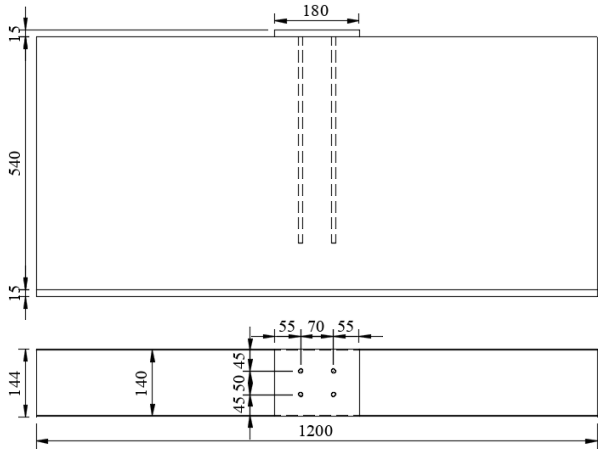
C. Experimental and calculations

C.1 Load rate and phases

Test specimen	Load case	Phase 1 Rate [kN/s]	Phase 1 Limit [kN]	Phase 2 Rate [kN/s]	Phase 2 Limit [kN]	Phase 3 Rate [kN/s]	Phase 3 Limit [kN]	Phase 4 Rate [mm/min]	Limit, end of test - ΔF$_{max}$ [%]	Deformation
N200_A_01	A	0.42	25	0.32	6	0.21	*1500 s	-	20	-
N200_A_02	A	0.54	32	0.40	8	0.27	*1500 s	-	20	-
Pe_8.2_160_A	A	0.65	39	0.50	9	0.33	*1500 s	-	20	-
N225_B	B	0.79	47	0.59	12	0.39	118	1.0	10	27
Pa_7.0_160_B	B	0.91	55	0.68	13	0.46	142	1.0	10	27
Pe_7.0_160_B	B	0.75	44	0.55	11	0.37	142	1.0	10	27
Pe_8.0_180_B	B	0.84	50	0.63	12	0.42	126	1.0	20	30
Pe_8.0_200_B	B	0.93	56	0.70	14	0.47	140	1.0	20	30
Pe_8.2_160_B	B	0.61	36	0.45	9	0.30	178	1.0	20	30
S_7.0_160_B	B	0.91	54	0.68	13	0.46	167	1.0	10	27
S_8.0_160_B	B	0.91	54	0.68	13	0.46	180	1.0	20	30
S_8.0_180_B	B	1.00	60	0.75	15	0.50	209	1.0	20	30
S_8.0_200_B	B	1.10	65	0.82	16	0.55	165	1.0	20	30
S_8.2_160_B	B	0.77	46	0.37	11	0.39	179	1.0	10	27
S6_7.0_160_B	B	1.07	64	0.80	16	0.33	161	1.0	20	30
N540_B	B	0.85	51	0.65	12	0.43	128	1.0	20	60
Pa_9.0_440_B	B	1.25	75	0.95	18	0.63	188	1.0	20	60
Pe_8.0_300_B	B	1.19	71	0.89	17	0.59	179	1.0	20	30
Pe_9.0_440_B	B	1.25	75	0.95	18	0.63	188	1.0	20	60
S_8.0_300_B	B	1.39	83	1.04	20	0.70	209	1.0	20	30
S_8.0_340_B	B	1.39	83	1.04	20	0.70	209	1.0	20	30
S_9.0_440_B	B	1.52	91	1.15	22	0.76	229	1.0	20	60
S6_9.0_440_B	B	1.19	107	0.90	26	0.90	270	1.0	20	60
N225_C	C	0.59	35	0.45	8	0.30	89	1.0	20	30
S_7.0_160_C	C	0.88	53	0.67	13	0.44	137	1.0	20	30
S_8.0_160_C	C	0.91	54	0.68	13	0.46	152	1.0	20	30
S_8.2_160_C	C	0.77	46	0.58	11	0.39	151	1.0	10	27
Pe_7.0_160_C	C	0.76	43	0.55	10	0.36	108	1.0	20	30
Pe_8.2_160_C	C	0.60	36	0.45	9	0.30	120	1.0	10	27
N540_C	C	0.67	40	0.50	10	0.33	100	1.0	20	60
Pe_9.0_440_C	C	0.83	50	0.63	12	0.42	125	1.0	20	60
S_9.0_440_C	C	1.10	66	0.83	16	0.55	182	1.0	20	60
T_7.0_160	Torx	0.089	5	0.067	1	0.045	40	-	20	-
T_8.2_160	Torx	0.110	6	0.083	1	0.056	50	-	20	-
T_8.0_160	Torx	0.120	7	0.100	1	0.061	55	-	20	-
T_8.0_180	Torx	0.120	7	0.100	1	0.061	55	-	20	-
T_8.0_200	Torx	0.120	7	0.100	1	0.061	55	-	20	-
T_8.0_300	Torx	0.120	7	0.100	1	0.061	55	-	20	-
T_8.0_340	Torx	0.120	7	0.100	1	0.061	55	-	20	-
T_9.0_440	Torx	0.150	8	0.100	2	0.073	66	-	20	-

C.2 Example test sheets, Test specimen 540 mm and 225 mm
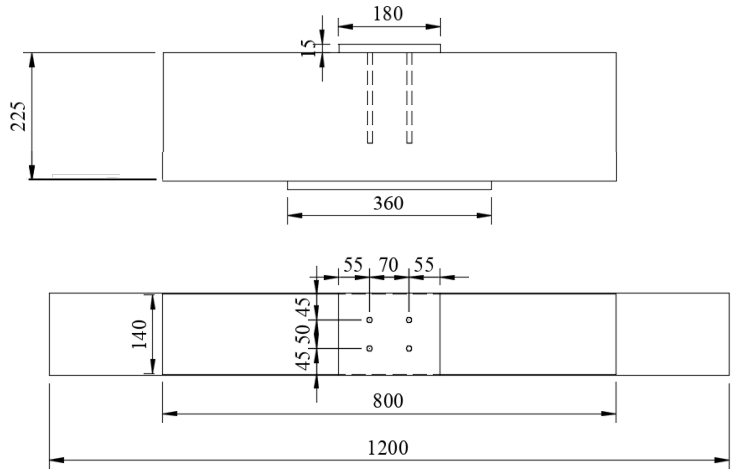
Test: S_9.0_440_01   Date: 19.04 2022

Set-up	
	Load case B

Reinforcement	4 x VGZ 9 x 440	n_0: 2, n_{90}: 2
Predictions	Failure mode: Comp., A_1: 228.6	$F_{c,90,k}$ = 228.6 kN
	Failure mode: Timber, A_2: 332.5	
Loading rate	0.76 kN/s	Time: 300 s + 120 s

Detail, Loading rate	1 – 1.52 kN/s
	    91 kN
	2 – 1.15 kN/s
	    22 kN
		3 - 0.76 kN/s
		    228.6 kN
		4 – 1.0 mm/min
		Stop limit:
		    ΔF = - 20 %
		    δ_{max} = 60 mm

Comments under test execution	Predrilled with 6 mm drill Test stopped due to - 20 % reduction of the maximum forxe	
Failure, Surface observations	Assumed failure of the screws, A_1. Wider hole, some spacing between the screw and the timber on one side. No cracks between the screws.	

C.2 Example test sheets, Test specimen 540 mm and 225 mm

Test: S_8.0_160_C_01   Date: 13.04 2022

Set-up		
	Load case C	
Reinforcement	4 x SFS HT-T-CS-FT-8 x 160	n_0: 2, n_{90}: 2
Predictions	Failure mode: Comp., A_1: 147.0	$F_{c,90,k}$ = 136.5 kN
	Failure mode: Timber, A_2: 136.5	
Loading rate	0.46 kN/s	Time: 300 s ± 120 s

Detail, Loading rate	1 - 0.91 kN/s
	  54 kN
	2 - 0.68 kN/s
	  13 kN
		3 - 0.46 kN/s
		  152.1 kN
		4 – 1.0 mm/min
		Stop limit:
		  ΔF = - 20 %
		  δ_{max} = 60 mm

Comments under test execution	Achieved relatively high load, ca. 220 kN, Countersunk head, seems that the capacity is better. The achieved capacity is significantly higher than the predicted capacity according to the design model.	
Failure, Surface observations	Assumed failure of the screws, not timber A_2. Screws are flush with the surface. Surfaced is some pushed in under the contact plate. Cracks occurred on both sides of the bottom contact plate. Additional small cracks under the contact plate.	

C.3 Calculation load case B

[8.1.6.2] Compression perpendicular to the grain with reinforcement

Load case B - S 7.0 160 C

Input properties: Comments:

Timber GL30c:
$$f_{c.90.k} := 2.5 \ \frac{N}{mm^2}$$

$$h := 225 \ mm$$
$$b := 140 \ mm$$

$$\rho_k := 390 \ \frac{kg}{m^3}$$

Screws VGZ 7.0x160:
$$d := 7.0 \ mm$$
$$d_1 := 4.6 \ mm$$
$$l_r := 160 \ mm$$
$$f_{y.k} := 1000 \ \frac{N}{mm^2}$$

Load arrangement: $k_{c90} := 1.75$ Discrete support,
Effective contact with: $b_c := 140 \ mm$ uniformly distirbuted load
Effective contact length: $l_c := 180 \ mm$
Length support to edge: $l_e := 310 \ mm$
Length support to concentrated load: $l_s := 0 \ mm$
Spacing parallel to the grain: $a_1 := 70 \ mm$
Distance edge to screws: $a_{3.c} := 365 \ mm$
Number fo screws: $n := 4$
Number of screws in grain direction: $n_0 := 2$

Withdrawal:

$$k_w := 1.0$$
$$k_{mat} := 1.0$$
$$k_p := 1.10$$
$$l_w := 160 \ mm$$

Characteristic withdrawal strength:
$$f_{w.k} := 8.2 \cdot k_w \cdot k_{mat} \cdot 7^{(-0.33)} \cdot \left(\frac{390}{350}\right)^{k_p} = 4.86$$

$$f_{w.k} := 4.86 \ \frac{N}{mm^2}$$

Characterisitc withdrawal resistance:
$$F_{w.k} := \pi \cdot d \cdot l_w \cdot f_{w.k} = 17.1 \ kN$$

Buckling:

$$N_{pl.k} := \pi \cdot \frac{d_1^2}{4} \cdot f_{y.k} = 16.6 \ kN$$

$$N_{kik} := \sqrt[2]{(0.19 + 0.012 \cdot 7) \cdot 390 \cdot 210000 \cdot \pi \cdot \frac{4.6^4}{64}} \cdot N = 22.2 \ kN$$

$$\lambda_k := \sqrt[2]{\frac{N_{pl.k}}{N_{kik}}} = 865.1 \cdot 10^{-3}$$

C.3 Calculation load case B

prEN 1995 - 1- 1 (November)
[8.1.6.2] Compression perpendicular to the grain with reinforcement

$$k := 0.5 \cdot \left(1 + 0.49 \cdot \left(\lambda_k - 0.2\right) + \lambda_k^{\,2}\right) = 1.037$$

$$k_c := \frac{1}{k + \sqrt[2]{k^2 - \lambda_k^{\,2}}} = 0.621$$

$$F_{c.k} := 1.18 \cdot k_c \cdot N_{pl.k} = 12.19 \; \textbf{\textit{kN}}$$

minimum(Fck, Fwk) -> Fck = 12.19 kN

Design model:

$$l_{ef.1} := l_c + 30 \; \textbf{\textit{mm}} + 30 \; \textbf{\textit{mm}} = 240 \; \textbf{\textit{mm}}$$

$$l_{ef.2} := \left(n_0 - 1\right) \cdot a_1 + 2 \cdot l_r = 390 \; \textbf{\textit{mm}}$$

$$A_1 := k_{c90} \cdot f_{c.90.k} \cdot b_c \cdot l_{ef.1} + n \cdot F_{c.k} = 195.7 \; \textbf{\textit{kN}}$$
$$A_2 := f_{c.90.k} \cdot b_c \cdot l_{ef.2} = 136.5 \; \textbf{\textit{kN}}$$

A2 gives the decisive capacity

C.4 Calculation load case C

[8.1.6.2] Compression perpendicular to the grain with reinforcement

Load case C - S 9.0 440 C

Input properties:

<div style="float:right">Comments:</div>

Timber GL30c:

$$f_{c.90.k} := 2.5 \; \frac{N}{mm^2}$$

$$h := 540 \; mm$$
$$b := 140 \; mm$$

$$\rho_k := 390 \; \frac{kg}{m^3}$$

Screws VGZ 7.0x160:

$$d := 9.0 \; mm$$
$$d_1 := 5.9 \; mm$$
$$l_r := 440 \; mm$$
$$f_{y.k} := 1000 \; \frac{N}{mm^2}$$

Load arrangement: $k_{c90} := 1.0$ Discrete support,
Effective contact with: $b_c := 140 \; mm$ uniformly distirbuted load
Effective contact length: $l_c := 180 \; mm$
Length support to edge: $l_e := 460 \; mm$
Length support to concentrated load: $l_s := 0 \; mm$
Spacing parallel to the grain: $a_1 := 70 \; mm$
Distance edge to screws: $a_{3.c} := 515 \; mm$
Number fo screws: $n := 4$
Number of screws in grain direction: $n_0 := 2$

Withdrawal:

$$k_w := 1.0$$
$$k_{mat} := 1.0$$
$$k_p := 1.10$$
$$l_w := 440 \; mm$$

Characteristic withdrawal strength:

$$f_{w.k} := 8.2 \cdot k_w \cdot k_{mat} \cdot 9^{(-0.33)} \cdot \left(\frac{390}{350}\right)^{k_p} = 4.47$$

$$f_{w.k} := 4.47 \; \frac{N}{mm^2}$$

Characterisitc withdrawal resistance:

$$F_{w.k} := \pi \cdot d \cdot l_w \cdot f_{w.k} = 55.6 \; kN$$

Buckling:

$$N_{pl.k} := \pi \cdot \frac{d_1^{\;2}}{4} \cdot f_{y.k} = 27.3 \; kN$$

$$N_{kik} := \sqrt[2]{(0.19 + 0.012 \cdot 9) \cdot 390 \cdot 210000 \cdot \pi \cdot \frac{5.9^4}{64}} \cdot N = 38.1 \; kN$$

$$\lambda_k := \sqrt[2]{\frac{N_{pl.k}}{N_{kik}}} = 847.1 \cdot 10^{-3}$$

C.4 Calculation load case C

[8.1.6.2] Compression perpendicular to the grain with reinforcement

$$k := 0.5 \cdot \left(1 + 0.49 \cdot \left(\lambda_k - 0.2\right) + \lambda_k^2\right) = 1.017$$

$$k_c := \frac{1}{k + \sqrt[2]{k^2 - \lambda_k^2}} = 0.633$$

$$F_{c.k} := 1.18 \cdot k_c \cdot N_{pl.k} = 20.41 \ \textbf{\textit{kN}}$$

minimum(Fck, Fwk) -> Fck = 20.41 kN

Design model:

$$l_{ef.1} := l_c + 30 \ \textbf{\textit{mm}} + 30 \ \textbf{\textit{mm}} = 240 \ \textbf{\textit{mm}}$$

$$l_{ef.2} := \left(n_0 - 1\right) \cdot a_1 + 2 \cdot l_r = 950 \ \textbf{\textit{mm}}$$

$$A_1 := k_{c90} \cdot f_{c.90.k} \cdot b_c \cdot l_{ef.1} + n \cdot F_{c.k} = 165.6 \ \textbf{\textit{kN}}$$
$$A_2 := f_{c.90.k} \cdot b_c \cdot l_{ef.2} = 332.5 \ \textbf{\textit{kN}}$$

A2 gives the decisive capacity

C.5 Performed test summary

Name	Load case	Reinforced/Non	1 % def, F	F_{max}	A1	A2	Timber capacity	Valid	Failure mode, screw	Moisture 1	Moisture 2	Horizontal Front [mm]	Horizontal Back [mm]	Horizontal Fram [mm] 1 % def	Horizontal Bakside [mm] 1% def
N200_A_01	A	Non-reinforced	79	94	-	-	63	Yes	Timber	12,4 %	-	7,968	25,120	0,772	0,614
N200_A_02	A	Non-reinforced	97	107	-	-	63	Yes	Timber	12,4 %	-	3,773	1,768	1,178	0,708
Pe_8.2_160_A_01	A	Reinforced	93	103	93,9	63,0	-	Yes	Withdrawal	-	-	14,437	11,136	1,813	1,718
Pe_8.2_160_A_02	A	Reinforced	99	104	93,9	63,0	-	Yes	Withdrawal	10,7 %	-	6,599	5,371	-	-
N225_B_01	B	Non-reinforced	152	202	-	-	117,9	Yes	Timber	12,4 %	-	0,972	0,963	-	-
Pa_7.0_160_B_01	B	Reinforced	172	174	171,4	136,5	-	Yes	Withdrawal	12,6 %	-	0,618	0,803	-	-
Pe_7.0_160_B_01	B	Reinforced	172	177	171,4	112,0	-	Yes	Withdrawal	12,3 %	12,3 %	0,628	0,445	-	-
Pe_8.0_180_B	B	Reinforced	196	207	177,8	126,0	-	Yes	Withdrawal/Compression	11,5 %	-	0,417	0,760	-	-
Pe_8.0_200_B	B	Reinforced	205	213	177,8	140,0	-	Yes	Compression	11,4 %	-	0,473	0,360	-	-
Pe_8.2_160_B_01	B	Reinforced	170	199	177,9	91,0	-	Yes	Withdrawal	11,7 %	-	0,694	0,992	-	-
Pe_8.2_160_B_02	B	Reinforced	178	178	177,9	91,0	-	Yes	Withdrawal	12,5 %	-	0,645	0,643	-	-
S_7.0_160_B_01	B	Reinforced	143	199	195,7	136,5	-	No	Withdrawal	14,2 %	-	-	-	-	-
S_7.0_160_B_02	B	Reinforced	210	222	195,7	136,5	-	Yes	Withdrawal	12,8 %	-	0,653	0,542	-	-
S_8.0_160_B_01	B	Reinforced	194	200	210,0	136,5	-	Yes	Withdrawal	-	-	0,612	0,787	-	-
S_8.0_180_B	B	Reinforced	217	226	208,7	150,5	-	Yes	Withdrawal	13,2 %	12,1 %	0,927	0,919	-	-
S_8.0_200_B	B	Reinforced	217	228	208,7	164,5	-	Yes	Withdrawal	13,2 %	-	0,643	0,466	-	-
S_8.2_160_B_01	B	Reinforced	189	191	208,8	115,5	-	Yes	Withdrawal	14,2 %	13,9 %	0,658	0,803	-	-
S6_7.0_160_B_01	B	Reinforced	311	339	220,1	161,0	-	Yes	Withdrawal	11,9 %	-	1,825	1,178	-	-
N540_B_01	B	Non-reinforced	165	210	-	-	127,7	Yes	Timber	12,3 %	13,0 %	0,092	0,849	-	-
Pa_9.0_440_B_01	B	Reinforced	230	231	187,8	332,5	-	Yes	Compression	12,5 %	12,3 %	0,524	0,409	-	-
Pe_8.0_300_B	B	Reinforced	234	234	177,8	210,0	-	Yes	Compression	11,0 %	-	1,266	-0,761	-	-
Pe_9.0_440_B_01	B	Reinforced	202	209	187,8	308,0	-	Yes	Compression	12,4 %	12,5 %	0,425	0,648	-	-
Pe_9.0_440_B_02	B	Reinforced	249	249	187,8	308,0	-	Yes	Compression	13,6 %	-	1,154	0,665	-	-
S_8.0_300_B	B	Reinforced	256	256	208,7	234,5	-	Yes	Compression	11,2 %	-	0,625	0,707	-	-
S_8.0_340_B	B	Reinforced	271	272	208,7	262,5	-	Yes	Compression	13,7 %	-	-	-	-	-
S_9.0_440_B_01	B	Reinforced	277	284	228,6	332,5	-	Yes	Compression	12,6 %	12,6 %	0,869	0,621	-	-
S_9.0_440_B_02	B	Reinforced	307	307	228,6	332,5	-	Yes	Compression	12,8 %	-	0,921	0,911	-	-
S6_9.0_440_B_01	B	Reinforced	455	457	379,7	350,0	-	Yes	Compression	12,8 %	-	1,477	1,467	-	-
N225_C_01	C	Non-reinforced	155	182	-	-	89,1	Yes	Timber	12,5 %	-	0,805	1,136	-	-
Pe_7.0_160_C_01	C	Reinforced	173	188	108,4	112,0	-	Yes	Withdrawal	12,5 %	-	1,102	1,792	-	-
Pe_8.2_160_C_01	C	Reinforced	169	171	114,9	91,0	-	Yes	Withdrawal	-	-	0,947	1,088	-	-
S_7.0_160_C_01	C	Reinforced	196	229	132,7	136,5	-	Yes	Withdrawal	11,2 %	-	1,983	1,716	-	-
S_7.0_160_C_02	C	Reinforced	188	210	132,7	136,5	-	Yes	Withdrawal	-	-	1,131	1,934	-	-
S_8.2_160_C_01	C	Reinforced	191	220	147,0	136,5	-	Yes	Withdrawal	12,5 %	-	2,362	1,742	-	-
S_8.2_160_C_01	C	Reinforced	183	184	145,8	115,5	-	Yes	Withdrawal	12,4 %	-	0,904	0,907	-	-
N540_C_01	C	Non-reinforced	182	237	-	-	100,7	Yes	Timber	13,0 %	14,3 %	1,789	0,818	-	-
Pe_9.0_440_C_01	C	Reinforced	214	222	124,8	308,0	-	Yes	Compression	12,6 %	12,8 %	0,708	1,737	-	-
Pe_9.0_440_C_02	C	Reinforced	244	251	124,8	308,0	-	Yes	Compression	12,8 %	-	0,955	1,110	-	-
S_9.0_440_C_01	C	Reinforced	235	257	165,6	332,5	-	No	Timber	13,2 %	12,5 %	0,954	2,826	-	-
T_7.0_160_01	Torx	Reinforced	-	21,7	13,4	-	-	Yes	Withdrawal	12,0 %	-	-	-	-	-
T_7.0_160_02	Torx	Reinforced	-	22,1	13,4	-	-	Yes	Withdrawal	12,3 %	12,6 %	-	-	-	-
T_8.2_160_01	Torx	Reinforced	-	19,6	16,8	-	-	Yes	Withdrawal	12,0 %	-	-	-	-	-
T_8.2_160_02	Torx	Reinforced	-	23	16,8	-	-	Yes	Withdrawal	13,2 %	-	-	-	-	-
T_8.0_160_01	Torx	Reinforced	-	29,1	18,3	-	-	Yes	Compression	13,2 %	-	-	-	-	-
T_8.0_160_02	Torx	Reinforced	-	27,4	18,3	-	-	Yes	Compression	11,7 %	-	-	-	-	-
T_8.0_180_01	Torx	Reinforced	-	29,3	18,3	-	-	Yes	Compression	12,3 %	-	-	-	-	-
T_8.0_180_02	Torx	Reinforced	-	29,1	18,3	-	-	Yes	Compression	11,0 %	-	-	-	-	-
T_8.0_200_01	Torx	Reinforced	-	26,3	18,3	-	-	Yes	Compression	10,3 %	-	-	-	-	-
T_8.0_200_02	Torx	Reinforced	-	28,6	18,3	-	-	Yes	Compression	11,5 %	-	-	-	-	-
T_8.0_300_01	Torx	Reinforced	-	26,0	18,3	-	-	Yes	Compression	12,3 %	-	-	-	-	-
T_8.0_300_02	Torx	Reinforced	-	25,9	18,3	-	-	Yes	Compression	12,4 %	-	-	-	-	-
T_8.0_340_01	Torx	Reinforced	-	29,2	18,3	-	-	Yes	Compression	12,4 %	-	-	-	-	-
T_8.0_340_02	Torx	Reinforced	-	27,8	18,3	-	-	Yes	Compression	11,7 %	-	-	-	-	-
T_9.0_440_01	Torx	Reinforced	-	38,7	22,1	-	-	Yes	Compression	12,0 %	-	-	-	-	-
T_9.0_440_02	Torx	Reinforced	-	42,8	22,1	-	-	Yes	Compression	12,5 %	-	-	-	-	-

C.6 Calculations Proposal 1

Proposal 1- S 9.0 440 C

Input properties:

Timber GL30c:

$$f_{c.90.k} := 2.5 \ \frac{N}{mm^2}$$

$$h := 540 \ mm$$
$$b := 140 \ mm$$

$$\rho_k := 390 \ \frac{kg}{m^3}$$

Screws VGZ 7.0x160:

$$d := 9.0 \ mm$$
$$d_1 := 5.9 \ mm$$
$$l_r := 440 \ mm$$
$$f_{y.k} := 1000 \ \frac{N}{mm^2}$$

Load arrangement: $k_{c90} := 1.75$

Discrete support, direct load

Effective contact with: $b_c := 140 \ mm$

Effective contact length: $l_c := 180 \ mm$

Length support to edge: $l_e := 460 \ mm$

Length support to concentrated load: $l_s := 0 \ mm$

Spacing parallel to the grain: $a_1 := 70 \ mm$

Distance edge to screws: $a_{3.c} := 515 \ mm$

Number fo screws: $n := 4$

Number of screws in grain direction: $n_0 := 2$

Withdrawal:

$$k_w := 1.0$$
$$k_{mat} := 1.0$$
$$k_p := 1.10$$
$$l_w := 440 \ mm$$

Characteristic withdrawal strength:

$$f_{w.k} := 8.2 \cdot k_w \cdot k_{mat} \cdot 9^{(-0.33)} \cdot \left(\frac{390}{350}\right)^{k_p} = 4.47$$

$$f_{w.k} := 4.47 \ \frac{N}{mm^2}$$

Characterisitc withdrawal resistance: $F_{w.k} := \pi \cdot d \cdot l_w \cdot f_{w.k} = 55.6 \ kN$

Buckling:

$$N_{pl.k} := \pi \cdot \frac{d_1^2}{4} \cdot f_{y.k} = 27.3 \ kN$$

$$N_{kik} := \sqrt[2]{(0.19 + 0.012 \cdot 9) \cdot 390 \cdot 210000 \cdot \pi \cdot \frac{5.9^4}{64}} \cdot N = 38.1 \ kN$$

$$\lambda_k := \sqrt[2]{\frac{N_{pl.k}}{N_{kik}}} = 847.1 \cdot 10^{-3}$$

Created with PTC Mathcad Express. See www.mathcad.com for more information.

140

C.6 Calculations Proposal 1

$$k := 0.5 \cdot \left(1 + 0.49 \cdot \left(\lambda_k - 0.2\right) + {\lambda_k}^2\right) = 1.017$$

$$k_c := \frac{1}{k + \sqrt[2]{k^2 - {\lambda_k}^2}} = 0.633$$

$$F_{c.k} := 1.18 \cdot k_c \cdot N_{pl.k} = 20.41 \ \pmb{kN}$$

minimum(Fck, Fwk) -> Fck = 20.41 kN

Design model:

$$l_{ef.1} := l_c + 30 \ \pmb{mm} + 30 \ \pmb{mm} = 240 \ \pmb{mm}$$

$$l_{ef.2} := \left(n_0 - 1\right) \cdot a_1 + 2 \cdot l_r = 950 \ \pmb{mm}$$

$$A_1 := k_{c90} \cdot f_{c.90.k} \cdot b_c \cdot l_{ef.1} + n \cdot F_{c.k} = 228.6 \ \pmb{kN}$$
$$A_2 := k_{c90} \cdot f_{c.90.k} \cdot b_c \cdot l_{ef.2} = 581.9 \ \pmb{kN}$$

A1 gives the decisive capacity

C.7 Calculations Proposal 2

Proposal 2 - S 9.0 440 C

Input properties:

Timber GL30c:

$$f_{c.90.k} := 2.5 \ \frac{N}{mm^2}$$

$$h := 540 \ mm$$
$$b := 140 \ mm$$

$$\rho_k := 390 \ \frac{kg}{m^3}$$

Comments:

Screws VGZ 7.0x160:

$$d := 9.0 \ mm$$
$$d_1 := 5.9 \ mm$$
$$l_r := 440 \ mm$$
$$f_{y.k} := 1000 \ \frac{N}{mm^2}$$

Load arrangement: $k_{c90} := 1.75$

Effective contact with: $b_c := 140 \ mm$

Effective contact length: $l_c := 180 \ mm$

Length support to edge: $l_e := 460 \ mm$

Length support to concentrated load: $l_s := 0 \ mm$

Spacing parallel to the grain: $a_1 := 70 \ mm$

Distance edge to screws: $a_{3.c} := 515 \ mm$

Number fo screws: $n := 4$

Number of screws in grain direction: $n_0 := 2$

Discrete support, direct load

Withdrawal:

$$k_w := 1.0$$
$$k_{mat} := 1.0$$
$$k_p := 1.10$$
$$l_w := 440 \ mm$$

Characteristic withdrawal strength:

$$f_{w.k} := 8.2 \cdot k_w \cdot k_{mat} \cdot 9^{(-0.33)} \cdot \left(\frac{390}{350}\right)^{k_p} = 4.47$$

$$f_{w.k} := 4.47 \ \frac{N}{mm^2}$$

Characterisitc withdrawal resistance: $$F_{w.k} := \pi \cdot d \cdot l_w \cdot f_{w.k} = 55.6 \ kN$$

Buckling:

$$N_{pl.k} := \pi \cdot \frac{d_1^{\ 2}}{4} \cdot f_{y.k} = 27.3 \ kN$$

$$N_{kik} := \sqrt[2]{(0.19 + 0.012 \cdot 9) \cdot 390 \cdot 210000 \cdot \pi \cdot \frac{5.9^4}{64}} \cdot N = 38.1 \ kN$$

$$\lambda_k := \sqrt[2]{\frac{N_{pl.k}}{N_{kik}}} = 847.1 \cdot 10^{-3}$$

C.7 Calculations Proposal 2

$$k := 0.5 \cdot \left(1 + 0.49 \cdot \left(\lambda_k - 0.2\right) + \lambda_k{}^2\right) = 1.017$$

$$k_c := \frac{1}{k + \sqrt[2]{k^2 - \lambda_k{}^2}} = 0.633$$

$$F_{c.k} := 1.18 \cdot k_c \cdot N_{pl.k} = 20.41 \; \textbf{\textit{kN}}$$

minimum(Fck, Fwk) -> Fck = 20.41 kN

Design model:

$$l_{ef.1} := l_c + 30 \; \textbf{\textit{mm}} + 30 \; \textbf{\textit{mm}} = 240 \; \textbf{\textit{mm}}$$

$$l_{ef.3} := \left(n_0 - 1\right) \cdot a_1 + a_1 \cdot 2 = 210 \; \textbf{\textit{mm}}$$

$$c := \frac{1}{0.48}$$

$$A_1 := k_{c90} \cdot f_{c.90.k} \cdot b_c \cdot l_{ef.1} + n \cdot F_{c.k} = 228.6 \; \textbf{\textit{kN}}$$
$$A_2 := k_{c90} \cdot c \cdot f_{c.90.k} \cdot b_c \cdot l_{ef.3} = 268 \; \textbf{\textit{kN}}$$

A1 gives the decisive capacity